MODELING THE VULNERABILITY OF A HIGHLY INDUSTRIALIZED ESTUARY TO STORM SURGE WITH A COUPLED ADCIRC, SWAN, AND EFDC SYSTEM

A Dissertation

Presented to

the Faculty of the Department of Civil & Environmental Engineering

University of Houston

In Partial Fulfillment

of the Requirements for the Degree

Doctor of Philosophy

in Environmental Engineering

by

Daniel Wesley Burleson

August 2015

MODELING THE VULNERABILITY OF A HIGHLY INDUSTRIALIZED ESTUARY

TO STORM SURGE WITH A COUPLED ADCIRC, SWAN, AND EFDC SYSTEM

Daniel Wesley Burleson

Approved:

Chair of the Committee
Hanadi S. Rifai, Professor
Civil & Environmental Engineering
University of Houston

Committee Members:

Philip B. Bedient, Professor
Civil & Environmental Engineering
Rice University

Clint N. Dawson, Professor
Institute of Computational
Engineering and Science
University of Texas-Austin

Debora F. Rodrigues, Assistant Professor
Civil & Environmental Engineering
University of Houston

William G. Rixey, Associate Professor
Civil & Environmental Engineering
University of Houston

Robert W. Gilmer, Director
Institute for Regional Forecasting
C.T. Bauer College of Business
University of Houston

Suresh K. Khator, Associate Dean
Cullen College of Engineering

Hanadi S. Rifai, Director
Environmental Engineering
Graduate Program

ACKNOWLEGEMENTS

Over five and half years ago, I was given a great opportunity to follow my now wife to Houston and pursue a PhD in Environmental Engineering at the University of Houston. I am gratefully indebted to my advisor, Dr. Hanadi Rifai, for taking me on as a student in the middle of the academic year. She has continually provided me with interesting projects and opportunities to grow both as a researcher and instructor. I wish to thank my committee members, Dr. William Rixey, Dr. Debora Rodrigues, Dr. Philip Bedient, Dr. Clint Dawson, and Dr. Robert Gilmer for their beneficial comments and input. I would also like to acknowledge my funding sources: the Texas Commission on Environmental Quality, the Houston Endowment through the Severe Storm Prevention Education and Evacuation from Disaster (SSPEED) Center and the National Science Foundation GK-12 program.

I have been fortunate to have been surrounded by people at the University of Houston that have supported me in a variety of ways. In particular, I would like to thank all of the students in the Rifai research group, current and past that I had the honor to work beside. They were there to listen to my ideas, provide me with an energizing cup of coffee, and give me technical and personal advice. You are all are not just colleagues, but life-long friends.

Lastly, but most importantly, I would like to thank my family for their encouragement and support. My wife, Heather, is always a loving support for me and is my rock. Thank you for your patience and always being there for me. To my parents, thank you for being a great example of hard work. I would not be here without your constant encouragement.

MODELING THE VULNERABILITY OF A HIGHLY INDUSTRIALIZED ESTUARY TO STORM SURGE WITH A COUPLED ADCIRC, SWAN, AND EFDC SYSTEM

An Abstract

Presented to

the Faculty of the Department of Civil & Environmental Engineering

University of Houston

In Partial Fulfillment

of the Requirements for the Degree

Doctor of Philosophy

in Environmental Engineering

by

Daniel Wesley Burleson

August 2015

ABSTRACT

Environmental and economic losses from hurricanes have emerged as an important topic due to the extensive damages from recent hurricanes Katrina, Rita, Ike, and Sandy on the Gulf and Eastern Coasts of the United States. Loss models developed to date fall short of modeling losses from industrial activities in coastal areas, especially economic losses from facility damage and environmental losses due to spills into waterways and ecosystems. This dissertation defines the vulnerability of industrial complexes, develops a framework for modeling environmental and economic losses due to storm surge, and develops a water and sediment quality model with storm surge boundary conditions to simulate the relative amount of pollution that would reach an open bay from a spill within an industrial facility. The developed framework, simulation tools, and models are applied to the Houston Ship Channel Industrial-Corridor (HSC-IC) using Hurricane Ike to generate three hurricane scenarios representing Hurricane Ike, Hurricane Ike landing further south along the coast, and the relocated Hurricane Ike with 30% higher winds. Data defining facility scale vulnerability are stored in a Geographic Information Systems database; the data are used to estimate inundation under surge using SWAN+ADCIRC simulations of Hurricane Ike completed by others. The resulting inundation projections are used in conjunction with infrastructure and environmental damage relationships in the developed FEDERAP loss estimation tool to estimate facility losses. Pollutant transport is simulated by coupling the SWAN+ADCIRC and EFDC models. A conservative tracer is simulated in the resulting model, known as EFDC-SS, to examine the effects of spill location and timing relative to peak surge on pollution extent and mass released to Galveston Bay. Results from FEDERAP indicate facility level

losses ranging from $10 to $25 billion based on 12 facilities that were analyzed in detail and projected losses for the HSC-IC ranging from $10 to $90 billion for all facilities. The EFDC-SS results show a significant dependence between the time of the spill and the distribution of pollutants in the HSC-IC system. Modeling results also indicate that at least half the spilled mass will reach the open bay waters within 10 days of being spilled under surge.

TABLE OF CONTENTS

LIST OF FIGURES

LIST OF TABLES

CHAPTER 1. INTRODUCTION

A hurricane is a type of tropical cyclone that starts as a low-pressure system and intensifies over warm tropical waters creating circulation around a center (hurricane eye). Once fully organized, the wind area of a hurricane storm has an average diameter of 100 miles (Weather Research Center, 2015) with central pressures lower than 994 mbar (metric unit of pressure) and sustained winds exceeding 74 miles per hour. As a result, a significant storm surge, or a rise in water level above typical conditions, develops as the storm moves towards a coastal region. This phenomenon is primarily driven by wind-imposed water surface stresses (Figure 1-1). The three damage-causing aspects of hurricanes are strong winds, significant rainfall, and storm surge. Of the three, storm surge is the most costly (Santella et al., 2010) and will be the focus of this dissertation.

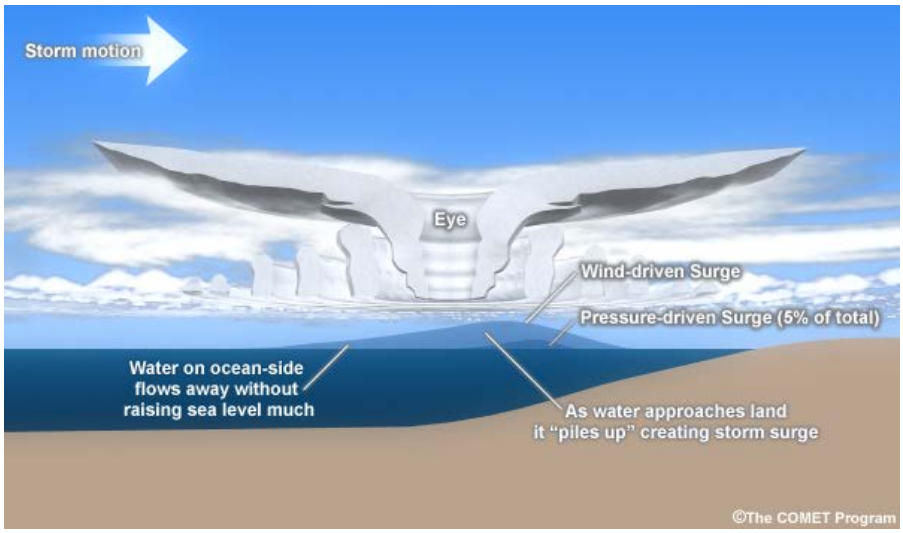

Figure 1-1. Components of storm surge as a hurricane approaches the coast line (NOAA – COMET Program, 2015)

The United States has an extended history of hurricane strikes. Over 290 hurricane events have made landfall since 1851 with 12 events occurring in the last 10 years as shown in Table 1-1. Tropical cyclones (i.e., hurricanes) account for less than a

quarter of the significant loss events from natural disasters (billion dollar events); however, more than 53% of losses (Consumer Price Index-adjusted (CPI) losses of $452 billion) resulted from tropical cyclones between 1980 and 2010. The data in Table 1-2 indicate that hurricane event losses average around $15 billion per event. Most recently, Hurricane Sandy moved across the east coast in October of 2012 causing more than $68 billion in damages. Recent studies about Hurricane Sandy have discussed the devastating social and economic damage that affected residential areas (Cutter et al., 2014), public infrastructure (Zimmerman, 2014), and the environment (Wilson, 2014). However, post-event inventories of damages and losses are not sufficient; it is important to be able to forecast the losses associated with hurricanes in order to develop resilience and sustainability in coastal communities.

Table 1-1. Hurricanes that made landfall in the United States since 2005

Year	Hurricanes
2012	Isaac
	Sandy
2011	Irene
2008	Dolly
	Gustav
	Ike
2007	Humberto
2005	Cindy
	Dennis
	Katrina
	Rita
	Wilma

Table 1-2. Billion dollar events to affect the U.S. from 1980 to 2010 – CPI adjusted (NOAA, 2015)

Disaster Type	Number of Events	Percent Frequency	CPI-Adjusted Losses (billions)	Percent of total loss	Average event loss (billion)
Drought	18	13.40%	$148	17.50%	$8.20
Flooding	15	11.20%	$79	9.30%	$5.30
Freeze	7	5.20%	$25	3.00%	$3.60
Severe Storm	43	32.10%	$86	10.20%	$2.00
Tropical Cyclone	30	22.40%	$452	53.40%	$15.10
Wildfire	10	7.50%	$24	2.80%	$2.40
Winter Storm	11	8.20%	$33	3.90%	$3.00

Disaster loss estimation has evolved in recent years. The most comprehensive model is HAZUS-MH (Vickery et al., 2006) from FEMA that provides regional losses. HAZUS-MH uses general categories to determine losses. Like a majority of current tools, HAZUS-MH does not differentiate the complexities associated with industrial activities, nor does it consider the effect that storm surge has on coastal communities. In addition, current models of hurricane damage and losses do not incorporate environmental effects that have been extensively documented from prior hurricane events (Pardue et al., 2005; Pine, 2006; Reible et al., 2006; Adams et al., 2007; Fries et al., 2007; Wilson, 2014). In particular, along the gulf coast (Texas and Louisiana) the coastlines have a high density of very productive chemical and petrochemical complexes that would incur substantial losses if subjected to storm surge. This proved to be the case in New Orleans during Hurricane Katrina at the Murphy Oil USA Meraux Refinery where over one million gallons of crude oil was released when an aboveground storage tank was lifted by floodwaters (Reible et al. 2006).

This dissertation addresses the aforementioned gaps in damage and loss estimation from a hurricane by defining vulnerability of industrial complexes and

developing a framework for estimating potential environmental and economic losses due to storm surge. This work involves database development and the use of ArcGIS spatial tools, spreadsheet analysis based on modeling, loss estimation algorithms, and a coupled SWAN+ADCIRC and EFDC model for water quality impact forecasting.

The overall goal of this research is to develop a framework for incorporating storm surge as a key driver for vulnerability and economic losses in coastal regions that contain an extensive industrial land use component. Specific objectives include:

- develop a framework for modeling storm surge impacts on industrial facilities;
- develop an ArcGIS database of industrial facilities and their relevant characteristics for an representative gulf coastal community;
- develop algorithms for economic and environmental losses at industrial facilities resulting from storm surge using facility-specific characteristics of tanks and unit-processes as well as facility elevation;
- integrate the developed algorithms into a spreadsheet-based model for estimating damages and losses at industrial facilities for various storm surge levels;
- link the SWAN+ADCIRC hurricane storm surge predictive model to the EFDC sediment and water quality model to develop a modeling system for estimating the fate of spills from industrial facilities during hurricanes; and
- illustrate the use of the developed loss estimation framework and the linked SWAN+ADCIRC and EFDC model to the Houston Ship Channel Industrial Corridor along the Gulf Coast.

This thesis has six chapters. Chapter 1 (the current chapter) is the Introduction. The next chapter (Chapter 2) will provide the theoretical background that formed the basis for the developed approach and methodology in this dissertation. In addition, Chapter 2 will provide context regarding the usefulness of the developed framework and other models in the field of hurricane impact. Chapter 3 presents the developed regional framework for modeling vulnerability of an industrial region to storm surge. Chapter 4 focuses on the development of the FEDERAP model for estimating environmental and economic losses at the facility level and for an entire industrial corridor using regression. Chapter 5 outlines the model development and results for the coupled SWAN+ADCIRC and EFDC model for contaminant transport and water quality during hurricane events. Finally, the findings of all chapters are summarized in Chapter 6.

CHAPTER 2. BACKGROUND

Storm surge can be readily simulated using a number of existing hurricane models. The next section will focus on the two most widely used models (ADCIRC and SLOSH) with emphasis on the ADCIRC model that was relied upon for storm surge predictions in this research.

2.1 STORM SURGE MODELING

2.1.1 HURRICANE STORM SURGE

Hurricane storm surge is primarily caused by low barometric pressures and high winds that cause significant wave action (Harris County Flood Control District 2009). The quantity and height of water results in extensive coastal flooding and is the primary cause of death and damage from a hurricane (Santella et al., 2010).

Storm surge height is dependent on the features of a hurricane (e.g., storm size, pressure, forward speed and maximum winds) and the bathymetry of the impacted coastline (Irish et al., 2008). The inundation from storm surge depends on the shoreline elevation and slope of the continental shelf, a large area of the seabed where there is shallow water depth close to the coast. Weaver and Slinn (2010) and Walton and Dean (2009) noted the significant impact bathymetry had on the wind stress of a hurricane and showed that the severity of storm surge was minimized in areas of Florida due to steep coastlines. In contrast, the Houston-Galveston region features a shallow sloping coastline, highlighting the vulnerable nature of this region to storm surge.

2.1.2 HURRICANE STORM SURGE MODELS

Storm surge was first modeled by Jelesnianski et al. (1992) creating the Sea, Lake, and Overland Surges from Hurricane (SLOSH) model. This finite difference, two-

dimensional model uses a polar grid (Figure 2-1) and numerically solves the governing equations of fluid motion. SLOSH is not “tuned” for specific locations but uses universal values for drag coefficient, and bottom stress, among others. (Jelesnianski et al., 1992). The SLOSH model uses open boundary conditions that are placed far from the primary area of interest (Mercado, 1994; Zhang et al., 2008). Based on observed high water marks (HWM), SLOSH has been found to be accurate to within +/- 20% (Blake and Gibney, 2011). While the model uses inputs of pressure, size, forward speed, track, and wind from the hurricane, the model fails to account for tide, precipitation/evaporation, riverine flow or wind-driven waves. SLOSH has been used nationally by NOAA including for Puerto Rico (Mercado, 1994) to assess storm surge over large areas and has previously been used for FEMA Flood Insurance Rate Maps (FIRM) in coastal regions. The advantages of SLOSH are seen in its ability to resolve flow through barriers, gaps, passes and the overtopping of levees and barriers. It is computationally efficient (Lin et al., 2010) allowing the model the make computations over large areas with high process speed.

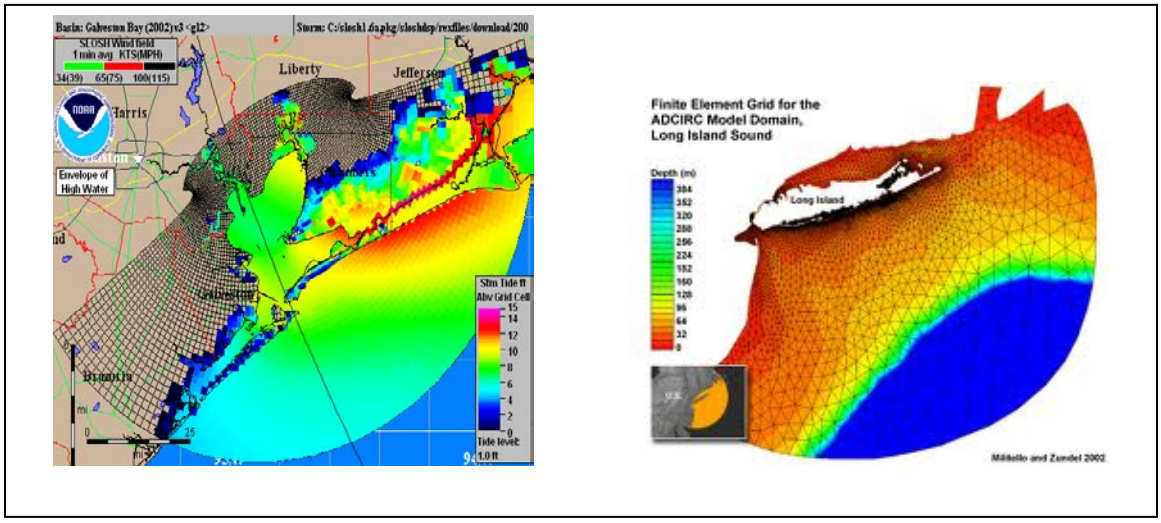

Figure 2-1. (Left) SLOSH model grid, (Right) ADCIRC model grid

The ADvanced CIRCulation (ADCIRC) model was developed by Luettich et al. (1992); storm surge predictions from ADCIRC for the Gulf Coast are used in this thesis. The model contains a large-domain unstructured grid (Figure 2-1) that allows for computational efficiency and better accuracy near the coast. As mentioned earlier, bathymetry plays an important role in predicting storm surge height. The ADCIRC model uses a more detailed base bathymetry near the coast thus allowing for results that are more accurate. The model can be run in 2-dimensions (2D) or 3-dimensions (3D) thereby enabling calculation of both water level and water velocities. However, because of the detailed nature of the grid used in modeling, ADCIRC requires relatively large computational power and detailed local data for its input.

The ADCIRC model has been used extensively to date. Mattocks and Forbes (2008) used the two-dimensional, depth-integrated ADCIRC model to create a storm surge forecasting system for the state of North Carolina. As part of the analysis by (Mattocks and Forbes, 2008), the accuracy of the SLOSH model was compared to that of ADCIRC. While the SLOSH model showed error in peak surge of approximately 20%, the ADCIRC model produced errors ranging from 4% to 16% with the largest error occurring in regions with low-resolution bathymetry. Velocities were also calculated in ADCIRC to within 0.72-0.93 error accuracy of their measured counterparts illustrating another advantage of ADCIRC over SLOSH.

Bunya et al. (2010) presented the “SL15” storm surge model for Louisiana and Mississippi. This model incorporated the wave models WAM (The Wamdi Group, 1988) and STWAVE (Smith et al., 2001) into the ADCIRC unstructured coastal ocean

circulation model. Bunya et al. (2010) modified the existing ADCIRC model by updating Manning-n values (representing the roughness or friction applied to the flow) and bottom friction while utilizing a localized refinement to the coastal floodplain grid for cells that are as small as 30 m. Wave radiation boundary conditions were used to ensure that surge does not bounce back into the system and distort the surge computations (Westerink et al., 2008). This resulted in an accurate representation of storm surge with measured peak storm surge values and modeled values having a correlation coefficient of 0.92.

Sheng et al. (2010) used the ADCIRC model in coordination with WaveWatch III, SWAN, and CH3D (Sheng, 1990) to create an integrated storm surge modeling system called CH3D-SSMS (CH3D-Storm Surge Modeling System). CH3D is a coarser coastal grid model coupled with SWAN that allows for better computational efficiency in examining the effects of 3D surge modeling on the accuracy of simulated storm surge elevation and currents. Similar to models used for Louisiana, Mississippi, and Texas (Westerink et al., 2008; Wamsley et al., 2009; Bunya et al., 2010; Smith et al., 2010), CH3D creates high-resolution grids close to the coast of Florida while still taking advantage of the coarse ADCIRC grid offshore.

The SWAN model developed by Booij et al. (1999) is a third generation coastal wave model that solves wave action density via wave and current interaction. To account for the influence of wave stresses on storm surge height, the Simulation Waves Nearshore (SWAN) model was dynamically coupled with ADCIRC (Chen, 2005; Funakoshi, 2008; Pandoe and Edge, 2008; Dietrich et al., 2011). A dynamical coupling means wave induced stresses are adapted back into the ADCIRC model where they are used for the radiation boundary condition. This modeling effort has been applied in the

aforementioned regional applications of ADCIRC yielding acceptable results (Chen, 2005; Funakoshi, 2008; Pandoe and Edge, 2008; Dietrich et al., 2011).

The SWAN+ADCIRC modeling system has been successfully validated for recent hurricanes Katrina, Rita, Gustav, and Ike (Westerink, et al. 2008; Dietrich et al., 2010; Hope et al., 2013). When compared to high water marks from Hurricane Ike, for instance, 94% of modeled high water marks were within 0.50 m of the measured values (Hope et al. 2013).

Inputs to SWAN+ADCIRC include a data assimilated Ocean Wind Field (OWF) and a high resolution computational domain encompassing the Western North Atlantic, Gulf of Mexico, and Caribbean Sea. The unstructured finite element mesh incorporates a significant amount of detail around the Houston-Galveston region, and consists of 3,323,388 nodes with resolution down to 30 m in the nearshore. The grid represents a subset of the grid (SL18TX33) presented in Hope et al. (2013) without the refinement that was undertaken for Louisiana. Storm surge data for calibration used 206 verified data locations that were derived from several sources including the U.S Geological Survey (USGS), the National Oceanic and Atmospheric Organization (NOAA), Texas Coastal Ocean Observation Network (TCOON), and the State of Louisiana Coastwide Reference Monitoring Station (CRMS).

2.2 ASSESSING VULNERABILITY TO HURRICANES

2.2.1 RISK, RESILIENCE, AND VULNERABILITY

Risk is the expected loss (people or property) that would be caused by a particular hazard. It is a function of resilience, vulnerability and hazard where the hazard is the

probability of the event occurring, resilience is the ability of the system to protect itself from the event, and vulnerability is characteristics of a system that may results in damage or losses from the event. The probability of storm surge events has yet to be determined and is currently the subject of much research. Thus, a risk-based approach was not used in this work due to the lack of probability data that can be associated with storm surge. Instead, this research is focused on vulnerability as will be described later in this section.

Resilience has its own diversity of definitions and applications. Holling (1973) described resilience as having the ability to "absorb" an event. From a geographic standpoint, Zhou et al. (2010) defines resilience as the ability of a region to resist losses during a disaster and recover after the event has passed. 'Absorption' (Carpenter et al., 2001) and 'adaptive capacity' (Folke et al., 2002; Walker et al., 2004; Adger et al., 2005; Folke, 2006; Lopez Marrero, 2008; Folke et al., 2010) are two terms that have been used throughout the literature to describe the resistance to losses or the ability of a system to 'absorb' some damages during an event.

For vulnerability related to natural hazards such as hurricanes and flooding, Birkmann (2006) argues that vulnerability is "prerequisting of reducing disaster risk." Vulnerability, in general, has been defined as the degree to which a system is susceptible to adverse effects from an event (Lei et al., 2014); however, Hufschmidt (2011) argues that there is no universal model for vulnerability. From a natural hazards perspective, social vulnerability was emphasized by Cutter et al. (2003) to include the exposure conditions to the event and resistance to the hazard by society. In the case of the work presented in this thesis, the event is storm surge from hurricanes and the adverse effects include economic and environmental losses.

2.2.2 ENVIRONMENTAL VULNERABILITY TO STORM SURGE

Storm surge, as discussed previously, is the most devastating aspect of a hurricane due to the retention time of inundated areas, currents, and water pressures within the affected region (Godoy, 2009; Naito et al., 2012). Several studies have demonstrated catastrophic impacts of storm surge on residential areas (Robertson et al., 2007; Frazier et al., 2010) and industrial regions (Godoy, 2007; Hallegatte et al., 2011; Burleson et al., 2015a) focusing mainly on physical damage related to infrastructure, e.g., building damage and storage tank damage. Residential regions are typically located at elevations that make storm surge less of a factor with the impact to these regions mostly due to structural damage from wind (Huang et al., 2007). Industrial facilities, in contrast, tend to be on waterways near shipping canals and thus may be at increased risk from storm surge due to their proximity to water and relatively lower land elevations (Santella et al., 2010).

Hurricane vulnerability studies to date have focused on community vulnerability and developing resilience in coastal areas (Wu et al., 2002; Wang and Yarnal, 2012) and on addressing wind damage (Unanwa et al., 2000; Stewart, 2003). Some studies have investigated the vulnerability of a region to storm surge; however, these studies have focused on larger regional impacts to the community (Kleinosky et al., 2007; Rao et al., 2007). Place-based models for understanding community response to natural hazards have been proposed and include additional ecological aspects such as biodiversity and erosion rates (Cutter et al., 2008). However, these models do not consider the impact industrial facilities have on the ecological or environmental vulnerability of a region.

Another aspect that has yet to be addressed has to do with the impact on the environment related to the inundation of infrastructure and industry. Some work has moved beyond studies by Vickery et al. (2006) and Ding et al. (2008), which demonstrated the limited application of HAZUS. Marc and Carol (2005) focused on the vulnerability of industrial and petrochemical facilities but only from the perspective of extreme winds associated with hurricanes. Stearns and Padgett (2011) demonstrated the impact that storm surge had on bridge infrastructure but their work was limited to bridge crossings. Ultimately, a definitive investigation of storm surge and its relationship to the vulnerability of industrialized regions has yet to be undertaken. The research presented in this thesis addresses this need.

Disaster vulnerability, in general, has been well studied (Petrova, 2006; Sharma and Patwardhan, 2008; Christopher et al., 2012). Hurricane vulnerability also has received significant attention because of hurricanes that have affected the Gulf Coast in the past 10 years (e.g., Hurricanes Katrina, Rita, and Ike) causing significant damage and loss of human life (Cauffman et al., 2006; Cigler, 2009; Link, 2010). While the impact of storm surge on the environment has been observed in Hurricanes Katrina and Rita, the economic impact related specifically to storm surge has yet to be fully understood. Pine (2006) noted over 50 oil spills that had been reported in the nearshore environment in Hurricane Katrina. The spills were attributed mostly to pipelines and tanks that were damaged by inundation and were thought to have short-term and long-term impacts on the environment. Godoy (2007) and Santella et al. (2010) found significant damage to 21 affected storage tanks in Hurricanes Katrina and Rita; the most severe effects being due mainly to surge and inundation related tank failures. In addition to potential cleanup

costs, the economic damage associated with facility inundation could include production downtime and supply loss that may represent a significant component of the total economic impact of storm surge on a region.

Past studies have reported on damages experienced by industrial facilities during hurricanes. Harris and Wilson (2008) provided a detailed evaluation of the DeLisle Plant in Pass Christian, MS during Hurricane Katrina and reported on significant failure of electrical centers, processing buildings, and control centers due to rising water from storm surge. Cruz et al. (2001) examined petroleum refineries and reported that flooding caused structural failure, floating tanks and significant production downtime due to power failure. Godoy (2007) and Santella et al. (2010) found storm surge to be the major cause for failures and releases in their studies on tank inundation during hurricanes Katrina and Rita, respectively. However, like the studies on industrial facilities, the investigation of tank inundation does not predict failure based on locations and elevation; instead the focus is on hindcast reporting of damages from previous storm surge events (Cauffman et al., 2006; Pine, 2006; Godoy, 2007; Naito et al., 2012). Some studies have reported damages and discussed the potential environmental impact during hurricanes (Adams et al., 2007; Ashley et al., 2008; Santella et al., 2010; Sengul et al., 2012), however none have accounted for environmental cleanup and/or downtime of industrial production.

The specificity of production units, storage and distribution systems, coupled with geospatial characteristics such as land elevation and proximity to coastal systems complicates the evaluation of storm surge impact on an industrial facility. Additionally, most industrial facilities will have intrinsic economic value based on their contribution to

the local, regional, and/or national economy. Thus, losses during hurricanes most certainly entail secondary losses from environmental cleanup and downtime that may result from inundation and catastrophic losses of units/processes which have been previously discussed in work done regarding hurricanes (Cauffman et al., 2006; Pine, 2006; Santella et al., 2010; Burleson et al., 2015a) and tsunamis (Srinivas and Nakagawa, 2008; Naito et al., 2012). Following Hurricane Isaac in 2012, for example, gasoline prices jumped five cents because of the perception that refined fuel supplies will be interrupted by the hurricane (Fahey, 2012). The need for a damage assessment framework in industrial regions that encompasses physical damage from inundation as well as secondary losses from environmental spills and releases and downtime effects on productivity is evident.

Frameworks for assessing vulnerability of critical infrastructure and the impact on a region have been presented for other areas of study (Yang et al., 2009; Francis and Bekera, 2013). Environmental decision support systems have been utilized to assess population impact (Qi and Altinakar, 2011) and hazardous waste transport (Zografos et al., 2000; Verter and Kara, 2001; Kim et al., 2011). However, specific decision-based frameworks for inundation of industrial facilities have yet to be fully studied.

2.3 MODELING WATER QUALITY AND POLLUTANT TRANSPORT DURING STORM SURGE

Very little has been presented to date on water quality and pollutant transport during hurricanes and more specifically resulting from storm surge. Hagy et al. (2006) investigated the effects of Hurricane Ivan on water quality in Florida using water quality

surveys 20 and 50 days after the storm. Immediate effects and potential deposition of contaminants discussed in work by Pardue et al. (2005) for Hurricane Katrina found high levels of toxic metals and depleted dissolved oxygen. Modeling of the water and sediment quality effects of hurricane and storm surge has yet to be elucidated. The result of such modeling, when completed, will provide insight into the variables that affect water quality and the spatial distribution of pollutants in coastal environments that would occur due to hurricane storm surge.

2.3.1 POLLUTANT TRANSPORT MODELING DURING A HURRICANE EVENT

Many studies have simulated pollutant transport in coastal environments though their focus was mainly on oil spills and did not include the effect of storm surge. The GNOME (General NOAA Oil Modeling Environment) is used for emergency response to oil spills but fails to include the physical and chemical reaction of oil with its environment (Beegle-krause, 2005). The coupling of spill simulation with hydrodynamic models successfully accounts for this interaction (Guo and Wang, 2009; Wang and Shen, 2010). Liu et al. (2011) simulated offshore oil spills under wave induced circulation, conditions that would be present in a hurricane event and included the vertical movement of oil in the water column. The result of the work indicated a significant wave impact on the transport of this contaminant as it increased the magnitude and direction of currents near shore. However, and as noted above, no work to date has modeled industrial spills during a storm surge event or modeled the potential for movement of pollutants upstream and their eventual distribution once the surge event has receded. The research presented in this thesis addresses this gap and links the SWAN+ADCIRC hurricane prediction

model with the EFDC water quality and sediment model. The next section will describe the EFDC model and its applications found in the literature.

2.3.2 ENVIRONMENTAL FLUID DYNAMICS CODE (EFDC) MODEL DESCRIPTION AND APPLICATION

The Environmental Fluid Dynamics code (EFDC) simulates flow, transport and biochemical processes in three-dimensions for water systems such as rivers and estuaries (Hamrick, 1992; Hamrick, 1996). While the model was originally developed at the Virginia Institute of Marine Science for coastal applications, the United States Environmental Protection Agency (US EPA) currently supports its development and is recommended for TMDL development. It is public domain software with hydrodynamic capabilities coupled with salinity and temperature transport, cohesive and non-cohesive sediment transport (Anderson, 2010) and fate and transport of toxic contaminants (Jie et al. 2002). The governing equations of momentum and continuity are solved from a Boussinesq approximation. EFDC utilizes a finite difference method on a curvilinear, orthogonal grid and applied using the Fortran 77 language. Additional details regarding the hydrodynamic and transport theory are found in Tetra Tech, Inc. (2007). Biochemical changes in algae and bacteria are modeled in EFDC using modeled water quality parameters such as temperature, salinity, and dissolved though biochemical processes are not the focus in this thesis. Craig (2012) through Dynamic Solutions, LLC (DSLLC) developed a streamlined and visual pre- and post-processing tool EFDC_Explorer7. While it has not been previously used for hurricane applications, EFDC has been used for water and sediment quality model in estuary systems (Ji et al., 2001; Alarcon et al.,

2014). Since the model is supported by the US EPA and has been applied in particular for the Houston Ship Channel (Howell, 2012) with success, EFDC was used in this work (Chapter 5).

2.4 HOUSTON SHIP CHANNEL – INDUSTRIAL CORRIDOR

The Houston Ship Channel Industrial Corridor (HSC-IC) (Figure 2-2) is located in Harris County, Texas. The HSC-IC, covering an area of 225 square kilometers, is highly industrialized with 866 industrial facility parcels covering 60 square kilometers and including more than 3,400 above ground storage tanks. Because of the chemical and petrochemical nature of this industrial complex, the potential for environmental releases during hurricanes and severe storms is significant and provides an ideal study area for the work presented in the thesis.

From an economic standpoint, the HSC-IC generates more than $150 billion in economic activity and over 1 million jobs. The Port of Houston, located on the west end of the HSC-IC, is one of the busiest ports in the United States based on foreign tonnage and the second largest in the world in terms of tonnage (Port of Houston, 2015).

As mentioned previously, there have been over 120 storm surge events related to hurricanes along the Gulf Coast since 1880; 14 of which have landed in the Houston-Galveston Region and affected the entire region including the HSC-IC. The sensitivity of this region to these events is noted from the Emergency Response Notification System (ERNS) database Harris County shown in Figure 2-3. Significant spikes in spills and accidents from facilities for recent events like Tropical Storm Alison (2001), Hurricane Rita (2006), and Hurricane Ike (2008) indicate for this region, a need for greater

understanding of storm surge impact. However, the work presented in this thesis does not focus on the port and damages associated with shipping losses due to closure of the channel or destruction of port-related facilities.

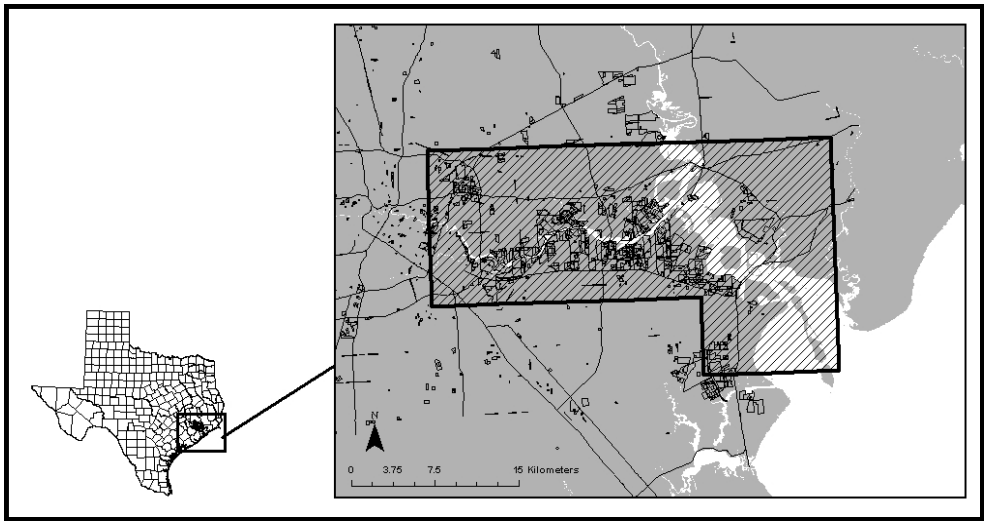

Figure 2-2. The Houston Ship Channel – Industrial Corridor (HSC-IC) along the Gulf coast in Texas. The parcels outlined in black are industrial facilities with the shaded-in region representing the study area.

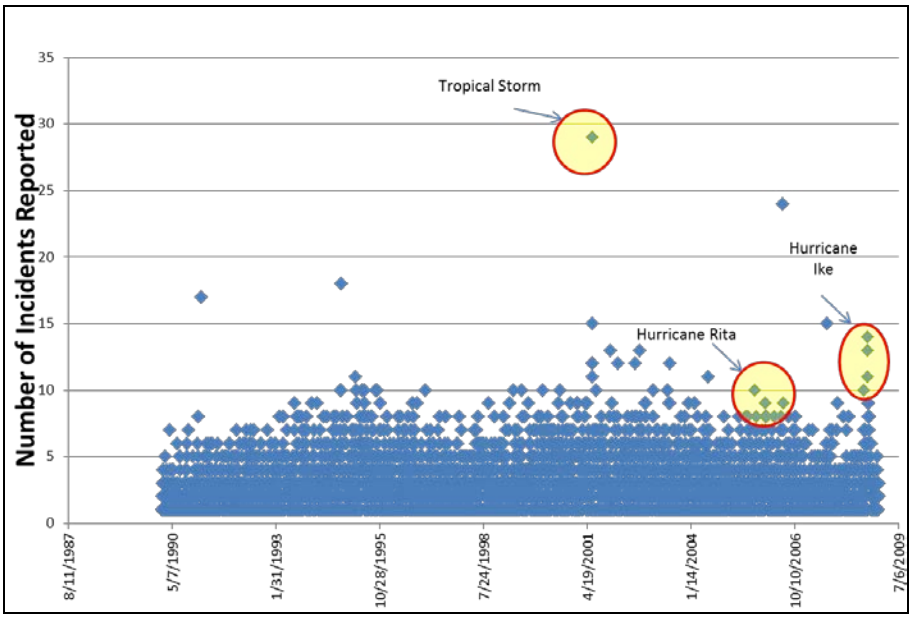

Figure 2-3. ERNS incidents for Harris County, Texas from 1990 to 2009.

CHAPTER 3. VULNERABILITY OF AN INDUSTRIAL CORRIDOR TO STORM SURGE

The developed framework in this research (Figure 3-1) relates storm surge predictions from an SWAN+ADCIRC model (Hope et al., 2013) for hurricanes that approach the Texas Gulf Coast to the topography of the HSC-IC, its environmental characteristics, and industrial infrastructure using a customized geodatabase for the region. Environmental characteristics in this research specifically refer to the potential for releases from facilities based on their chemical storage profile, past history of releases, and toxic storage amounts. As can be seen in Figure 3-1, the framework hinges on developing modeling scenarios for hurricane landfall, modeling landfall scenarios with the SWAN+ADCIRC model, developing a geodatabase for the region, and linking the latter two to allow an analysis of geospatial and environmental vulnerabilities. Each component of this framework is described briefly below for completeness; more detail can be found in Burleson et al. (2015a).

3.1 HURRICANE SCENARIOS

Hurricane Ike made landfall in 2008 along the Texas Gulf coast on Galveston Island (landfall location shown in Figure 3-2 and annotated as “original”). While not a catastrophic event for the HSC-IC, Ike was characterized by its unusually wide spatial coverage upon landfall. Within the Houston-Galveston region and the HSC-IC, Ike generated the equivalent of the 100-yr flood event in the HSC-IC (Burleson et al. 2015a).

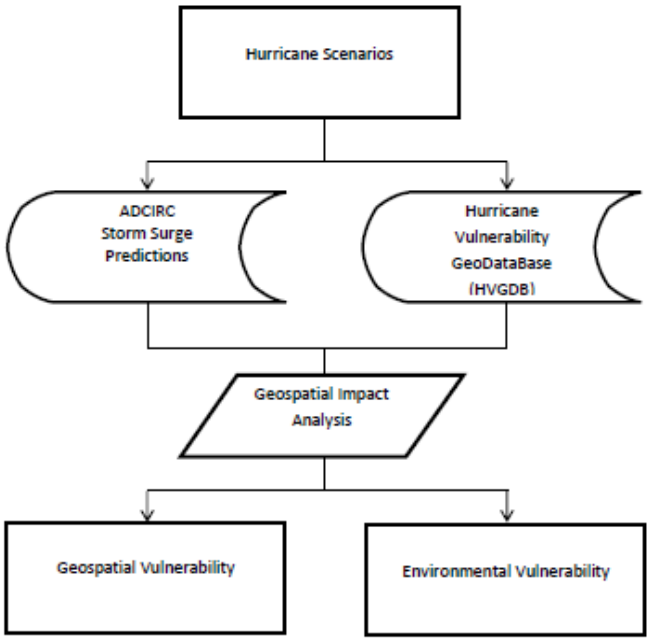

Figure 3-1. A schematic of the conceptual model developed for characterizing vulnerabilities to storm surge

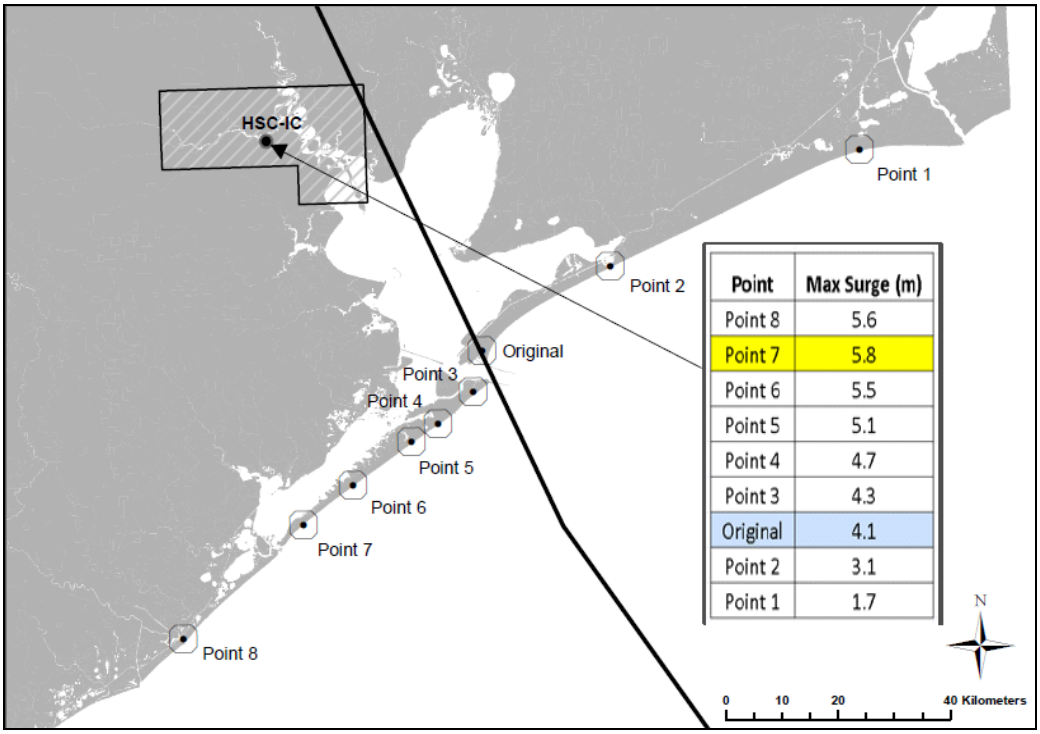

Figure 3-2. Landfall locations for SWAN+ADCIRC modeling of Hurricane Ike with change in storm surge by location shown in the table. The solid black line represents the original track of Hurricane Ike.

While the Sea, Lake, and Overland Surges from Hurricane (SLOSH) model has previously been used extensively by the National Oceanic and Atmospheric Administration (NOAA) for hind casting and forecasting storm surge events, a newly developed SWAN+ADCIRC wave and circulation model was used to simulate storm surge during Hurricane Ike. In particular, Kerr et al. (2013) performed an analysis comparing the water level results from the two models during Hurricane Ike and found that SLOSH produced less accurate results compared to the SWAN+ADCIRC model for the Houston-Galveston region. This model was chosen for use in this thesis since it has been extensively validated on a variety of storms in the Louisiana and Texas coastal shelf (Dietrich et al., 2012; Hope et al., 2013; Sebastian et al., 2014) and is considered an ideal simulation tool for quantifying storm surge in the region. In particular, the model was validated for Hurricane Ike (Hope et al., 2013) and successfully applied the SWAN+ADCIRC model for Galveston Bay using various storm locations and strengths related to Hurricane Ike (Sebastian et al., 2014)

Weisberg and Zheng (2006) indicated that the location of a hurricane's landfall has a significant impact on localized storm surge levels. Thus, for the modeled scenarios in this thesis, Ike's track was shifted to eight different landfall locations along the coast to the southwest and to the northeast to determine the effect of the landfall location on storm surge in the HSC-IC. Figure 3-2 shows the actual Hurricane Ike landfall location (labeled "original") and the eight additional modeled landfall locations. It is important to note that while landfall location changed in the modeled scenarios, the track alignment shown in Figure 3-2 was maintained for all scenarios. The landfall location approximately 31 miles

to the southwest of Hurricane Ike's actual landfall location (referred to in this thesis as Point 7) provided the highest storm surge elevations in the HSC-IC, and was thus considered the worst-case scenario and used to illustrate the vulnerability framework developed in this chapter of the thesis.

In addition to landfall location, wind speed as it affects storm surge is an important consideration. This is because the stress caused by wind accounts for approximately 95% of the storm surge height (Weisberg and Zheng, 2006; Irish et al., 2008; NOAA, 2012). Prior to making landfall, Hurricane Ike was a Category 4 hurricane with winds exceeding 135 mph but it quickly subsided to a Category 2 storm upon landfall, a 30% reduction in wind speed. Thus and in order to incorporate the effect of wind speed into the modeled scenarios, Hurricane Ike's winds were increased by 30% thereby elevating Hurricane Ike back to a Category 4 hurricane upon landfall (Sebastian et al., 2014). For the purposes of illustrating the vulnerability framework developed in this study, results from Hurricane Ike at the "original" location, Hurricane Ike at Point 7, and Hurricane Ike at Point 7 with 30% stronger winds are presented. It should be noted that the focus of the modeling scenarios is on assessing vulnerabilities; the modeled scenarios were not intended to be used to develop relationships between wind speed, landfall, and impacts.

3.2 SWAN+ADCIRC STORM SURGE PREDICTIONS

Model results for the landfall location scenarios indicated that as Ike was moved from Point 1 to Point 7 (a distance of approximately 120 kilometers southwest), storm surge in the HSC-IC increased from approximately 4 m for the actual landfall location to approximately 5.8 m at Point 7 (a 1.8 m increase, identified as worst-case scenario for

landfall location as mentioned previously). At Point 8, storm surge begins to decrease. As shown in Figure 3-2 for a select location within the HSC-IC, there is a steady increase in storm surge as Hurricane Ike is shifted to the southwest because of the strongest component (Northeast corner) of the storm hitting the HSC-IC directly. When the winds were increased by 30% at Point 7, the storm surge level increased to approximately 7.7 m in the HSC-IC (1.9 m increase over the lower wind scenario), supporting the importance of wind speed effects on storm surge. When taken together, the swath defined by potential landfall locations between points 3 and 7 represents the critical zone of influence for storm surge in the HSC-IC from both a landfall and wind speed perspective. Figure 3-3 illustrates the extent of inundation based on the maximum storm surge elevation simulated in the HSC-IC in the three SWAN+ADCIRC scenarios (Ike, Ike at point 7, and Ike at point 7 with 30% increased wind speed). As can be seen from the figure, and while most of the inundation is reasonably contained in the Ike scenario, inundation is extensive, widespread, and completely submerges the HSC-IC in Ike at Point 7 with 30% higher wind. In this manner and based on the modeled scenarios, vulnerability of the HSC-IC to landfall location and wind speed of hurricanes was characterized.

3.2.1 HSC-IC HURRICANE VULNERABILITY GEODATABASE (HVGBD) DEVELOPMENT

A specialized GIS geodatabase for the HSC-IC was developed to include topography, parcel boundaries, and critical infrastructure. The main purpose of developing the Hurricane Vulnerability GeoDataBase (HVGDB) was to link the modeled

storm surge from the scenarios described in the previous section with the geospatial land-use, topography, industrial facility, and environmental data. The HVGDB can be envisioned as a tool to analyze, interpret, map, and store the resulting vulnerabilities that can also serve as a means of communication and decision-making among its users (e.g., scientists, engineers, hurricane modelers, decision makers). Therefore, while not all stakeholders may be experts in SWAN+ADCIRC or hurricane modeling, they can still readily access the modeled results and make interpretations. Because of its dynamic format (e.g., direct linkage to existing spatial datasets), the HVGDB can be readily updated and expanded to include additional scenarios as they are developed as well as additional variables or considerations for analysis and decision-making. The HVGDB includes geographic and topographic data for the HSC-IC, facility critical infrastructure information, data on Aboveground Storage Tanks (ASTs) at each facility, information from Toxic Release Inventories (TRI) and information on Risk Management Plans (RMPs). These components will be described briefly below.

Geographic and Topographic Data. The geography of the region was defined using Light Detection and Ranging (LIDAR) data from the Harris County Flood Control District (HCFCD) that was developed in their Tropical Storm Allison Recovery Project (TSARP). The vertical datum for TSARP data that were collected in 2006 is the North American Vertical Datum of 1988 (NAVD88). Inundation depth within the HSC-IC was calculated as the difference between the modeled water level and the ground elevation above sea level. The LIDAR data were also used to determine the specific ground elevation of industrial facilities and select infrastructure along the HSC-IC.

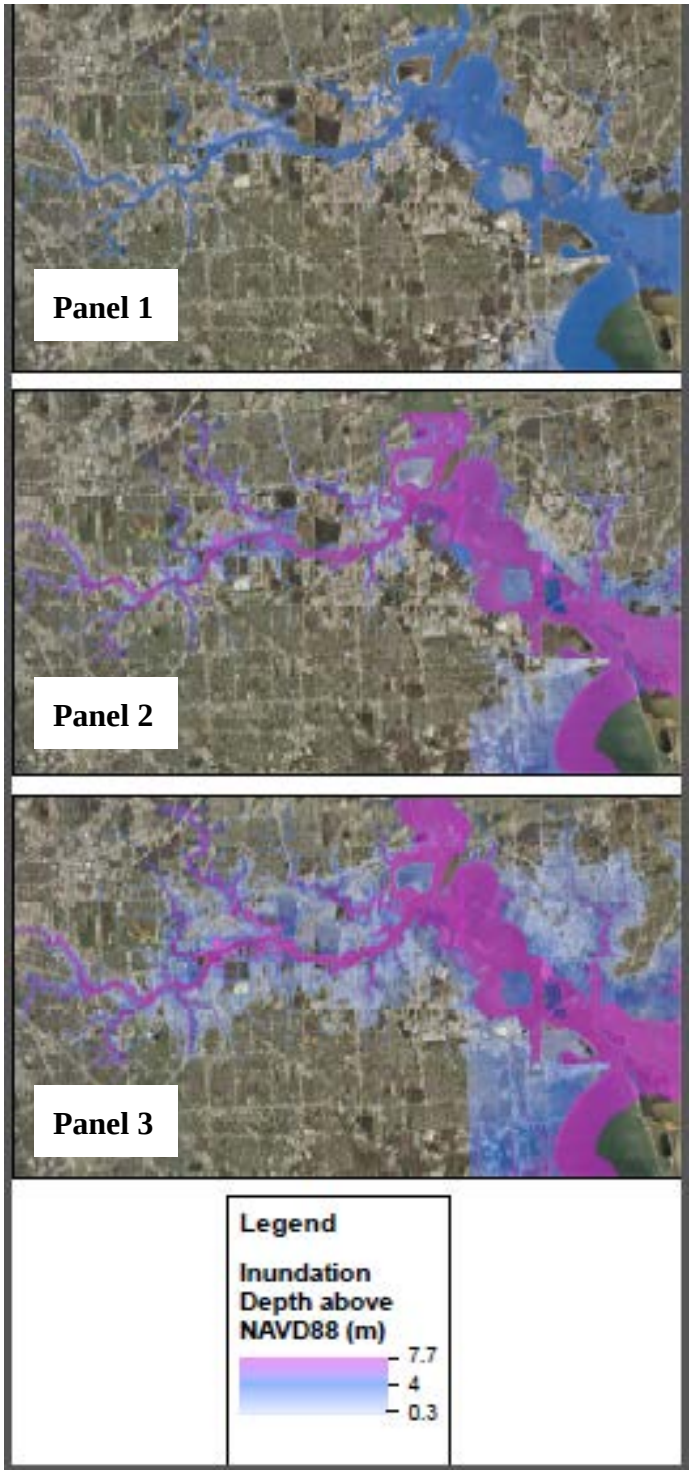

Figure 3-3. Depth of inundation (m) at maximum storm surge for the three runs of interest Hurricane Ike (panel 1), Hurricane Ike at point 7 (panel 2), and Hurricane Ike at point 7 with 30% increased winds (panel 3).

Industrial Facility Data. Industrial facility information was obtained from EPA's EnviroFacts database (http://www.epa.gov/enviro/) and Harris County Appraisal District (HCAD) data. While EnviroFacts provides facility information and latitudes and longitudes from the Facility Registry System (FRS), it does not document facility boundaries. These were developed by spatially linking latitude and longitude data from the Envirofacts database to parcel boundaries from HCAD data. The parcels associated with each facility were tagged and used to develop the property boundary for each facility within the HVGDB.

Above Ground Storage Tanks (ASTs). Tank locations were determined using visual inspection of aerial photography. Within the study area, 1-ft by 1-ft aerial photography from the Houston-Galveston Area Council (HGAC) database from 2008 (http://www.h-gac.com/rds/gis_data/default.aspx) were used to identify locations of ASTs; a spatial point was then placed in the center of the tank within the HVGDB. Tank elevations were determined using the LIDAR data.

Toxic Release Inventory (TRI). Past toxic releases from facilities along the HSC-IC were downloaded from EPA's EnviroFacts database (http://www.epa.gov/enviro/); data for facility ownership, past release yearly totals, and chemicals released to water bodies were assimilated. These data, as will be seen subsequently in this thesis, were used to select facilities with a greater potential for releases based on their historical records.

Risk Management Plans (RMPs). Data from RMPs submitted to EPA were collected from the Right to Know Network (rtknet.org, Accessed: 08/2011) database. The data included basic facility information, process toxic chemical amounts, past accidents, and prevention plans. Other sources of information such as Tier II submittals

(http://www.epa.gov/oem/content/epcra/tier2.htm, Tier II are chemical inventory reports that are submitted to local emergency managers/responders) were also consulted but were deemed to overlap with the information in RMPs and thus were not used. Information regarding prevention plans and past accident histories lacked necessary details in order to be included in this assessment; therefore, the key data extracted from the RMPs were the process toxic chemical amounts (kg).

Data from the developed HVGDB, joined with the SWAN+ADCIRC modeling results, were analyzed to develop geospatial and environmental vulnerabilities for the HSC-IC as described below.

3.2.2 GEOSPATIAL VULNERABILITY

Geospatial vulnerability in this research refers to the potential for inundation from storm surge based on ground elevation. Inundated land was defined as any land with elevation that falls below the predicated storm surge height. As mentioned previously, and from a flooding perspective, Hurricane Ike was equivalent to a 100-yr flood event. Thus, the existing 100-yr FEMA floodplain areas were first identified since these areas would not be considered geospatially vulnerable to storm surge below the 100-yr level in the Hurricane Ike scenario. Storm surge inundation for the modeled Ike scenario was compared to the 100-yr FEMA floodplain, areas not in the 100-yr FEMA floodplain were then identified, and their geospatial vulnerability was delineated.

The initial findings confirm conclusions by Brody et al. (2012) that the 100-yr FEMA floodplain boundary is not sufficient for representing actual economic losses during a flood. Since the analysis of this thesis evaluates specific events without a

probability of occurrence, the results cannot be directly correlated to the FEMA 100-yr floodplain. Rather, the purpose of the geospatial analysis is to identify inundated areas by storm surge that are not within the FEMA 100-yr floodplain and to illustrate the potential for inundation of areas outside the 100-yr floodplain for storm surge levels that are commensurate with the 100-yr flood elevation. The FEMA 100-yr floodplain provides a protection level for facilities within the HSC-IC. Identifying regions that are inundated outside the standard protection is a necessary and important component to the overall vulnerability analysis for the HSC-IC. Similarly, land areas within the 100-yr FEMA floodplain that were not inundated during Hurricane Ike were also delineated and removed from the geospatial vulnerability analysis. The total area (km^2) of inundated land for each modeled scenario was calculated to determine the relationship between surge level (observed for each scenario) and geospatial vulnerability.

In addition, the geospatial vulnerability of individual facilities along the HSC-IC was quantified. Facilities with less than 40% inundation were delineated. For the purposes of this framework, facilities with greater than 40% inundation were identified as candidates for total loss and failure, and consequently high geospatial vulnerability.

3.3 ENVIRONMENTAL VULNERABILITY

Environmental vulnerability is defined as the potential for releases to the environment due to inundation as discussed previously which includes: (1) potential releases from inundated aboveground storage tanks, (2) potential releases of chemicals to the environment based on previous history of releases, and (3) potential releases of chemicals to the environment based on stored volumes of toxic chemicals. Two aspects should be noted regarding environmental vulnerability as defined in this research. First,

the quantity of stored chemicals is a surrogate indicator for environmental damage under storm surge. Second, inundation (geospatial vulnerability) is used to delineate impacted ASTs and the inundated ASTs are used as a surrogate for potential chemical releases to the environment as described below in more detail.

Releases from ASTs. In this research, the potential for releases from ASTs was determined by identifying the number of tanks that would be inundated for each modeled scenario. Since ASTs are typically surrounded by berms with berm elevation set at the 100-yr FEMA floodplain, the analysis included affected tanks that were outside the 100-yr FEMA floodplain level.

Other Toxic Releases. It was assumed that facilities with a history of releases to the water environment had a higher vulnerability for releases under storm surge. A given facility's historical annual amount released to the water environment over the past decade was calculated from the TRI data. It was assumed that the top 25% of facilities based on released volumes are the most vulnerable to releases during a hurricane. The facilities from the top 25% list within the modeled surge level were identified and their potential for pollutant releases was estimated based on their historical records and their relative inundation for the specific hurricane scenario. Facilities with greater than 450 million kg of chemicals released into the water environment were identified as having high environmental vulnerability (potential for release). In order to account for facilities with high geospatial vulnerability based on areal inundation and the potential for releases from such facilities (independent of ASTs), their inundation was factored in as the second aspect of environmental vulnerability.

Risk Management Plans. The RMP database was initially used to identify industrial facilities that had prevention plans in place to handle large amounts of hazardous materials. Of the total number of facilities in the study area, less than 10% had RMPs indicating a serious deficiency and signaling additional vulnerability in the HSC-IC. Due to this relatively low number of RMPs, they were not incorporated in the framework. The analysis focused on accounting for vulnerability using a similar approach to the one used in the AST analysis (i.e. determining which facilities with RMPs had greater than 40% inundation and were in the top 25% of facilities in terms of the amounts of toxic process chemicals).

3.4 VULNERABILITY ASSESSMENT RESULTS

This section will present the results from the vulnerability framework described above as it was applied to the Houston Ship Channel using the modeled SWAN-ADCIRC landfall and wind velocity scenarios.

3.4.1 GEOSPATIAL VULNERABILITY RESULTS

Figure 3-4 shows the inundated areas outside the 100-yr FEMA floodplain from Hurricane Ike, Hurricane Ike at Point 7, and Hurricane Ike at Point 7 with 30% increase in wind speed. A significant inundation area occurs at the mouth of the HSC-IC in the southeast corner of the study area. Figure 3-5 presents the developed correlation between the total inundated area and surge height. The storm surge values in the figure are based on the average storm surge observed in the HSC-IC (within the HSC-IC there is little observed variability in storm surge height from the model results, on the order of +/- 0.2

m). The figure demonstrates that the area of inundation increasing exponentially with increases surge level described mathematically using Equation (1),

$$Area\ Inundated\ Outside\ Floodplain\ = 2.0162e^{0.5939(Surge\ Height)}, \quad (1)$$

where Area is given in km^2 and Surge Height is given in meters.

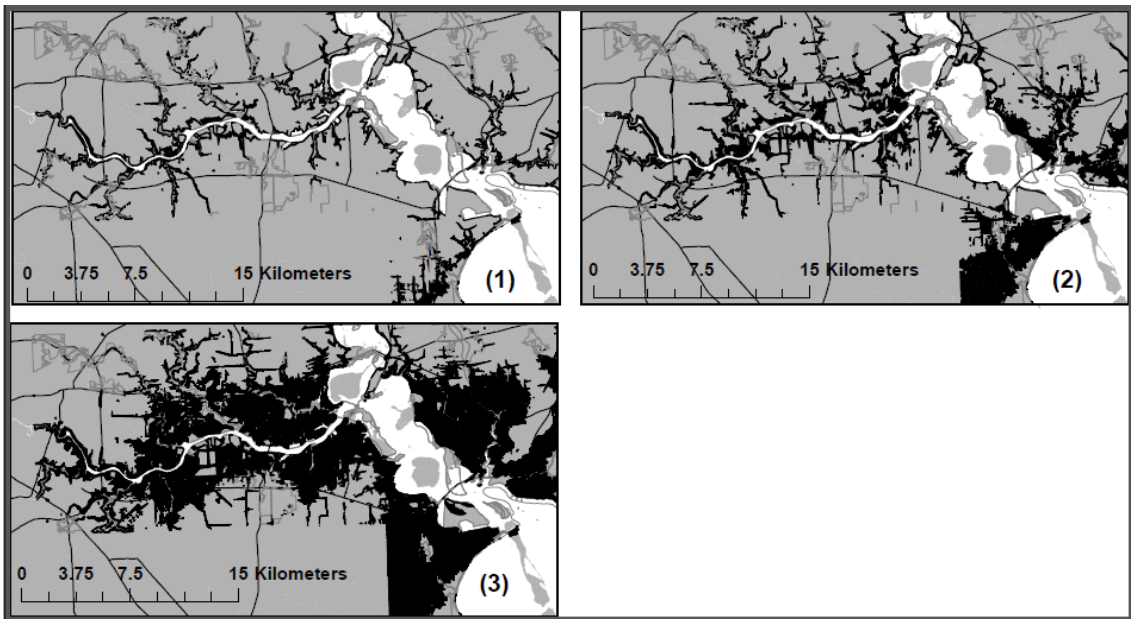

Figure 3-4. SWAN+ADCIRC modeled storm surge inundation outside the 100-yr floodplain (black region) for Hurricane Ike (1), Hurricane Ike at Point 7 (2) and Hurricane Ike at Point 7 with 30% higher wind speed (3).

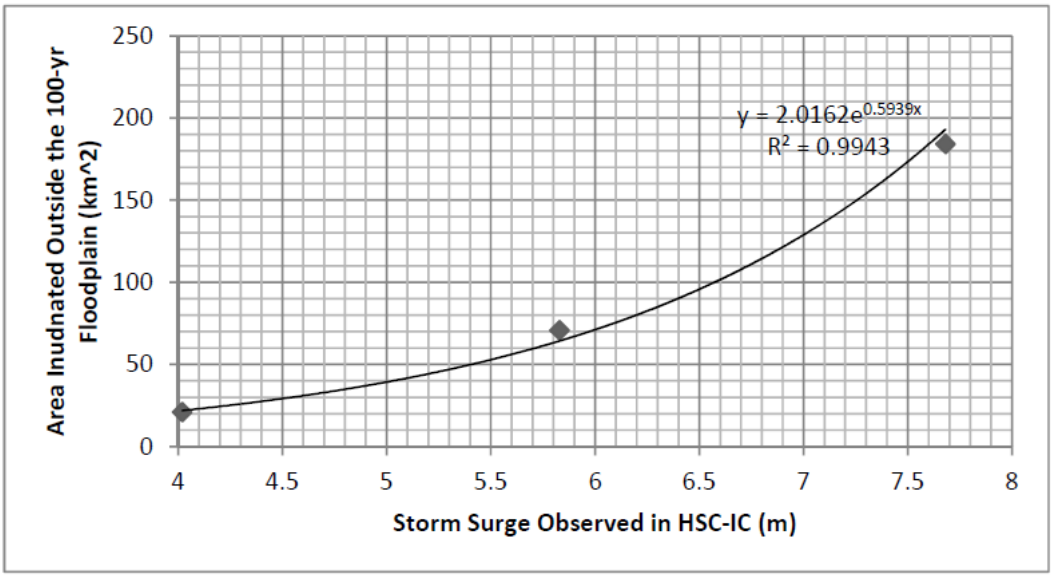

Figure 3-5. Correlation between inundated areas (outside of the 100-yr FEMA floodplain) and the modeled storm surge levels for the various hurricane scenarios

3.4.2 ENVIRONMENTAL VULNERABILITY RESULTS

Releases from ASTs. Figure 3-6 illustrates tank inundation for the modeled storm surge scenarios. The three panels in the figure represent the three modeled storm surge events with a dot representing an inundated tank. The number of impacted tanks increases significantly with an increase in severity of the storm surge for the region and summarized in Table 3-1. Almost four times the number of tanks are inundated when Ike is moved to point 7 and winds are increased by 30%. Similar to land inundation outside the FEMA 100-yr floodplain, as the storm surge in the region increases, the number of inundated tanks increases exponentially; this relationship (shown in Figure 3-7) can be represented mathematically using Equation (2),

$$Number\ of\ Inundated\ Tanks\ = 89.165e^{0.4716(Surge\ Height)}\ , \qquad (2)$$

where Surge Height is in meters.

Other Toxic Releases. The facilities with greater than 1 billion pounds of released chemicals to the water environment annually that fell in the top 25% of facilities historically reporting releases in the HSC-IC are identified in panel 1 of Figure 3-8 (27 total facilities). Panel 2 and Panel 3 of the figure combine the historical release information and modeled inundation by showing facilities having high tonnage of releases to the water environment and high geospatial vulnerability (greater than 40% inundation) for Hurricane Ike at Point 7 and Hurricane Ike at Point 7 with a 30% increase in wind speed, respectively. Facilities filled in black are vulnerable to toxic release. For the Hurricane Ike scenario, no facilities were deemed vulnerable to toxic releases (true in reality during Ike) and only two vulnerable facilities were identified when Ike was moved to Point 7. However, a storm surge of over 7 m produced by increasing winds by 30% for Ike at Point 7 showed significant number of facilities vulnerable to toxic release shown in Panel 3 of the figure. The number of vulnerable facilities for each scenario is shown in Table 3-1.

Risk Management Planning. Table 3-1 presents the number of RMP reporting facilities that had greater than 40% inundation for each of the modeled hurricane scenarios. Facilities with greater than 94 kg of stored chemicals (top 25% among HSC-IC RMP reporting facilities) were assumed to be the greatest threats to the environment. A total of 25 facilities fell into this category and these facilities are shown in Panel 1 of Figure 3-9. Similar to the analysis used for the toxic release facilities identified through the TRI database, Panel 2 and Panel 3 of the figure combine this environmental threat based on the RMP reported toxic process chemical amount with the facilities having high

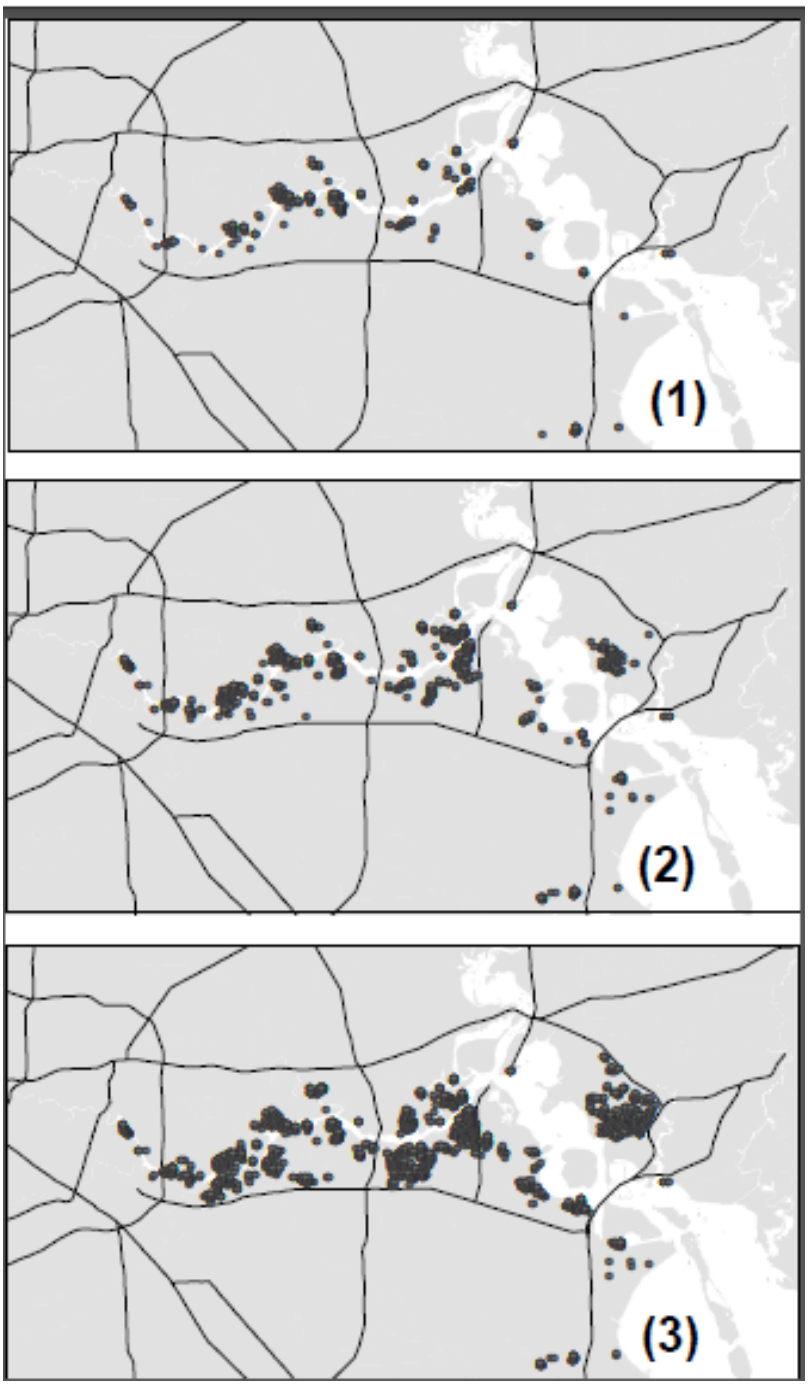

Figure 3-6. Inundated tanks for the modeled scenarios represented by each dot for Hurricane Ike (panel 1), Hurricane Ike at Point 7 (panel 2), and Hurricane Ike at Point 7 with 30% increase in wind speed (panel 3).

Table 3-1. Summary of geospatial and environmental vulnerability of facilities along the HSC-IC

		TRI Facilities with History of Release		**RMP Reporting Facilities**	
Hurricane Scenarios	Number of Tanks Inundated	Greater than 40% Inundation	High Geospatial and Environmental Vulnerability	Greater than 40% Inundation	High Geospatial and Environmental Vulnerability
Hurricane Ike	579	36	-	47	-
Hurricane Ike at Point 7	1464	88	2	57	12
Hurricane Ike at Point 7 with 30% increase in wind speed	3256	182	21	67	20

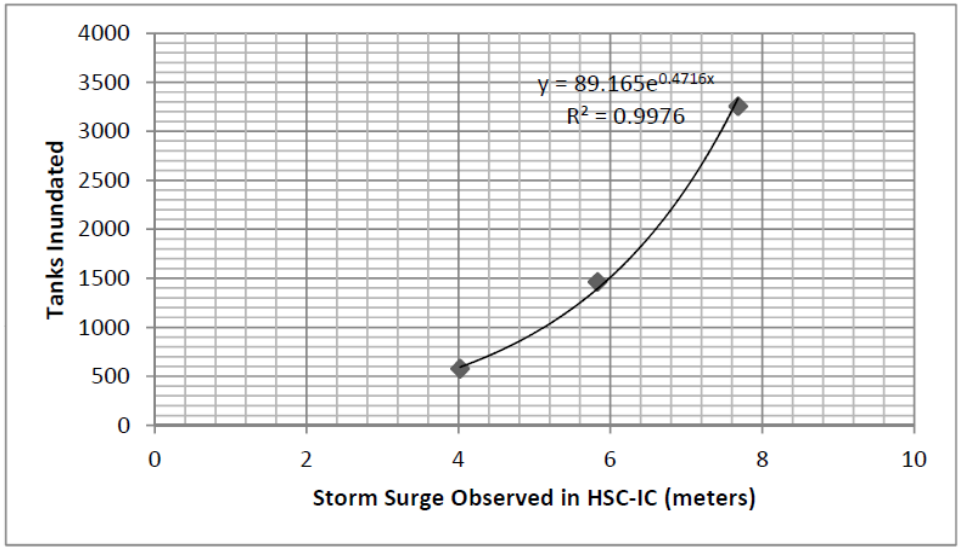

Figure 3-7. Correlation between the number of inundated tanks and storm surge levels in the HSC-IC.

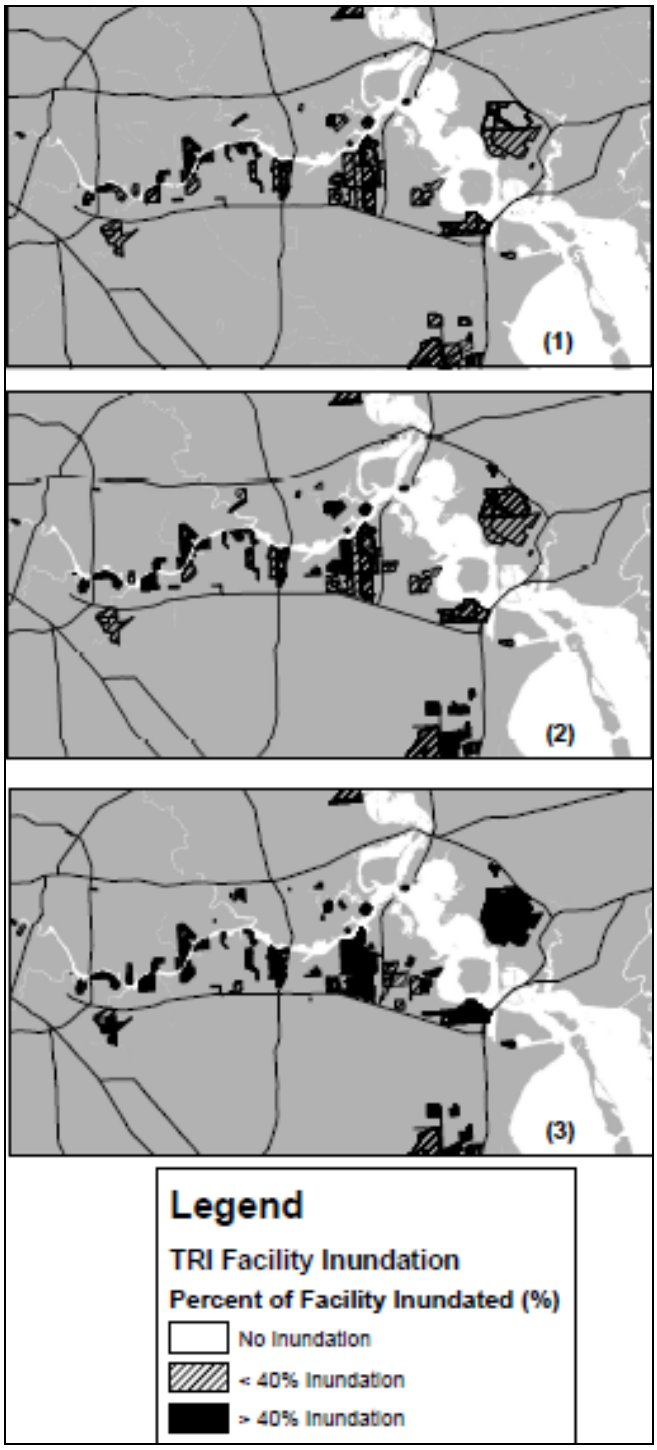

Figure 3-8. Facilities with high environmental vulnerability and high geospatial vulnerability from storm surge Inundation (black) for Ike (1), Ike at point 7 (2), and Ike at point 7 with 30% increase in wind speed (3).

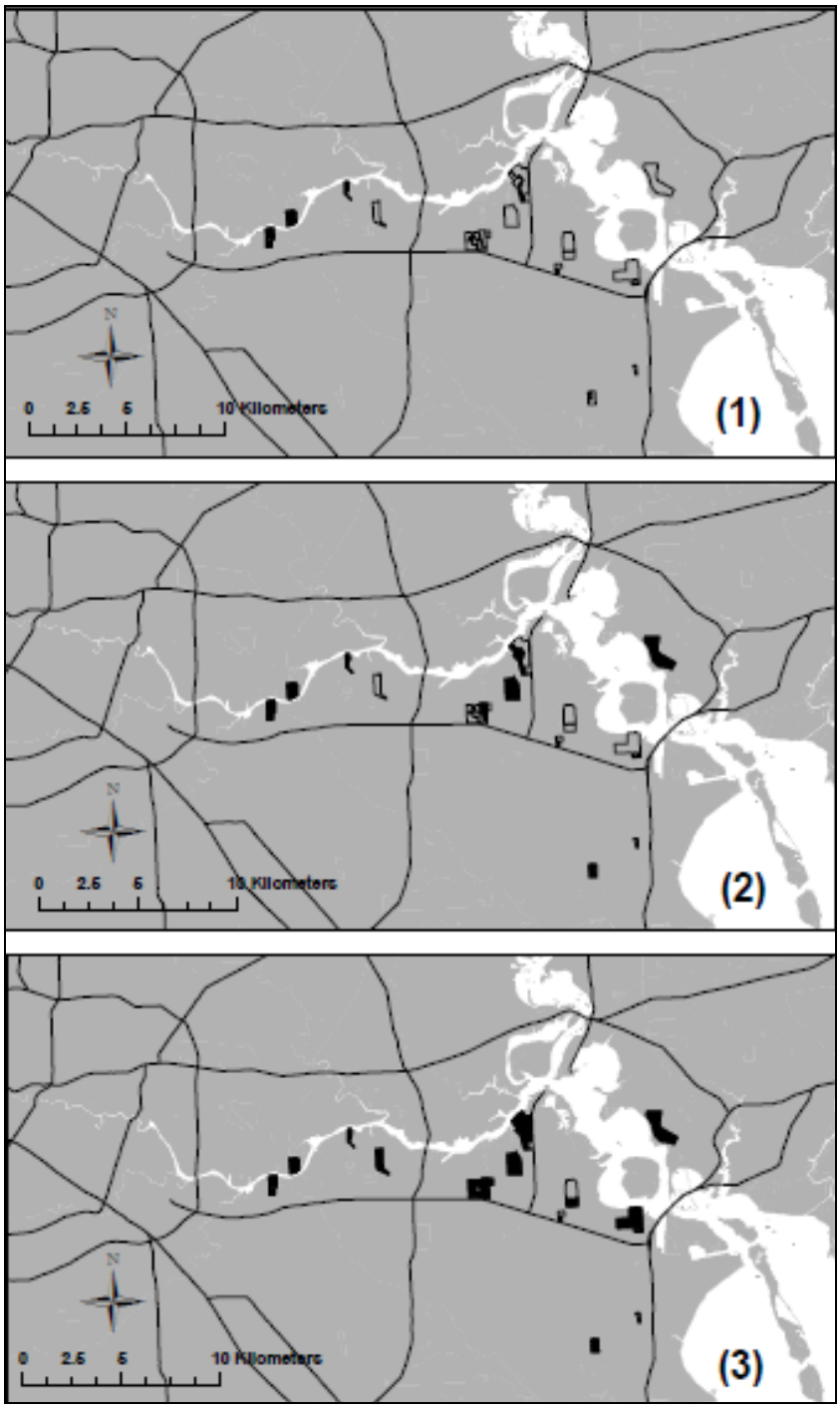

Figure 3-9. RMP facilities with high stored toxic volumes and high geospatial vulnerability due to storm surge inundation (black) for Ike (1), Ike at point 7 (2) and for Ike at point 7 with 30% increase in wind speed (3).

geospatial vulnerability (shaded in black). Confirming the reality of the Hurricane Ike, no facilities were deemed threats to the environment under the Ike scenario. Panel 2 of the figure presents a large number (12) of vulnerable facilities compared to the two facilities identified under this same scenario for the TRI facilities. In addition, Panel 3 of the figure and the data in Table 3-1 indicate that 20 facilities were vulnerable during Ike at point 7 with increased wind speed.

3.4.3 DISCUSSION

The geospatial and environmental vulnerability framework developed in this thesis illustrates the potential relationships between storm surge levels, inundation of areas outside the FEMA 100-yr floodplain, the potential for tank inundation, and the potential for releases at facilities with relatively large volumes of stored chemicals and/or RMP facilities that would experience more than 40% inundation for various storm surge levels. The aforementioned analysis was intended to highlight potential vulnerabilities of industrialized regions to storm surge. It is important to note the non-linear nature of the relationship between storm surge and its potential impacts; such a relationship will be important for decision-making at the facility as well as regionally.

While the main purpose of the innovative framework presented in this chapter is to evaluate vulnerability from a geospatial and environmental perspective, the human vulnerability, evaluated extensively as it directly relates to hurricanes and flooding (Chakraborty et al., 2005), can be readily incorporated. For example, census block data for the US Census of 2010 for the region surrounding the HSC-IC were incorporated into the evaluation of the results.

There are 489,089 people within the study area based on the 2010 US Census. More than half of those in the study area (274,262 people) are in the census blocks inundated from Ike at point 7 with 30% increase in winds. A detailed evaluation of census blocks directly affected by the facilities with high geospatial and environmental vulnerability shows that 18,461 persons would be potentially impacted (3.7% of the population for the study area). These census blocks represent the potential indirect human impact from releases of hazardous material because of inundation of tanks within these facilities. Studies have connected environmental risk and vulnerability to human health for industries (Topuz et al., 2011) and accidental spills (Cutter et al., 2003; Sengul et al., 2012; Bonvicini et al., 2014). However, natural hazards research has yet to incorporate this understanding to the vulnerability of facility failures in an extreme storm surge event. While more detailed population data would be required to make appropriate conclusions about facility impact on the surrounding human life, these details emphasize the need for a vulnerability analysis that incorporates the industrial characteristics of a region as is done here.

CHAPTER 4. A GIS FRAMEWORK AND TOOLBOX FOR MODELING INDUSTRIAL FACILITY DAMAGE AND ECONOMIC LOSSES DUE TO STORM SURGE

A GIS framework and toolbox containing built-in ArcGIS commands was developed to model industrial facility damage and economic loss due to storm surge named Facility Economic Damage and Environmental Release Planning (FEDERAP). Burleson et al. (2015b) describes FEDERAP in detail; their work is briefly incorporated here for completeness. In essence, FEDERAP addresses the gaps in damage and economic loss forecasting for industrial facilities and contains a GIS toolbox, economic loss algorithms, and an Excel-based spreadsheet model. Together, the framework, the tools in FEDERAP, and the spreadsheet model provide detailed qualitative and quantitative analyses of storm surge impacts for a specific facility. The result is an estimation of associated losses from direct impact but does not account for secondary impacts that tend to spread. The GIS toolbox is used to develop spatial analysis data for various storm surge levels for a given facility (for example, to determine areas within an industrial facility that are inundated at a given storm surge level). The Excel spreadsheet model allows the user to compile the spatial data from the GIS toolbox and use the information in conjunction with economic loss algorithms defined by the user in order to predict losses for a given storm surge level at a specific facility. The toolbox and Excel spreadsheet include a user interface with input screens designed to prompt the user to enter the required variables for the analysis.

4.1 FEDERAP SPATIAL ANALYSIS TOOLBOX

The FEDERAP framework requires a spatial analysis to determine the extent of inundation of a given facility, its unit-processes, and storage tanks for a given storm surge depth. In this research, ArcGIS spatial analysis capabilities were used to develop a FEDERAP toolbox using a combination of built-in ArcGIS commands with the Model Builder framework capability. The data sources for the inputs to FEDERAP vary depending on the region of interest; the current list of variables used in FEDERAP and their sources is defined below.

Facility boundary. Within FEDERAP, facility boundaries were derived from parcel boundaries and ownership information resulting in a polygon shapefile for ArcGIS. The facility boundary is accurately represented through a combination of multiple parcels. The facility boundary was derived from detailed parcel data acquired by the Harris County Appraisal District (HCAD) and verified with 1-ft by 1-ft aerial photography from the Houston-Galveston Area Council (HGAC) GIS database from 2006 (http://www.h-gac.com/rds/gis_data/default.aspx).

Storm surge levels of interest. The user specifies the minimum and maximum value for storm surge to be used in the analysis. The model loops over the storm surge range using a step of one unit. For example, for a minimum storm surge of 10 and a maximum of 15, storm surge levels of 10, 11, 12, 13, 14, and 15 would be evaluated within the toolbox (6 loops). The storm surge duration is not considered in the FEDERAP framework.

Unit-processes. A unit-process is the region within the facility where chemical or oil refining occurs and/or is processed. A polygon shapefile defining each unit-process is

used for this input. A single object is used to represent a single unit-process to allow estimating the total percent inundation for each individual unit-process. Unit-process data was obtained from detailed aerial photography of the region (HGAC 2008) and the shape of the object in the input file reflects the size and shape of the unit-process.

Storage Tanks. Storage tanks are used in industrial facilities to store feedstock and product. A unique polygon shapefile is used for each tank type in FEDERAP: horizontal, fixed-top vertical, and floating-top vertical tanks (illustrated in Figure 4-1). The tank locations are derived from detailed aerial photography of the region (HGAC 2008) and the shape of the object in the input file reflects the shape of the tank (circular for vertical tanks and oval for horizontal tanks).

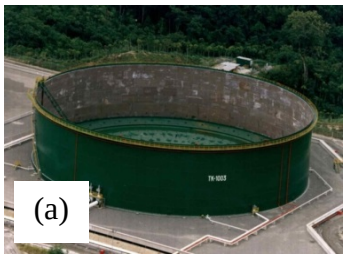

(http://www.inspection-for-industry.com/images/fix-roof.jpg)

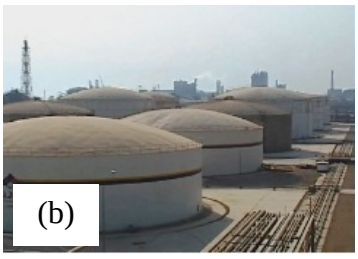

(http://i00.i.aliimg.com/img/pb/541/642/407/407642541_924.jpg)

(http://www.cmpea.fr/wp-content/uploads/2013/12/Equateur.jpg)

Figure 4-1. Examples of tank types applied in FEDERAP (a) Floating-top Vertical Tank (b) Fixed-top Vertical Tank (c) Horizontal Tank

Elevation for Region. The elevation for the region input is a point file with elevation locations throughout the region in which the facility is located. Typically, elevation data are available as a raster or point shapefile for large areas (TSARP 2005). The FEDERAP toolbox includes commands to extract the elevation for the facility within its specified boundaries. Within ArcGIS, a point to raster conversion is utilized based on least squares to provide a surface map for the facility.

The FEDERAP toolbox uses built-in ArcGIS commands and the aforementioned inputs to evaluate the inundation at each storm surge level of the facility itself, its tanks, and processing units. The uniqueness of FEDERAP does not relate to the addition of new commands but the combination of existing built-in commands to address the problem at hand. Built-in tools such as *Clip*, *Select by Location*, and raster conversion are used in an intentional order to accurately evaluate the inundation of the facility infrastructure. The result is several geodatabases of shapefiles and statistics that represent inundation at multiple storm surge levels as shown in Figure 4-2. The first seven geodatabases shown in Figure 4-2 contain the inundation results for facility elevations, unit-processes, and storage tanks. Data tables are stored within *Statistics.gbd*, the last geodatabase shown in Figure 4-2; these tables contain facility inundation area, unit-processes inundation percent, and counts for each of the tank types inundated under each storm surge level evaluated. This information is compiled using built-in count and ArcGIS field calculators from the spatial results of the other seven geodatabases. The results are exported into a tabular format that the user can then manually move to the FEDERAP Excel Analysis.

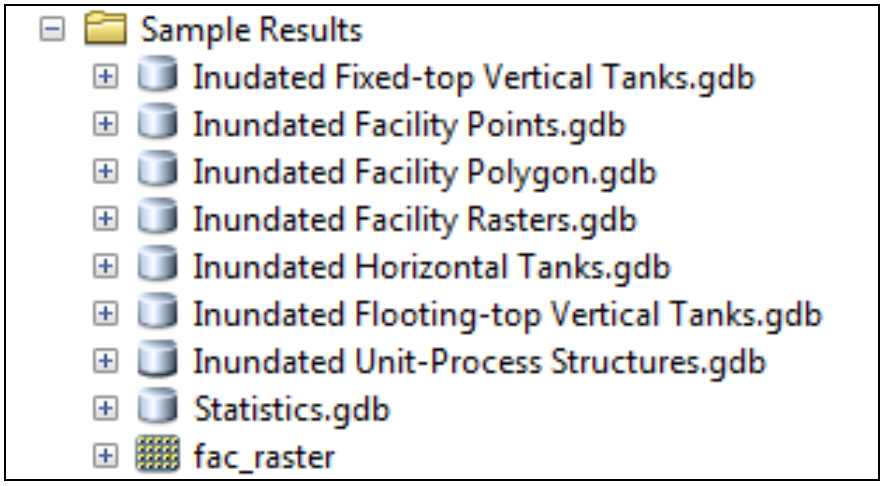

Figure 4-2. Geodatabase Results from FEDERAP ArcGIS Toolbox

4.2 FEDERAP MODELING FRAMEWORK

The FEDERAP modeling is categorized into four major components shown in Figure 4-3: (1) facility inundation loss, (2) unit-process loss, (3) environmental release loss, and (4) productivity loss. Each of these components is a function of inundation caused by the storm surge level and is associated with models of economic losses as will be described in detail below. This framework incorporates aspects of downtime, production, and potential cleanup costs that have not been addressed in prior studies in the literature. As can be seen from Figure 4-3, FEDERAP is well suited for decision-making at the facility level and more broadly, for an entire industrial region because it incorporates detailed spatial data of facility layout, topography, infrastructure, and inundation due to storm surge.

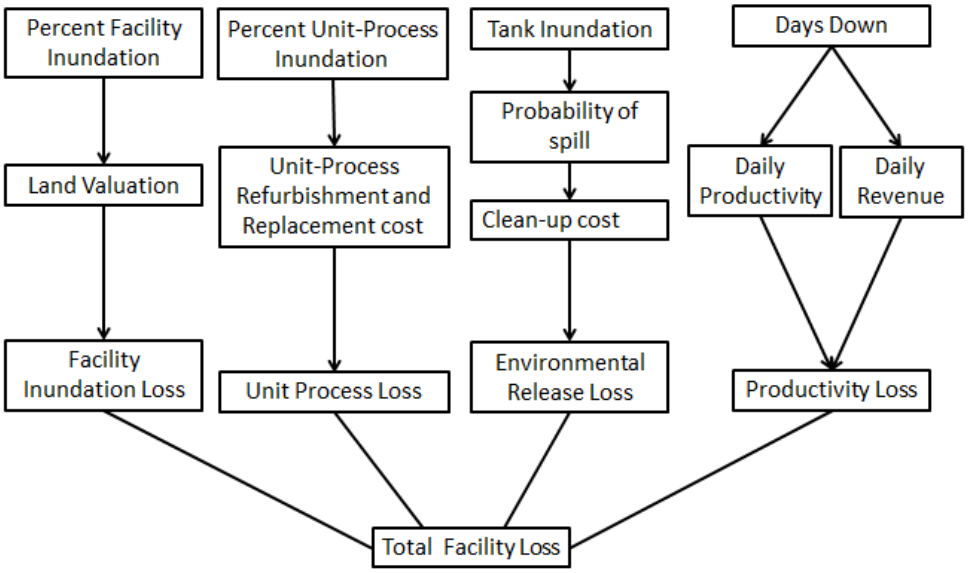

Figure 4-3. The FEDERAP modeling framework is categorized into four major components: (1) facility inundation loss, (2) unit-process loss, (3) environmental release loss, and (4) productivity loss.

4.2.1 CATEGORY 1: FACILITY LOSS

Storm surge height and the associated facility inundation is a key driver in FEDERAP and the basis of many of the developed models and regression equations. Land value is based on the property-appraised value of the land parcels for the facility from tax assessor publically available databases. Losses in facility value are modeled based on the percent of the facility that is under water for a given storm surge as shown in Table 4-1 Land value losses range from 0-100% based on a facility inundation that ranges from 0-75%; at 10% inundation, it is assumed that the land loses 25% of its value. The property value goes down by 75% at 50% inundation. The land value loss ranges were determined based on previous hazard model (Vickery et al., 2006; Vickery et al., 2006) as well as personal communication with facility managers and emergency personnel. Property value losses are not interpolated in between inundation levels. Instead, the relationship for loss is applied in a stepwise fashion until the next level is met or exceeded. Thus, between 10 and 50% inundation, a given facility would still accrue a property value loss of 25%. The modeled relationship in Table 4-1 is one of the input regression expressions in FEDERAP that can be altered by the user for their specific study. The effect of this variable on the modeled results is addressed in the sensitivity section of the thesis (Section 4.7).

Table 4-1. Land value Loss as a function of facility inundation

Facility Inundation (Percent)	**Land Value Loss (Percent of land value)**
0%	0%
10%	25%
25%	50%
50%	75%
75%	100%

4.2.2 CATEGORY 2 - INDUSTRIAL UNIT-PROCESS LOSS

Each unit-process at an industrial facility in FEDERAP has a value to the overall production of the facility in addition to the intrinsic value of the structure itself. For each unit-process, a cost of refurbishment or replacement is calculated based on the inundation percentage using the relationship shown in Table 4-2. As can be seen in the table, for 20% inundation of the unit process, refurbishment is modeled using a cost basis of $1 million dollars. However, when the unit experiences 50% inundation, a total loss is modeled using a cost basis of $10 million. While recent reports have estimated costs for construction of process-units at approximately $340 million with refurbishment estimated at $60 million (Eggleston, 2014), conservative estimates are used in the illustrative calculations used in the thesis. Here again, as in the previous category of facility losses, the condition applied to each unit-process is maintained until the next inundation level is met or exceeded. Therefore, unit-processes with inundation between 20% and 49% would fall under the refurbishment condition. As before, the cost relationships are readily modifiable by users and the model sensitivity to these cost valuations is described in Section 4.7.

Table 4-2. Unit processes inundation loss relationship

Percent Inundation of Unit Process (%)	**Description**	**Unit Damage ($)**
20%	Refurbishment Required	1,000,000
50%	Complete Loss	10,000,000

4.2.3 CATEGORY 3 - ENVIRONMENTAL RELEASE LOSS

Under surge conditions, storage tanks may fail. Tank failure is defined as a structural failure resulting in the release of tank contents of the tank into the environment.

Failure can be attributed to displacement of the tank via uplift from buoyant forces or buckling due to loss of tank integrity because of the surrounding static and dynamic water pressures.

The environmental losses modeled in FEDERAP are based on an estimate of the number of tanks that would be inundated for a specific storm surge level. A tank is designated as inundated if the elevation of the bottom of the tank is below the storm surge level. It is, however, unlikely that all inundated tanks would experience failure, thus a certain percentage of inundated tanks are modeled to fail. In this research, the percent of tanks that experience failure when inundated ranges from 20 – 50% depending on the type of tank (see Table 4-3). These modeled percentages are also a model variable that can be refined given specific data on tank structural integrity. The percent of total tanks inundated for each storm surge level is applied to the total stored product for the facility to determine the potential spill quantity. The cleanup cost is calculated as $31 per liter released during a spill (Etkin, 2000). The approximate cost is based on a spill in a port region (such as the Port of Houston) but can be changed to reflect different conditions in other regions.

Table 4-3. Storage tank types and modeled failure under surge

Tank Type	**Percent Failure for Inundated Tanks**
Fixed Top Vertical Tank	20%
Floating Top Vertical Tank	50%
Horizontal Tank	30%

The total environmental cost is the sum of the loss associated with cleanup of the spilled volume and an estimated cost for replacing the tank structure itself. For example, a facility having 10 fixed top vertical tanks that are inundated at a certain storm surge

level with a total volume of stored product of 500 gallons would experience a loss of 20% of the product or 100 gallons (i.e., 300 liters with an associated cleanup cost of 300 liters x $31/liter or $9,300). In this case, two tanks would fail and assuming a replacement cost of $1,000 per tank, the structural cost would be $2,000 yielding a total environmental cost of approximately $11,300 for the facility at the 20 ft surge level. This approach to modeling environmental losses is overly simplistic. Product release into waterways may also cause other damages such as to natural resources. Thus, and as will be seen later in the thesis, a more detailed treatment of environmental impacts of surge is presented using a water quality estuarine model (EFDC-SS) for pollutant fate and transport using a conservative dye.

4.2.4 CATEGORY 4 - PRODUCTIVITY LOSS

Productivity loss is defined as the loss resulting from a disruption of normal business operations. In FEDERAP, this is modeled using the number of days that the facility is not operational (also referred to as downtime) in addition to the loss of physical product (e.g., refined gasoline). The downtime is modeled using three key variables: (1) the percent inundation of the facility, (2) unit-process inundation, and (3) the volume of released product. The modeled relationship between the percent inundation of the facility and days down is shown in Table 4-4; for 75% inundation, for instance, 56 days of inactivity are projected. However, and as can be seen in Table 4, 20% inundation of process units will add 7 days to the 56 days and a release of 20 million gallons of product will add another 14 days down for a total of 77 days (56+7+14) of inactivity. The relationships shown in Table 4-4 were developed based on personal communications with

facility and emergency management personnel in Texas and can be customized for other regions.

The downtime loss is then estimated based on the number of days down and the daily revenue of the facility. Thus, for a facility that has daily revenue of $300K and using the 77 days down in the example above, the total downtime loss will be about $23.1 million.

Table 4-4. Modeled relationship between non-operational days and percent inundation of facilities

Facility Inundation	
Inundation Percent	**Days Down**
0	7
20	14
50	28
75	56
Unit-Processes Inundation	
Units Inundation Percent	**Additional Days Down**
0	0
20	7
50	14
75	21
Environmental Cleanup	
Volume of Release (in gallons)	**Additional Days Down**
0	0
10 million	7
20 million	14
30 million	21

Also included in the productivity loss is the cost associated with loss of production. Continuing the example in this section, based on an estimated 10,000 barrels of daily oil production at the facility with a cost of $100 per barrel, a total production loss of $1 million is accrued per day during the 77 days of downtime ($77 million for

production loss). The total productivity loss for the example is $100.1 million, the sum of the production loss of $77 million and the downtime loss of $23.1 million.

4.3 FEDERAP SPREADSHEET MODELING ANALYSIS

The statistic outputs from FEDERAP, described previously in the thesis in Section 4.1, are exported into a tabular format and used in conjunction with the damage relationships discussed in the previous section within an Excel Spreadsheet that is specifically designed to estimate the total damages for a given facility. The Excel model has seven sheets (see Table 4-5). The first sheet requires the user-inputs for general information about the facility including total land area, number of unit-processes, daily revenue and production.

The next four sheets determine the results for each of the four categories of losses in the FEDERAP framework. These sheets require the output statistics from the statistics geodatabase discussed previously (see Figure 4-3: *Statistics.gbd*). The losses are calculated for each category within the appropriate sheet in the Excel model. It is also here that users can modify the cost modeling relationships and customize them for their specific application.

The outputs from the FEDERAP Excel analysis are presented in the final two sheets shown in Table 4-5. For each storm surge level, the loss for each category and the total loss are both shown in tabular form as are loss curves showing the total loss and contribution from each of the four categories. Examples of the output are presented in the following sections that detail the FEDERAP calibration and expansion to a regression model with model validation.

Table 4-5. FEDERAP Excel sheets

Sheet name	Inputs	Outputs
Cover Page- Facility Information	Total number of unit-processes, tanks, daily revenue, property value, production, and total area (user-defined)	None
Facility Inundation	Total area inundated (*Statistics.gbd*)	Facility Land Damage ($)
Unit-Process Loss	Total number of facilities inundated of 20% and 50% (*Statistics.gbd*)	Unit-Process Damage ($)
Environmental Releases Loss	Total number of tanks inundated (*Statistics.gbd*)	Environmental Clean-up Damage ($)
Productivity Loss	None	Daily Revenue Loss, Production Loss, Total Productivity Loss
Facility Loss Summary Table	None	Summary of all the above outputs
Facility Loss Summary Graphs	None	Loss curves for each category and the total loss for the facility

4.4 FEDERAP CALIBRATION

Nine facilities in the HSC were modeled using FEDERAP for calibration. These facilities are identified as Facility 1 thru 9 going from left to right in Figure 4-4. Based on work presented in Chapter 3 of the thesis, the HSC could experience storm surge levels as high as 25 ft under a worst-case scenario involving an Ike landfall 100 miles to the southwest of the original landfall location and winds increased by 30% (Sebastian et al. 2014; Burleson et al. 2015a). Since significant facility inundation does not occur in this region until beyond the equivalent 100-yr floodplain event, the calibration of FEDERAP is run for storm surge levels between 15 and 25 ft.

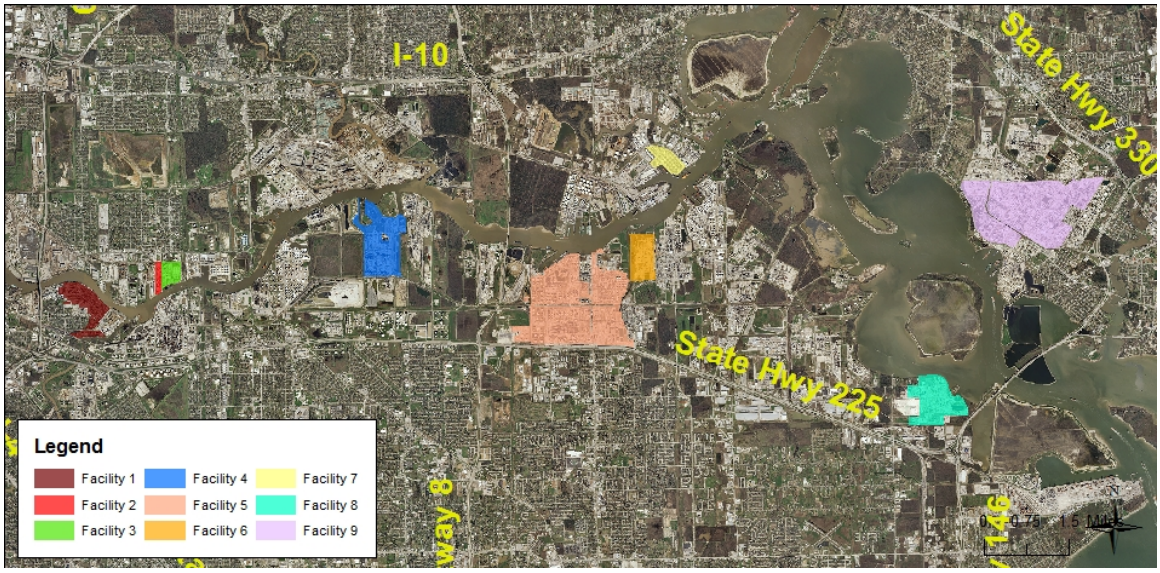

Figure 4-4. Facilities locations along the HSC used for calibration of FEDERAP

4.4.1 DESCRIPTION OF MODELED FACILITIES

Over 200 facilities in the HSC-IC produce chemicals, petrochemicals, and petroleum products; most have multiple production units and storage tanks as part of their infrastructure. Many of the industrial facilities bordering the channel are permitted for industrial discharge of treated effluents and runoff into the HSC.

Facility elevations within the HSC range from 1.5 to over 30 ft. Figure 4-5 shows the average elevation in the HSC, and as can be seen, many of the facilities are below 25 ft and would be expected to experience various degrees of inundation from storm surge between 15 and 25 ft. The nine facilities selected for the calibration represent variations among the facilities in size, location, and facility type. Table 4-6 shows the facility area and average elevation along with the total number of tanks and unit-processes for each of the nine facilities. Facilities 5 and 9 are the two largest facilities and are the closest to the opening of the HSC to Galveston Bay with the lowest average elevation. Therefore,

facilities 5 and 9 are expected to have more significant losses as compared to the other facilities for similar storm surge levels.

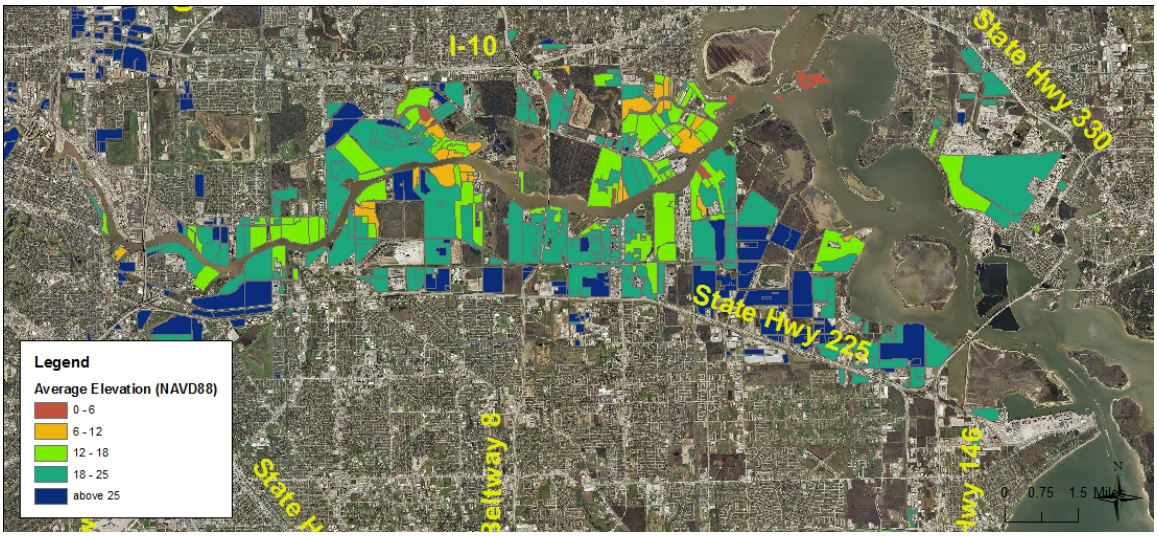

Figure 4-5. The average elevation for industrial facilities in the HSC above NAVD88 (ft) based on detailed LiDAR data (HGAC 2008).

Table 4-6. Characteristics for the modeled FEDERAP HSC calibration facilities

Facility Characteristic	Facility Number								
	1	**2**	**3**	**4**	**5**	**6**	**7**	**8**	**9**
Area (acres)	191	28	66	374	1752	174	92	304	1008
Average Elevation (ft)	20	22.2	18	21.6	23	16.7	16.4	23.7	21
Fixed top vertical tanks (#)	59	84	77	2	400	16	80	72	161
Floating top vertical tanks (#)	30	0	0	1	83	2	0	4	52
Horizontal Tanks (#)	22	5	18	0	17	0	0	0	7
Unit-Process (#)	15	0	5	4	25	2	0	9	34

4.4.2 DEVELOPMENT OF ECONOMIC LOSS DATASET

Detailed facility production and daily revenue have not been previously incorporated into published hurricane loss studies. The reasons for this gap could stem from the challenge in gathering such data or the implementation of such valuations into an appropriate framework. While FEDERAP provides this framework, a detailed process of gathering industrial productivity and economic output data was required to estimate losses for the facilities of interest more accurately. To maintain anonymity, facilities are not referenced by name in this dissertation. Similarly, the exact URL sources for the economic loss models in FEDERAP are not presented.

For each of the facilities of interest, company quarterly reports, stockholder information packets, and annual reports were reviewed to determine production and daily revenues. Typically, these values are delineated by continent and/or region of the United States. Based on facility descriptions from parent company websites, a determination was made as to the proportion of revenue associated with the facility in question. The resulting data were converted from an annual or quarterly value to daily revenue for application in FEDERAP.

The developed range of financial and productivity values gleaned from industry publications are presented in Table 4-7. Daily revenues were as high as $3.5 million per day and daily production was as high as 584,000 barrels per day for the nine calibration facilities.

Table 4-7. Facility daily revenue and productivity data for HSC-IC facilities

Variable	Range	Sources
Daily Revenue	Min: 0 (storage facilities) Max: $3,500,000	Annual reports to stockholders, quarterly reports
Productivity	Min: 0 (storage facilities) Max: 584,000 barrels	Facility descriptions, quarterly reports

4.4.3 FEDERAP CALIBRATION RESULTS

Figure 4-6 shows the total loss estimates using the FEDERAP toolbox and spreadsheet analysis for each of the facilities. The figure shows that the total losses ranged from $0.5 million to $7 billion for a storm surge level of 20-ft (top figure) and 25-ft (bottom figure).

The loss curves from four facilities (facilities 1, 3, 5, and 9) are presented in Figure 4-7 in order to illustrate the specific shape of the loss curve as surge levels increase from 15 to 25 ft. As can be seen in the figure, loss curves for Facility 1 and 3 are similar and distinctly different from 5 and 9. While loss curves for 1 and 3 increase gradually, the loss curves for facilities 5 and 9 are almost superimposed up to surge levels around 19 ft. Beyond this surge level, facilities 5 and 9 exhibit distinctly different losses that reflect the difference in facility characteristics (area, elevation, tanks, and unit processes). Facility 5 has a larger area (but more of the area is at a higher elevation) and more tanks, whereas Facility 9 has a lower average elevation and more process units. Thus, and as can be seen in Figure 4-7, the loss curves increase steadily for Facility 5 beyond surge levels of 19 ft whereas Facility 9 experiences an exponential rise in losses between 21 and 23 ft that stabilize beyond 23 ft.

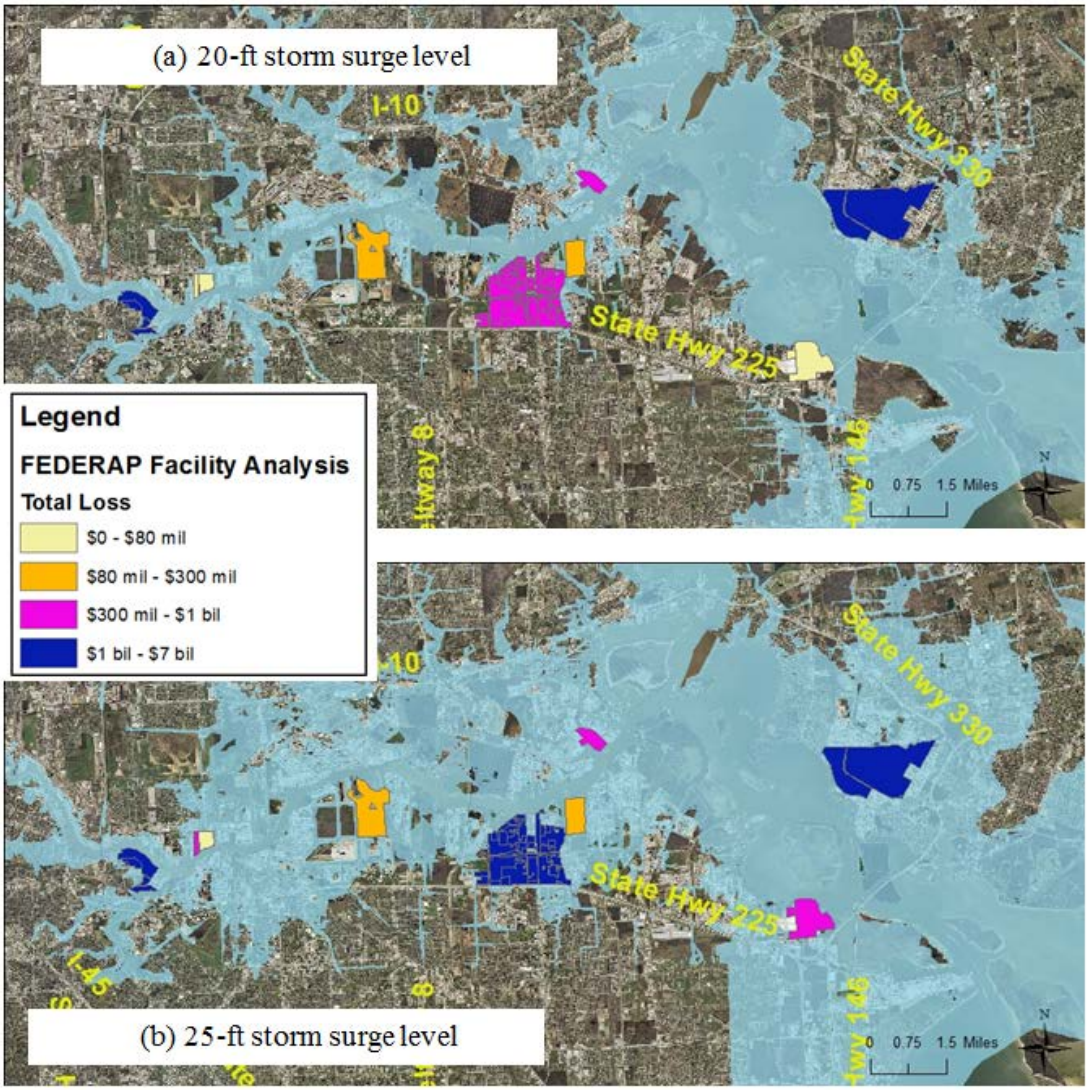

Figure 4-6. Total loss results from FEDERAP for the 9 calibration facilities modeled at 20 ft (top) and 25 ft (bottom) surge levels

The individual components of the total losses for each facility can be studied further to determine the main driver for losses as storm surge increases. As can be seen in Figure 4-8 for the modeled high losses estimates, as inundation increases, the downtime causes total losses to rise significantly. For three of the four facilities shown here, production loss is the most important driver for losses. For facilities 1 and 5, environmental release plays a significant role due to the number of tanks on site and the locations of the tanks. For Facility 5 in particular, environmental release is the largest loss

source. Facility 5 exhibits relatively high tank density (more than one tank per acre) and the resulting losses for this facility are due to the large number of tanks at low elevations as the majority of the plant and its unit-processes are not inundated even at high storm surge levels of approximately 23 ft.

The results from the analysis with these four facilities can be synthesized to allow general conclusions to be made for the entire HSC industrial region. Figure 4-9 presents this concept by relating the percent inundation for each of the facilities with the total losses that were estimated using FEDERAP. As can be seen from the figure, losses are at their lowest when the facility is less than 20% inundated and at their highest once inundation exceeds 75% as would be expected. The results on a spatial basis are somewhat less intuitive; for facilities to the east near the mouth of the HSC, the initial response to storm surge level rise is minimal but begins a step increase at approximately 20 ft (facilities 5 and 9).

Comparison to actual losses for facilities is not possible since hurricane losses to date are not differentiated based on specific industrial facilities or the parameters used in this framework. However, understanding the relationship between facility elevations, storm surge level, and expected losses is critical. Such a relationship, when developed as in this work, can be associated with the risk of different storm surge levels occurring during hurricanes thus allowing decision-makers to develop more rigorous hurricane damage mitigation strategies that are based on vulnerability, hazard, and risk in a projected losses framework.

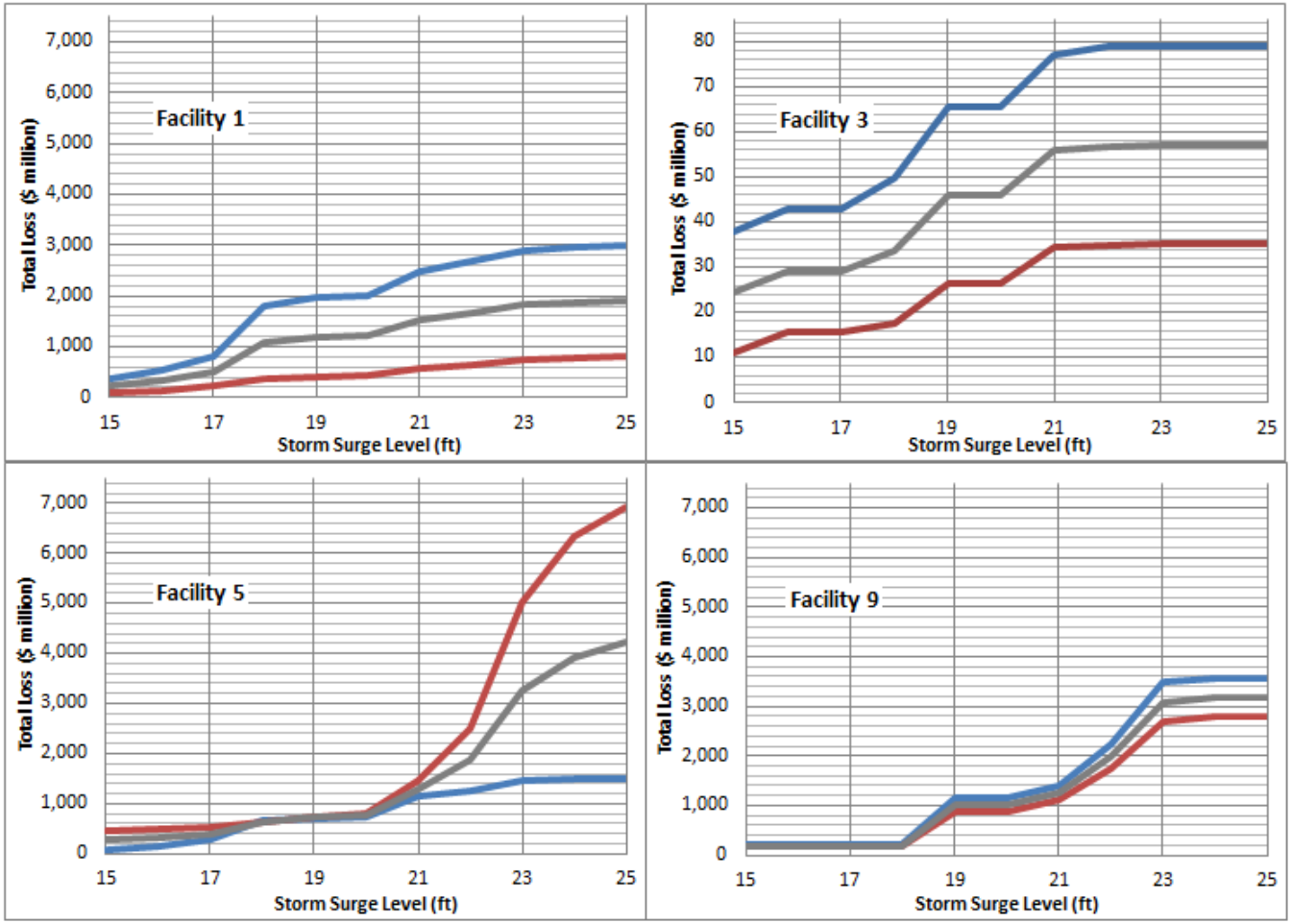

Figure 4-7. Total losses for four FEDERAP calibration facilities (blue line: higher estimate, grey line: average estimate, red line: lower estimate). Due to significantly lower loses, the range of losses for Facility 3 is presented using a different scale than the other facility losses for ease of viewing

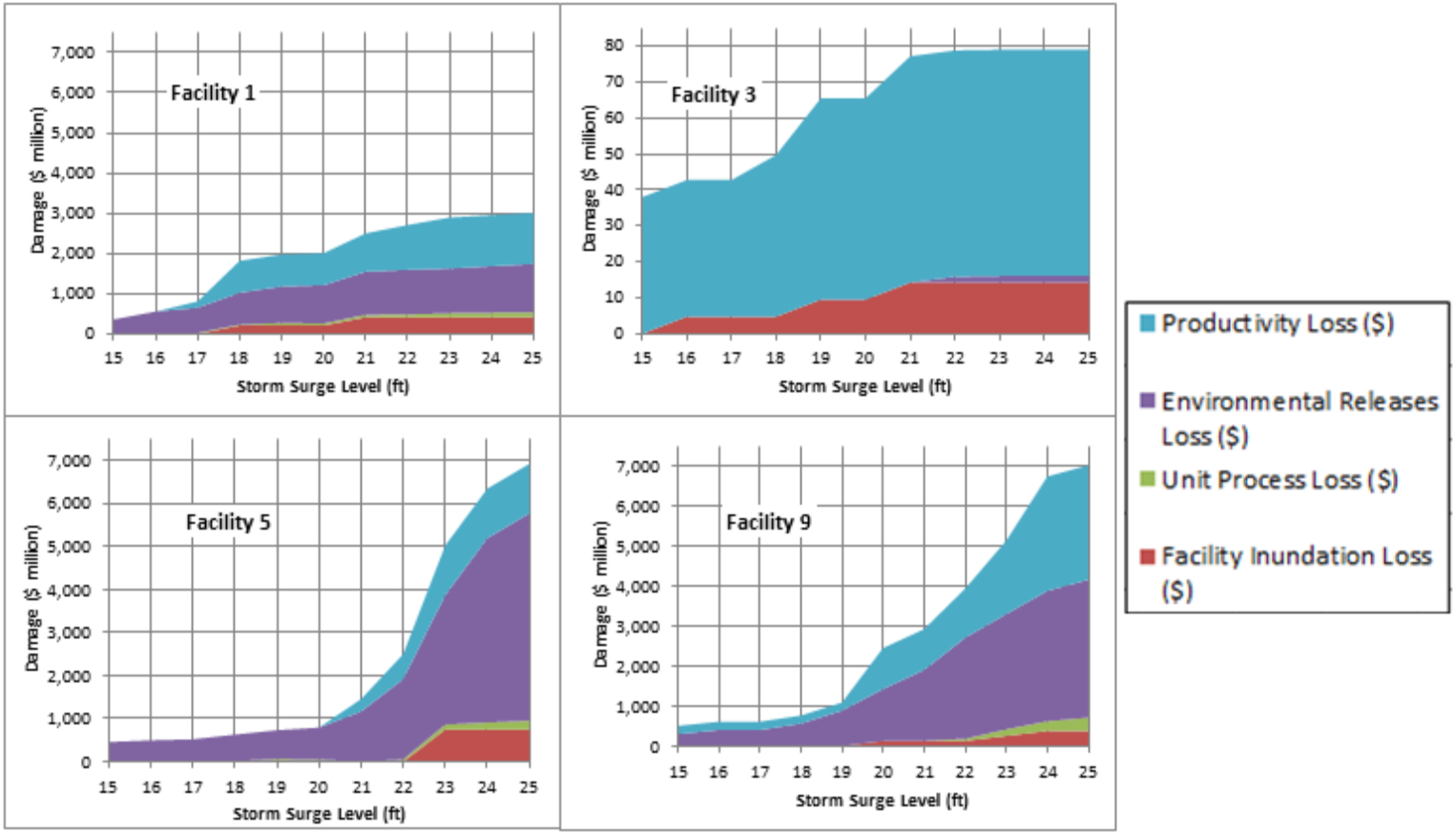

Figure 4-8. The FEDERAP modeled high loss estimates shown in terms of the 4 loss components in FEDERAP for four calibration facilities.

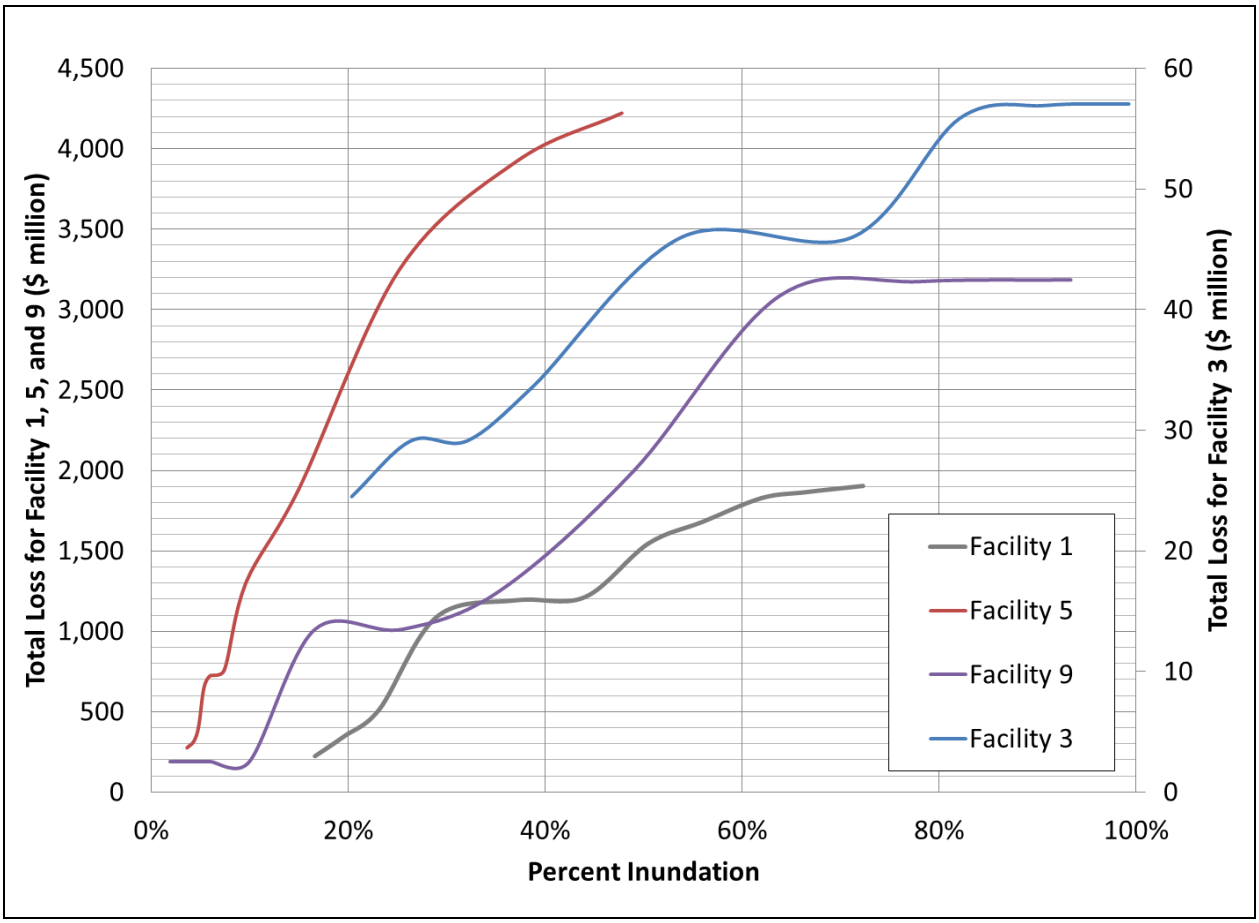

Figure 4-9. The inundation-loss curve for the FEDERAP calibration with the total facility loss as a function of percent inundation of the facility

4.5 REGRESSION MODELING WITH FEDERAP

Regression equations were developed that associate economic losses with facility characteristics. The loss curves for facilities were categorized into three domains identified from the ratio between the average facility elevation and the storm surge level (A_{inun}) (Figure 4-10). A regression model was derived separately for each domain to capture the shape of the loss curve.

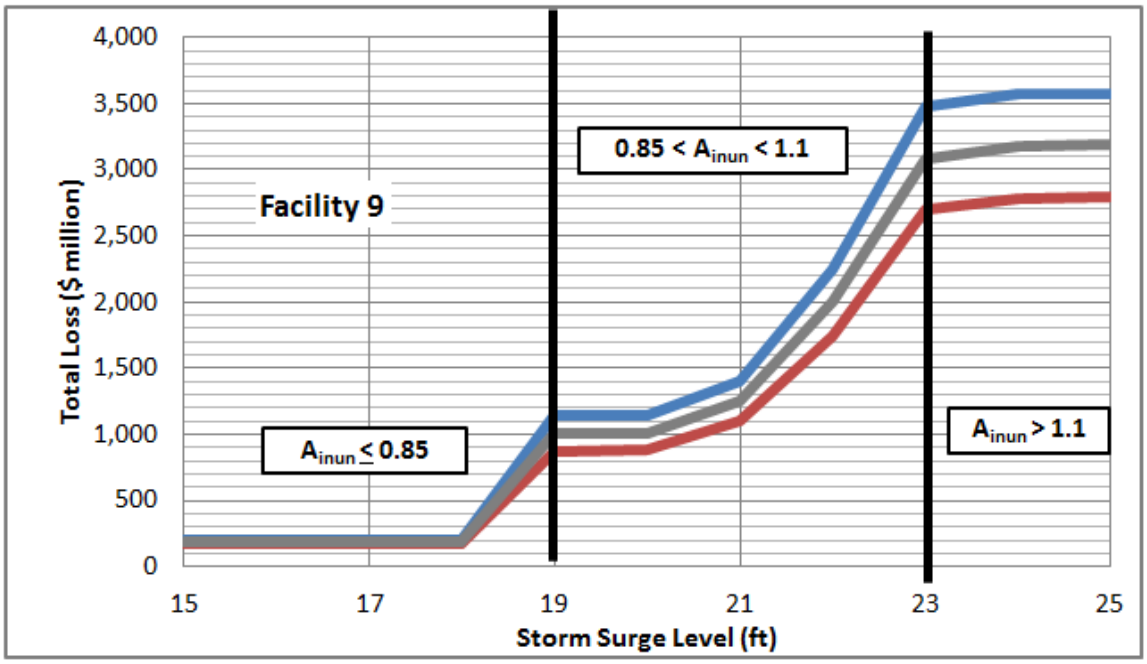

Figure 4-10. Facility 9 loss curve with the various domains within the curve related to a specified range of percent inundation.

The regression model accounts for key facility infrastructure such as area, unit-processes, and tank counts and average elevations as shown in Equation 3,

$$Loss_{total}\left(A,\ S_{level}, E_{facility}, Unit_p,\ E_H, V_{fixed}, E_{V_{fixed}}, V_{floating},\ E_{v_{floating}}\right) =$$

$$e^{C_1} * \left[A * \left(\frac{S_{level}}{E_{facility}}\right)\right] + e^{C_2} * \left[\left(Unit_p\right) * \left(\frac{S_{level}}{E_{unit_p}}\right)\right] + e^{C_3} * \left[(H) * \left(\frac{S_{level}}{E_H}\right)\right] + e^{C_4} *$$

$$\left[\left(V_{fixed}\right) * \left(\frac{S_{level}}{E_{V_{fixed}}}\right)\right] + e^{C_4} * \left[\left(V_{floating}\right) * \left(\frac{S_{level}}{E_{V_{floating}}}\right)\right], \quad (3)$$

where A is the area in acres, S_{level} is the surge level, $E_{facility}$ is the average facility elevation, H, V_{fixed}, and $V_{floating}$ are the counts of horizontal, fixed-top, and floating top tanks respectively, $E_{H,}$ E_{Vfixed}, and $E_{Vfloating}$ are the average elevations of horizontal, fixed-top, and floating top tanks respectively, $Unit_p$ is the count of unit-processes and E_{unitp} is the average elevation of the unit-processes.

A separate set of coefficients is determined for each domain of the loss curve based on A_{inun}. The coefficients are determined by minimizing the root mean squared error (RMSE) for oil refining, chemical processing, and storage facilities separately from the nine calibration facilities presented in the previous section (Section 4.4). Due to the limited number of facilities, there is a great deal of uncertainty in the resulting coefficients shown in Table 4-8. Each set of coefficients is unique to the facility type and A_{inun} range. At least ten facilities for each facility type would be necessary to improve the resulting coefficient.

4.6 FEDERAP VALIDATION

For validation of the regression model, three additional facilities of each facility type (chemical, oil, and storage) were selected as shown in Figure 4-11. These validation facilities are modeled for losses using FEDERAP and the regression model. Table 4-9 shows facility details for the three facilities that are inputs into the regression model described in the previous section.

Table 4-8. Regression Coefficients for the three facility types as a function of A_{inun}

Oil Refining (2 facilities)					
	C_1	C_2	C_3	C_4	C_5
$A_{inun} \leq 0.85$	2.6	0	17.0	13.3	0
$0.85 < A_{inun} < 1.1$	7.9	13.1	18.4	14.6	11.1
$A_{inun} > 1.1$	0	4.6	17.5	0	17.6
Chemical Processing (4 facilities)					
	C_1	C_2	C_3	C_4	C_5
$A_{inun} \leq 0.85$	9.0	16.7	16.5	0.0	13.5
$0.85 < A_{inun} < 1.1$	11.3	16.7	16.7	14.7	16.1
$A_{inun} > 1.1$	7.1	17.4	17.7	14.7	17.4
Storage (3 facilities)					
	C_1	C_2	C_3	C_4	C_5
$A_{inun} \leq 0.85$	14.9	5.0	5.1	0.0	5.0
$0.85 < A_{inun} < 1.1$	0.0	16.3	2.6	0.0	3.8
$A_{inun} > 1.1$	0.8	4.8	0.0	15.4	18.9

Note - A_{inun} is the ratio between the average facility elevation and the storm surge level

The developed regression models are compared to the estimated losses from FEDERAP for the three validation facilities in Figure 4-12. As can be seen in the figure, the regression model captures the calculated losses with relatively good accuracy for refining and chemical facilities. For the validation of the storage facility, the regression model over estimates the losses by approximately 100%. Future efforts should incorporate more detail on storage facilities to refine the regression models further.

The regression models developed above are be applied to the HSC to develop the region-wide estimates of losses under various storm surge levels as will be discussed in Section 4.8.

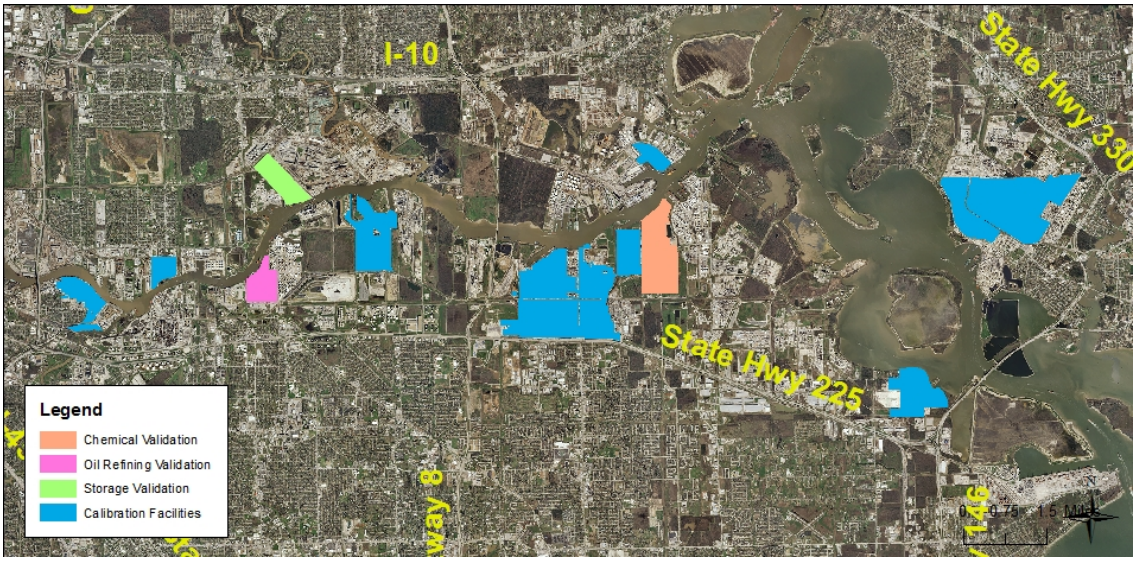

Figure 4-11. Selected facilities for validation of the regression model for FEDERAP in the HSC

Table 4-9. Validation facility inputs for regression model of HSC

Facility Characteristics	Chemical Facility	Oil Refining Facility	Storage Facility
Area (acres)	441	300	190
Average facility elevation (ft)	19.7	22.7	12.9
Fixed top vertical tanks (#)	66	57	98
Average elevation – fixed (ft)	14.13	23.8	14.4
Floating top vertical tanks (#)	3	11	5
Average elevation – float (ft)	11.2	23.0	19.8
Horizontal Tanks (#)	0	3	0
Average elevation – hor. (ft)	0	24.2	0
Unit-Process (#)	5	3	0
Average elevation – unit (ft)	19.8	21.6	0

4.7 FEDERAP SENSITIVITY ANALYSIS

In order to incorporate uncertainty, a sensitivity analysis of FEDERAP variables was undertaken to allow users to understand the relative impact of the loss relationships used within the model. In lieu of a hypothetical facility and to add rigor to the sensitivity analysis, Facility 1 was used in the run. With a relatively large area of 191 acres and an average elevation above 20 ft (NAVD88), the facility has a number of tank and process-units at various elevations and locations within the facility boundary as can be seen in Figure 4-13. The modeled losses for this facility as discussed above ranged from $360 million to $3 billion and were non-linear relative to storm surge levels as can be seen in Figure 4-14 (base run).

Table 4-10 shows the list of the sensitivity runs performed with a description of the variable that was changed for each run. Overall, ten cost inputs to the model were evaluated each with a lower and higher value relative to the base run. As can be seen in Figure 4-14, on the low end of the losses for a surge level of between 15 and 25 ft, the losses range from $280 million to $1.9 billion, whereas on the high end, the losses range from $750 million to $4.2 billion indicating a high degree of sensitivity in modeling results to the assumed cost relationships.

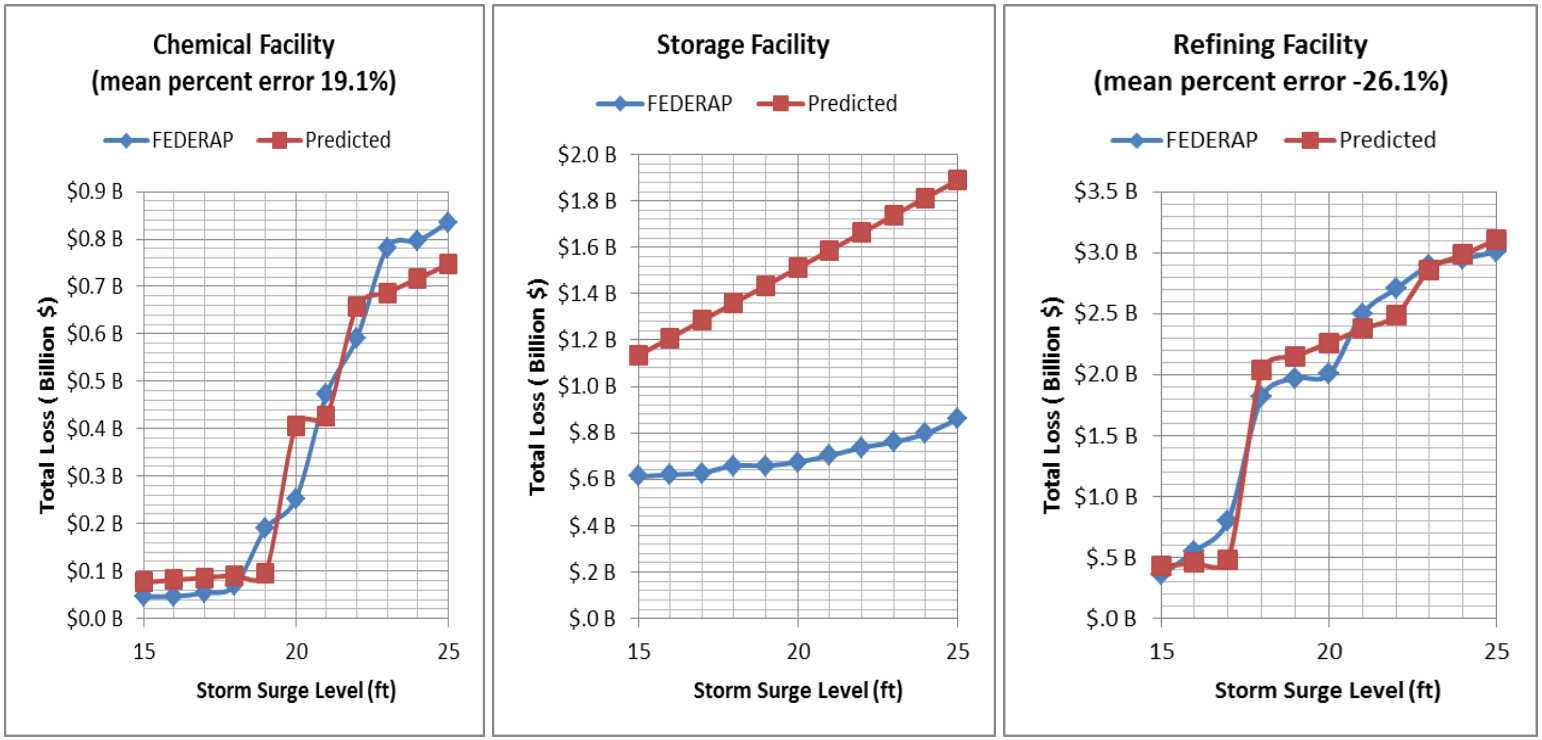

Figure 4-12. Regression modeled losses compared to FEDERAP estimated losses

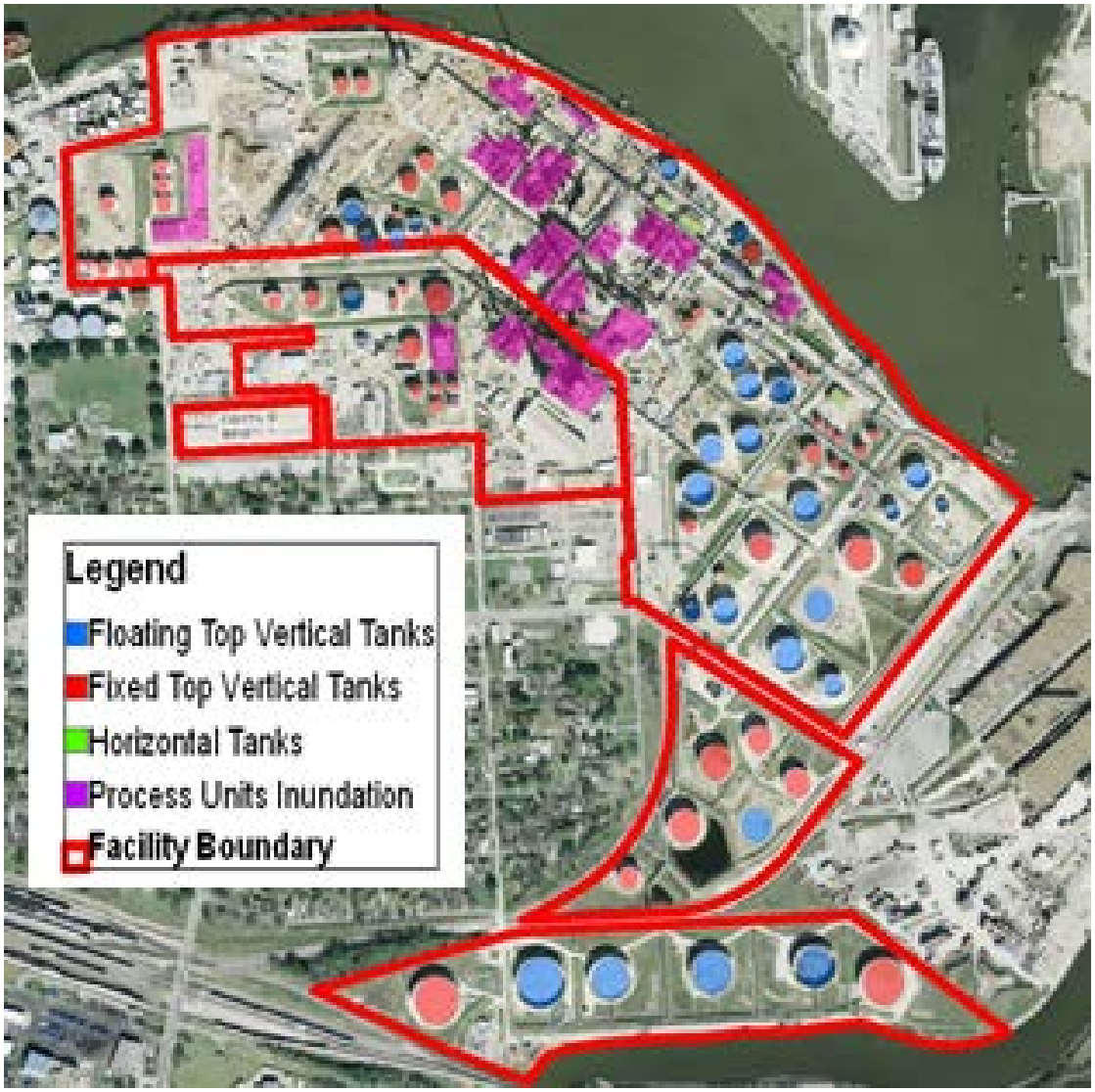

Figure 4-13. Aerial view of Facility 1 highlighting facility infrastructure

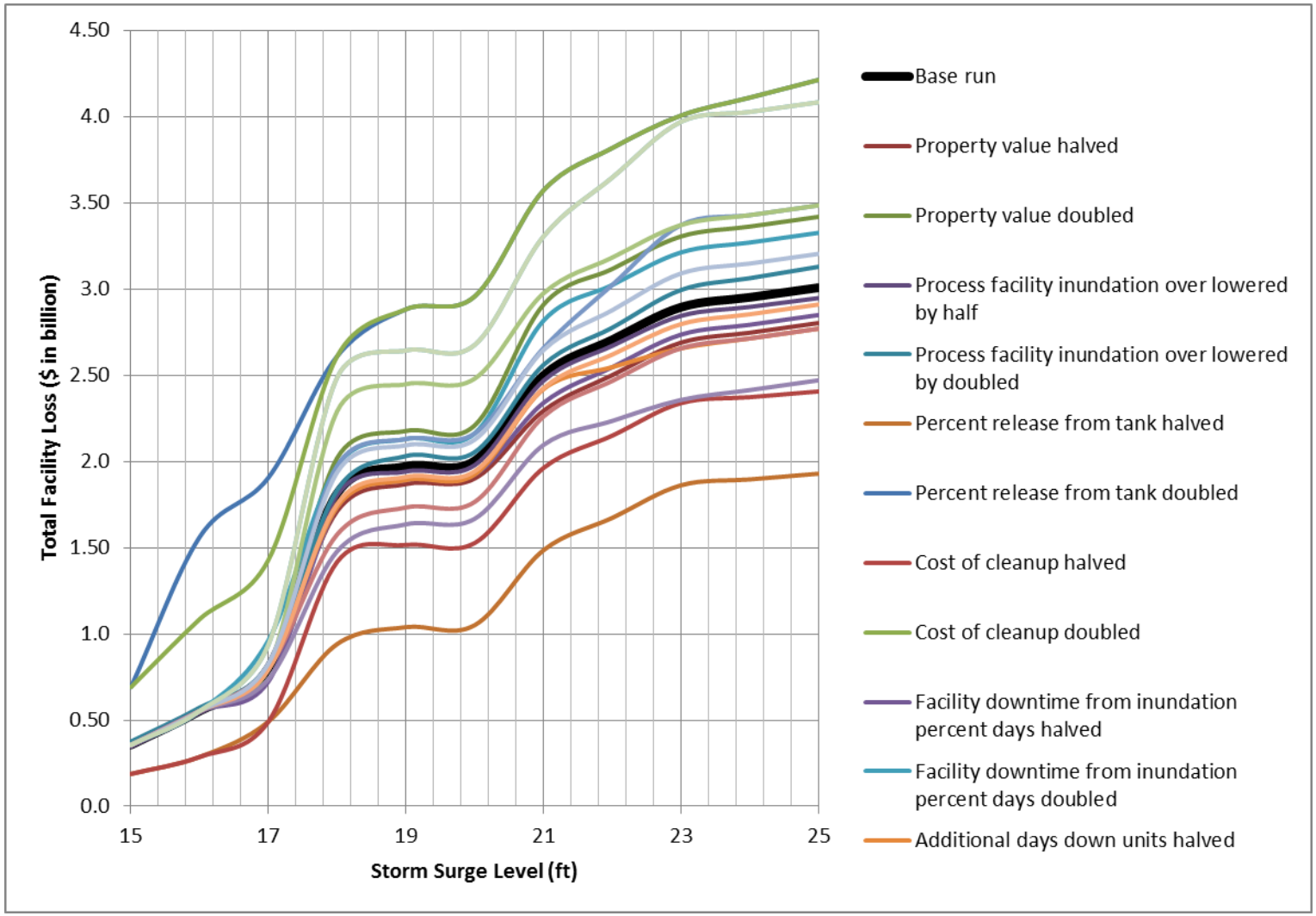

Figure 4-14. The FEDERAP sensitivity analysis results for Facility 1 with the base run shown with a thick black line

Table 4-11 presents the percent change in the total losses for Facility 1 for the sensitivity runs. As can be seen from this table and Figure 4-14, the FEDERAP model was most sensitive to environmental losses (cleanup cost and additional days down). Changes to environmental loss variables caused changes in the total loss for the facility ranging between -183% and 48% across the surge levels. At lower storm surge levels (15 to 18 ft), the model had limited sensitivity to changes in most inputs except for percent tank release and cleanup costs. This is to be expected since most of the facility area is above 20 ft in elevation. When the storm surge level exceeds 18 ft, more of the facility infrastructure becomes inundated causing higher dependence on values used for production losses. This expectation is confirmed in the sensitivity runs for production rate and cost per barrel. Overall, the loss model had limited sensitivity to daily revenue, property value, and losses related to unit-processes with the major driver being productivity and environmental (spill) losses.

In general, prior to the maximum total loss level being reached, the loss curve is non-linear and exhibits exponential behavior due to total loss of units and productivity and the damage relationships used to determine these losses. In addition, the key structure locations and the exponential elevation change of the facility in general as the distance from the main waterway increases contributes to this shape of the loss curve. This phenomenon is observed in most facilities in the region of study. On closer inspection of the sensitivity analysis results, it is noted that facility characteristics can influence the overall effect that the modeled variables have on the total losses as demonstrates in the calibration of FEDERAP. Thus, facilities that have a relatively significant number of

tanks (over 100), for example, will experience losses that are largely driven by product loss and additional days down from environmental cleanup. The interplay between facility characteristics and the modeled cost relationships and their effect on total losses highlights the need for tools such as FEDERAP and the importance of integrating this type of analysis into decision-making for addressing vulnerability of critical industrial infrastructure.

Table 4-10. Description of sensitivity analysis runs

Sensitivity Run Number	Variables of Interest	Base Run Values	New Values
Run 1	Property Value	$821 million	(1a) Value halved
			(1b) Value doubled
Run 2	Unit-process refurbishment and replacement cost	See Table 4-2	(2a) Refurbishment and Replacement cost halved
			(2b) Refurbishment and Replacement cost doubled
Run 3	Tank Percent Release	See Table 4-3	(3a) Percent Release from tanks halved
			(3b) Percent Release from tanks doubled
Run 4	Cleanup Costs (per liter)	$31	(4a) Cost of cleanup halved
			(4b) Cost of cleanup doubled
Run 5	Facility Inundation Days Down	See Table 4-4	(5a) Facility Downtime from Inundation Percent Days halved
			(5b) Facility Downtime from Inundation Percent doubled
Run 6	Additional Days Down (Unit-processes)	See Table 4-4	(6a) Additional Days down units halved
			(6b) Additional Days down units doubled
Run 7	Additional Days Down (Environmental Cleanup)	See Table 4-4	(7a) Additional Days down environmental cleanup halved
			(7b) Additional Days down environmental cleanup doubled
Run 8	Cost per barrel	$120	(8a) Cost per barrel (halved)
			(8b) Cost per barrel (doubled)
Run 9	Daily Revenue	$3.5 million	(9a) Daily Revenue halved
			(9b) Daily Revenue doubled
Run 10	Production Rate	160,000 barrels	(10a) Production Rate halved
			(10b) Production Rate doubled

4.8 ESTIMATION OF OVERALL LOSSES FOR HSC WITH FEDERAP

Overall losses for the HSC were determined using the regression model described in Section 4.5 and categorized based on the EPA's Facility Registry System (FRS), facilities into three categories: chemical, storage, and oil refining. Detailed aerial photography was used to delineate tank and process units for the entire region. Figure 4-15 summarizes the resulting facility and infrastructure inventory. Over 1000 parcels (200 facilities) were found with 126 unit-processes and 3,780 tanks. Using the 15-25 ft storm surge levels, the regression models produced the loss curve for the HSC shown in Figure 4-16. The shape of the curve matches the shape of the loss curves modeled for the previous facilities though the losses a significantly higher than expected. The higher losses from the regression model for the many storage facilities identified contributed to high losses modeled for the entire HSC-IC. In addition, by applying the regression model at a parcel level, more facilities fell in the higher loss region of the curve ($A_{inun} > 1.1$) resulting in higher losses. The results indicate the need for refinement of the FEDERAP model, in particular the environmental loss component.

Two alternate methods for estimating region-wide losses were evaluated. Additionally, tank spill probabilities from Kameshwar (2015) for the HSC-IC using a fragility tank model (Kameswhar and Padgett, 2015) were incorporated into the analysis to provide a comparison with the method used in FEDERAP for estimating environmental losses due to tank failure.

Table 4-11. Change in modeled cost estimates due to sensitivity to modeled variables and/or cost relationships for Facility 1

Storm Surge (ft)	Base Run ($ in Billion)	Run 1		Run 2		Run 3		Run 4		Run 5	
		(a)	(b)	(a)	(b)	(a)	(b)	(a)	(b)	(a)	(b)
15	0.36	0%	0%	3%	-6%	-94%	47%	47%	-94%	0%	0%
16	0.55	0%	0%	2%	-4%	-183%	48%	48%	-96%	0%	0%
17	0.80	0%	0%	1%	-2%	-137%	39%	39%	-78%	10%	-20%
18	1.82	6%	-11%	1%	-1%	-44%	48%	22%	-44%	4%	-9%
19	1.97	5%	-10%	2%	-3%	-46%	47%	23%	-46%	4%	-8%
20	2.00	5%	-10%	1%	-2%	-48%	48%	24%	-48%	4%	-8%
21	2.50	8%	-16%	1%	-2%	-43%	41%	21%	-43%	6%	-13%
22	2.71	8%	-15%	1%	-3%	-41%	38%	21%	-41%	6%	-12%
23	2.89	7%	-14%	2%	-3%	-38%	36%	19%	-38%	5%	-11%
24	2.95	7%	-14%	2%	-4%	-39%	36%	20%	-39%	5%	-11%
25	3.01	7%	-14%	2%	-4%	-40%	36%	20%	-40%	5%	-11%

Storm Surge (ft)	Base Run ($ in Billion)	Run 6		Run 7		Run 8		Run 9		Run 10	
		(a)	(b)	(a)	(b)	(a)	(b)	(a)	(b)	(a)	(b)
15	0.36	0%	0%	0%	0%	0%	0%	0%	0%	0%	0%
16	0.55	0%	0%	0%	0%	0%	0%	0%	0%	0%	0%
17	0.80	0%	0%	0%	0%	8%	-17%	2%	-3%	8%	-17%
18	1.82	4%	-9%	13%	-26%	19%	-37%	3%	-7%	19%	-37%
19	1.97	4%	-8%	12%	-24%	17%	-34%	3%	-6%	17%	-34%
20	2.00	4%	-8%	12%	-24%	17%	-34%	3%	-6%	17%	-34%
21	2.50	3%	-6%	10%	-19%	16%	-32%	3%	-6%	16%	-32%
22	2.71	6%	-12%	9%	-18%	17%	-35%	3%	-6%	17%	-35%
23	2.89	8%	-16%	8%	-16%	19%	-37%	3%	-7%	19%	-37%
24	2.95	8%	-16%	8%	-16%	18%	-36%	3%	-7%	18%	-36%
25	3.01	8%	-16%	8%	-16%	18%	-36%	3%	-7%	18%	-36%

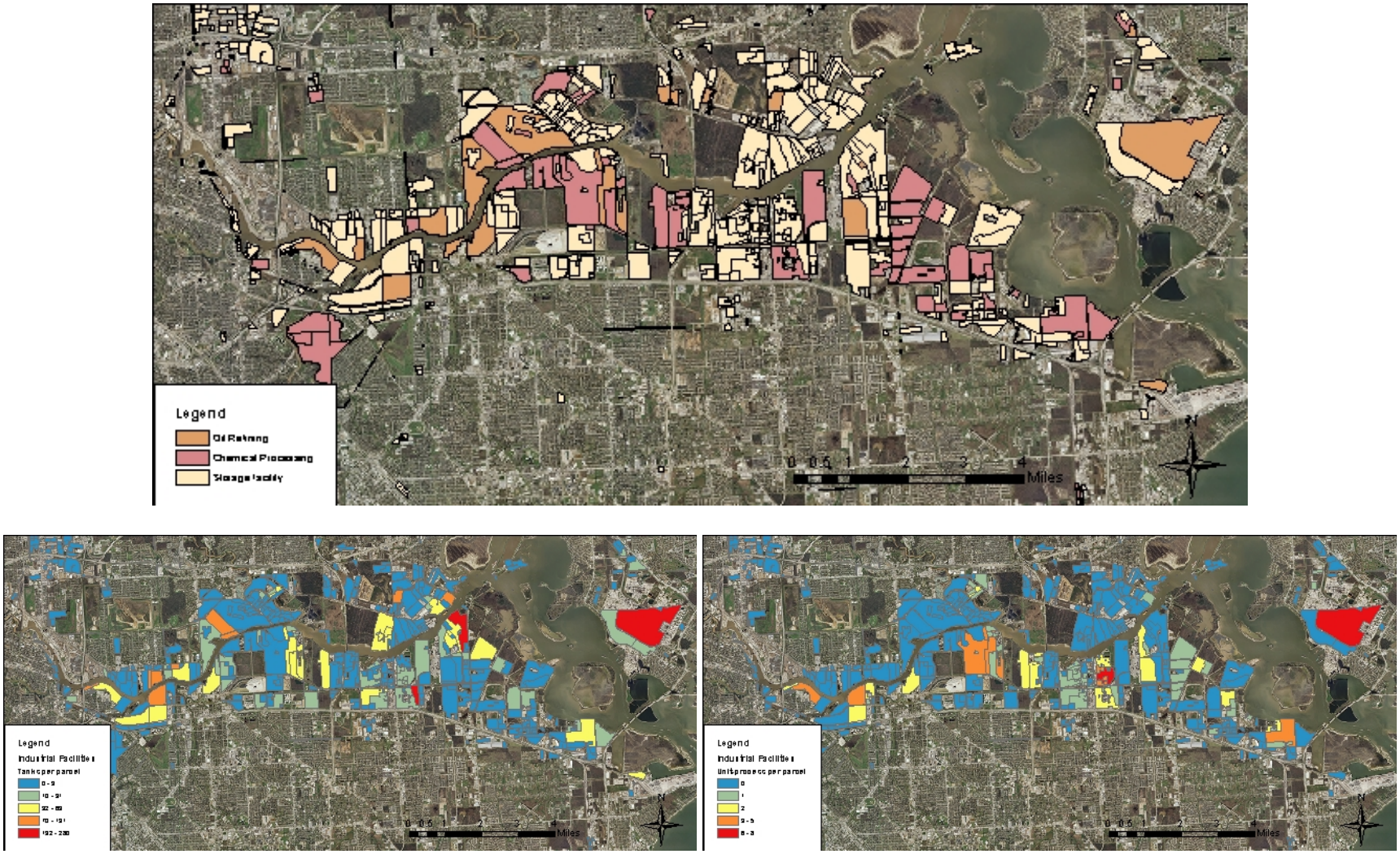

Figure 4-15. HSC facility categorization and infrastructure derived from aerial photography

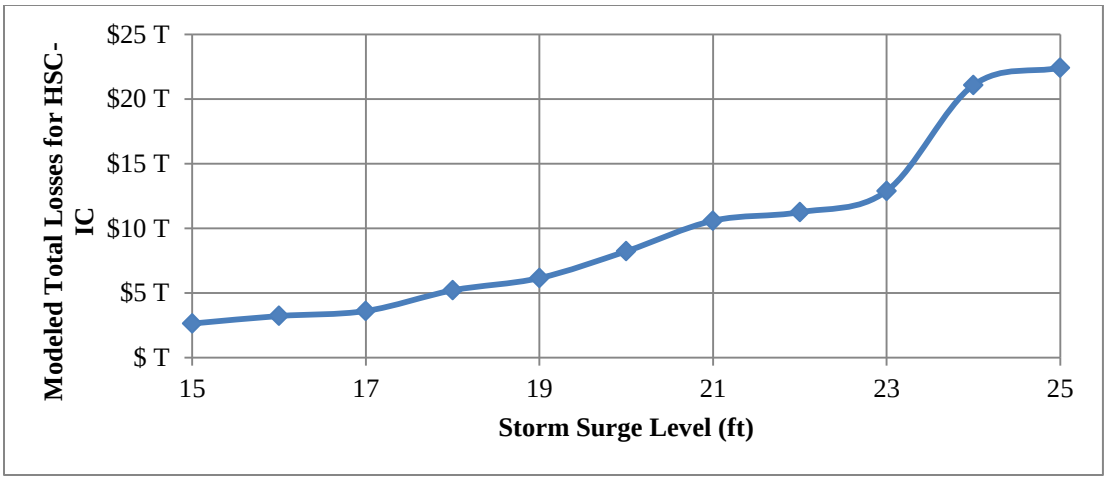

Figure 4-16. Modeled total loss curve based on regression model for HSC-IC

Alternative Method 1. In this method, the loss per acre of industrial facility based on data for the nine calibration facilities (4507 acres) modeled with FEDERAP is applied to the total acreage in the HSC-IC (21,305 acres); the results are shown in Table 4-13. The losses are estimated at $10.6 billion for 15 ft storm surge and increase to $90.7 billion at 25 ft surge. Figure 4-17 show the 4324 tanks identified in the HSC-IC from Kameshwar (2015). Over 1000 of these tanks are located within the nine facilities used to calibrate FEDERAP and the statistics for these tanks at various storm surge levels are shown in Table 4-12. The probabilities of failure consider only buckling and floatation failure (Kameshwar and Padgett, 2015) and are significantly lower than the 20 to 50% probability of failures assumed in FEDERAP. Hence, the results in spill amounts are significantly lower than those used in the FEDERAP model for the nine validation facilities. Hence, estimated losses using tank failure probabilities in place of FEDERAP default environmental loss estimates are much lower ranging from $3.6 billion to $51 billion for 15 and 25 ft surge, respectively. The cleanup costs for tank spill probabilities are based on the $30.6 per liter cleanup cost used in FEDERAP. It is also important to

note that while the FEDERAP model considered both vertical and horizontal tanks, the work done by Kameshwar (2015) is limited to vertical tanks.

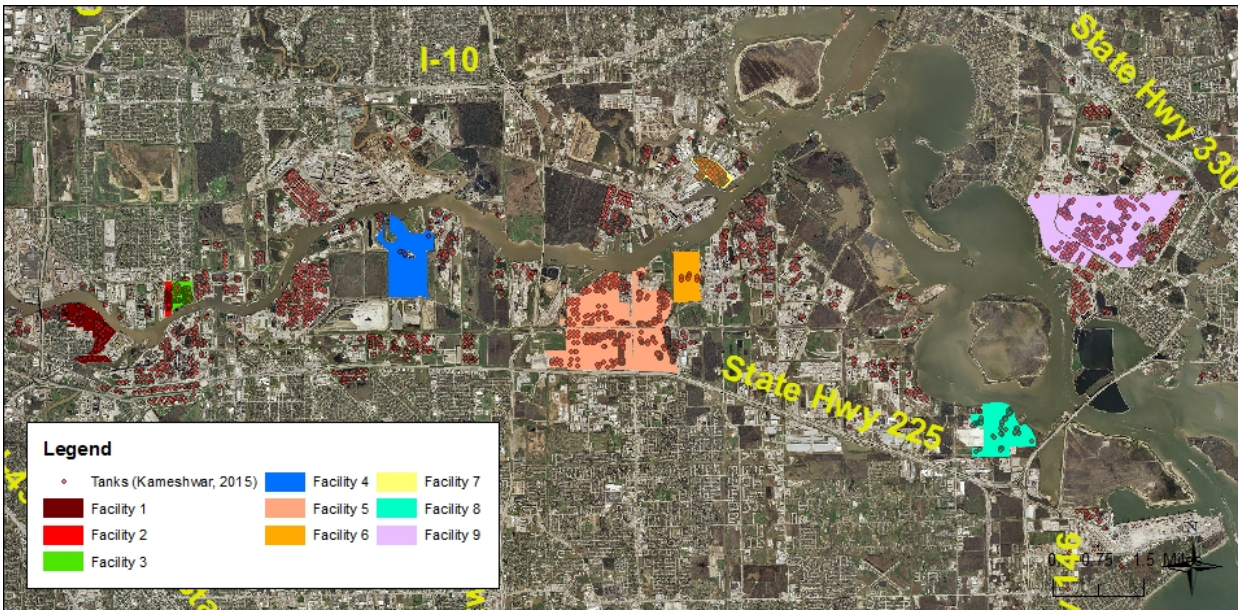

Figure 4-17. Tank locations from Kameshwar (2015) for the HSC-IC with nine calibration FEDERAP facilities

Table 4-12. Tank spill estimates for the nine calibration FEDERAP facilities using tank spill probabilities from Kameshwar (2015) compared to FEDERAP

Storm Surge Level	Kameshwar (2015)			FEDERAP	
	Tanks Inundated	Failure Probability	Spill Amount (million gallons)	Tanks Inundated	Spill Amount (million gallons)
16	15	0.3%	0.7	95	42.9
18	24	0.5%	1.4	174	78.0
20	55	1.0%	3.2	294	98.0
22	188	2.5%	17.0	543	191.7
24	478	11.4%	29.7	866	219.2

Table 4-13 compares FEDERAP estimates to those that incorporate tank failure probabilities for all surge levels analyzed. Figure 4-18 shows the total loss curve for the HSC-IC using both estimates and the resulting envelop can be thought of as the predicted

range of overall losses that is highly influenced by the number of tanks that would fail at a given surge level.

Table 4-13. Industrial loss estimates for HSC-IC using FEDERAP and tank spill probabilities (Alternative Method 1)

Storm surge level (ft)	Full FEDERAP Loss estimates	FEDERAP loss estimate using tank spill probabilities (Kameshwar, 2015)
15	$ 10.6 Billion	$ 3.6 Billion
16	$ 12.8 Billion	$ 4.2 Billion
17	$ 14.5 Billion	$ 5.6 Billion
18	$ 20.4 Billion	$ 9.3 Billion
19	$ 24.4 Billion	$ 11.3 Billion
20	$ 31.1 Billion	$ 16.0 Billion
21	$ 40.1 Billion	$ 21.1 Billion
22	$ 53.5 Billion	$ 27.6 Billion
23	$ 71.8 Billion	$ 39.2 Billion
24	$ 85.4 Billion	$ 47.1 Billion
25	$ 90.7 Billion	$ 51.0 Billion

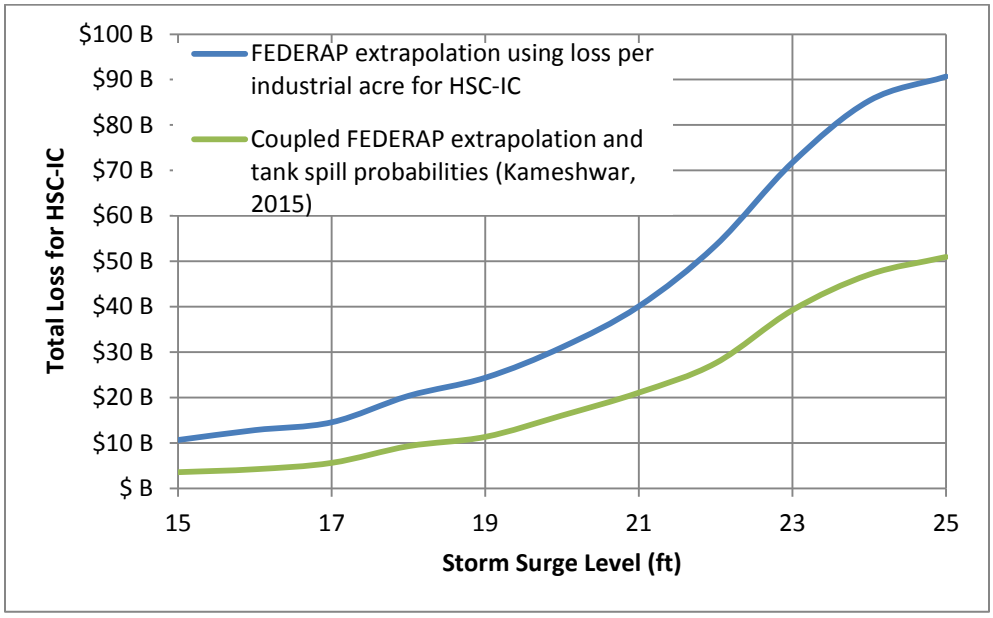

Figure 4-18. Total loss estimation for HSC-IC using the FEDERAP model and FEDERAP coupled with tank spill probabilities (Alternative Method 1)

Alternative Method 2. Since FEDERAP is largely driven by the acreage that is inundated for a given facility at a given surge level, alternative method 2 redevelops the regional estimate using the cost per inundated acre using the data from the nine modeled calibration facilities. The loss per inundated acreage ranged from approximately $5 million to $7.2 million with the range declining to between approximately $1 to $3 million per inundated acre when the tank component is removed. The results are shown in Table 4-14 and Figure 4-19. Compared to alternative method 1, estimated losses are higher at lower surge levels ($20.1 billion for the full FEDERAP extrapolation and $5.1 billion using refined tank spill probabilities). At high storm surge levels, the two methods converge to very similar regional estimates that is to be expected since inundated acreage increases with rising storm surge.

Table 4-14. Industrial loss estimates for HSC-IC estimates using FEDERAP and additional tank spill probabilities (Alternative Method 2)

Storm surge level (ft)	Full FEDERAP Loss Estimates	FEDERAP loss estimate using tank spill probabilities (Kameshwar, 2015)
15	$20.1 Billion	$5.4 Billion
18	$27.8 Billion	$11.7 Billion
20	$41.5 Billion	$20.0 Billion
22	$56.5 Billion	$24.6 Billion
25	$87.8 Billion	$49.8 Billion

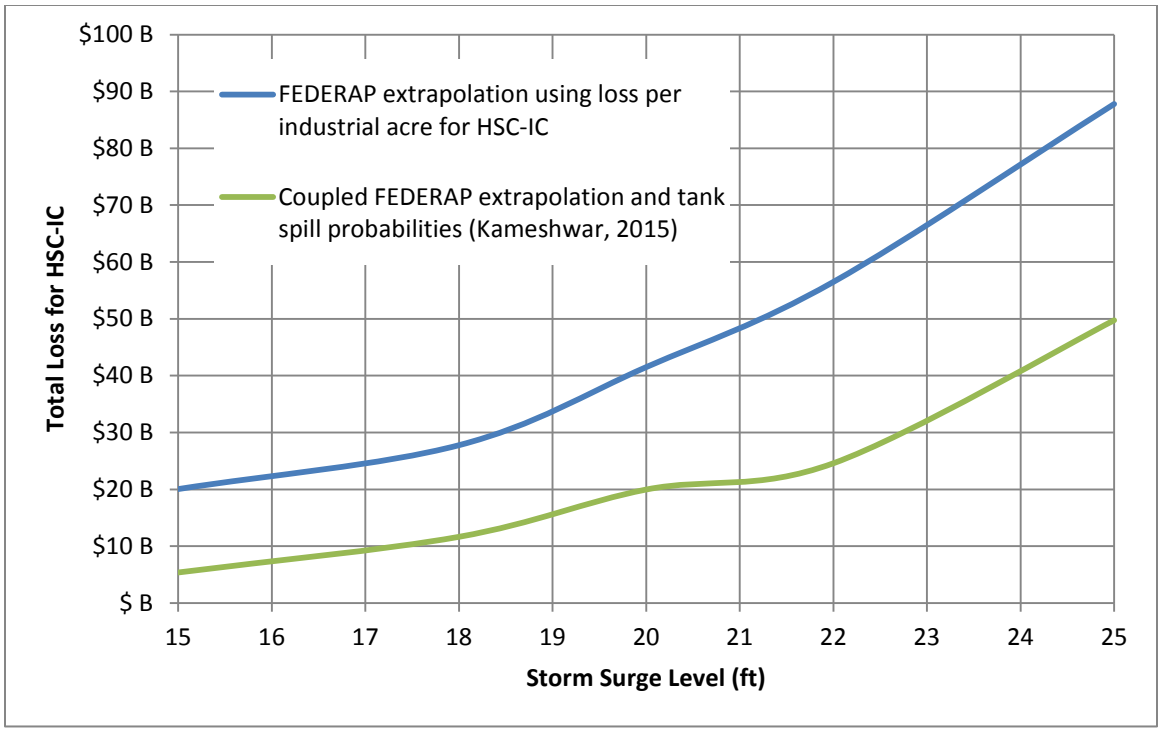

Figure 4-19. Total loss estimation for HSC-IC using the FEDERAP model and FEDERAP coupled with tank spill probabilities (Alternative Method 2)

CHAPTER 5. WATER QUALITY MODEL FOR CONTAMINANT TRANSPORT DURING STORM SURGE EVENTS

5.1 MODELING GOALS

The development of a water quality model for contaminant transport during storm surge links the SWAN+ADCIRC hurricane storm surge predictive model and EFDC hydrodynamic, sediment, and water quality model. The resulting model is referred to as EFDC-Storm Surge model or EFDC-SS and has three main goals as noted previously in the thesis objectives:

- To develop a modeling system for simulating the transport of spills from industrial facilities during hurricanes;
- To provide an alternate approach for estimating environmental losses that accounts for pollutant release to coastal environments; and
- To simulate the extent to which water and sediment quality in an industrialized estuary system such as the HSC changes as a result of storms surge event.

The EFDC model developed by Howell (2012) was modified in this research to simulate pollutant transport under surge. This chapter is intended to provide a summary of the EFDC model as developed by Howell (2012) and details of the adaptations made to link it with the SWAN+ADCIRC hurricane simulation model and model pollutant transport under surge.

5.2 EFDC MODEL DESCRIPTION FOR HSC (HOWELL, 2012)

The EFDC model adapted from Howell (2012) utilizes a detailed grid (2,649 cells) of the waterway derived from aerial photography taken in 2005 (the grid area is shown in blue in Figure 5-1). The model begins west near downtown Houston in Buffalo Bayou and is bounded in the north by the Lake Houston Dam on the San Jacinto River. It has an open boundary at the south along Tabbs Bay and Morgan's Point. The island to the northwest of the open boundary is called Alexander Island located in the Upper San Jacinto Bay. These areas are identified in Figure 5-1 and will be referred to when discussing the model results. The bathymetry was developed from the Harris County Flood Control District (HCFCD) transects and the National Oceanic Atmospheric Administration (NOAA) elevation charts (Vertical Datum 1988 – NAVD88). The model is contained to the waterway and does not account for wetting and drying in areas where inundation may occur from significant storm surge events.

EFDC employs the common vertical sigma scaling approximation whereby the total depth at each cell and time step is determined externally and is then subdivided into vertical cells according to pre-set fractions. There are five vertical fractions represented from bottom to top as 0.05, 0.10, 0.20, 0.30, and 0.35.

Calibration of EFDC by Howell (2012) used three model metrics that included water surface elevations, salinity, and total suspended solids (TSS) with boundary conditions as shown in Figure 5-2. In examining the long-term trends (three years) of water surface elevation, salinity, and TSS, Howell (2012) observed that storm events resulting in increased flows into the channel and a rise in the tidal boundary at Morgan’s point (orange circles in Figure 5-2) caused significant disturbances in the water quality of

the modeled system. Thus, in this research, their model is used in a scenario-based mode with storm surge as the tidal boundary condition to determine potential environmental impacts from spills within the HSC-IC during a hurricane. It should be noted that, unlike the storms modeled by Howell (2012), the emphasis is on the storm surge impact and not on rainfall within HSC watersheds.

5.3 EFDC MODEL ADAPTATION FOR POLLUTANT RELEASE IN STORM SURGE EVENT

5.3.1 SWAN+ADCIRC AND EFDC MODEL COUPLING

The SWAN-ADCIRC hurricane simulation model was linked to EFDC via the use of a surge-based boundary condition at Morgan's Point and Tabbs Bay along the navigable channel of the HSC-IC. The boundary condition extends from Morgan's Point east through Tabbs Bay (refer to Figure 5-2). The output from the SWAN+ADCIRC model that includes water surface elevations (WSE) in meters above North American Datum 1983 (NAVD83) and velocities (m/s) at each node within the grid were used as boundary conditions in the EFDC-SS model. An example of the water surface elevations for SWAN+ADCIRC for a location in the study area is shown in ; these data are used to validate EFDC-SS.

The NOAA tidal stage in the region is used for the lead up to the 4-day hurricane event and the long-term impact in post-storm simulations.

Figure 5-1. The EFDC-SS model area with key areas of interest.

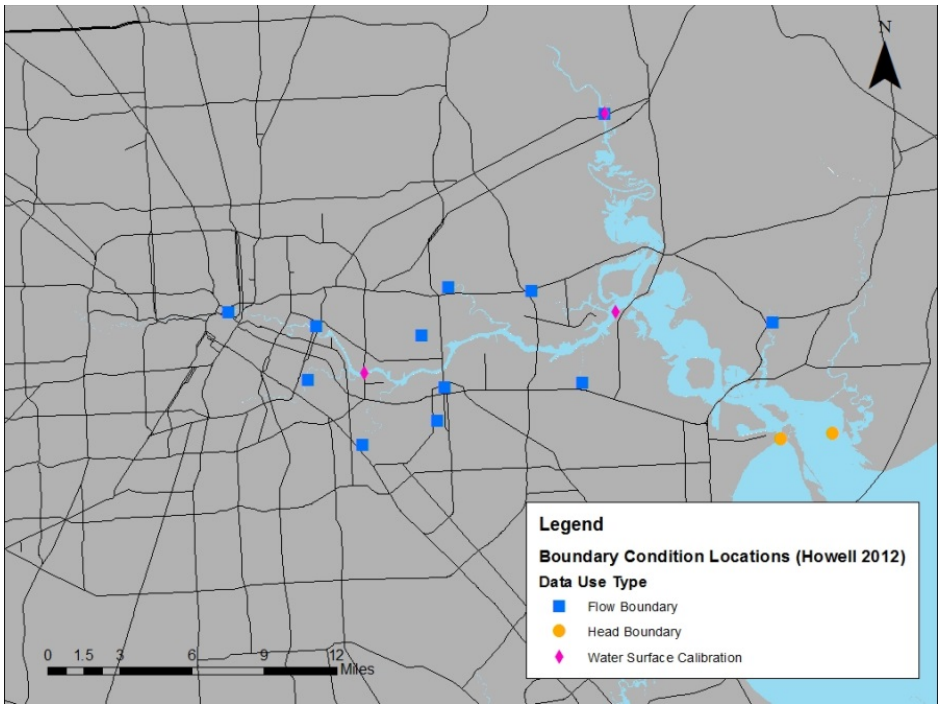

Figure 5-2. Boundary condition locations in the EFDC model for freshwater inflows (runoff flows – flow boundary) the HSC and tidal influence (storm surge – head boundary) from Howell (2012)

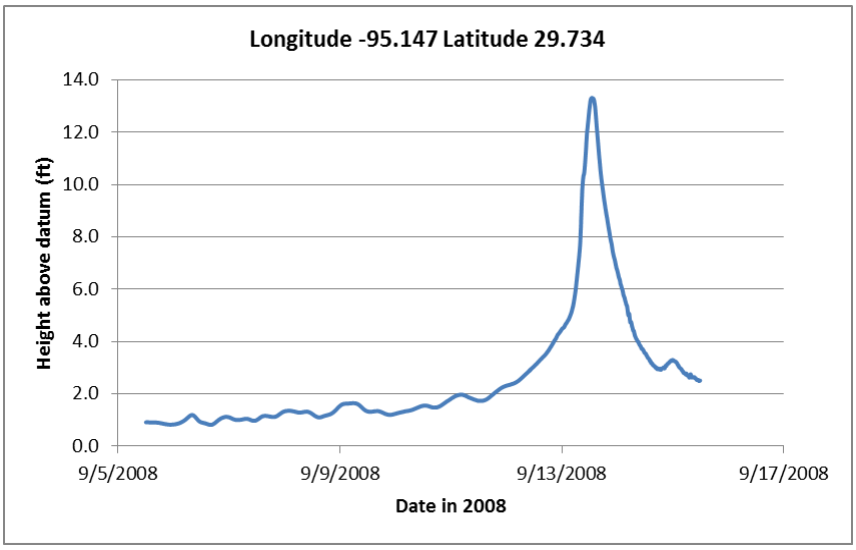

Figure 5-3. Sample SWAN+ADCIRC water surface elevation result for a location in HSC-IC

Table 5-1 shows the model time period associated with each source of boundary condition data used in EFDC-SS. One of the reasons for using the modeled WSE from SWAN+ADCIRC is the uncertainty and missing data from the NOAA tidal gages at this boundary. Figure 5-4 shows the recorded NOAA tidal WSE measured reading for September of 2008 (blue line). However, during Hurricane Ike, observed values are missing as indicated by the break in the blue line. The red line in this figure is the modeled WSE from SWAN+ADCIRC that is used to model Hurricane Ike for EFDC-SS. The WSE from SWAN+ADCIRC at Morgan's Point is used as the surge boundary condition for the 4-day period encompassing Hurricane Ike and additional storm surge events. To derive the storm surge hydrograph for each cell along the boundary, the average WSE at each time step is taken from the SWAN+ADCIRC nodes within each EFDC model cell indicated in Figure 5-5 (left). The result is a continuous head boundary condition for Hurricane Ike shown Figure 5-5 (right). In addition, the coupling of SWAN+ADCIRC results to EFDC allows for additional hurricane scenarios to be modeled (Ike at Point 7 and Ike at Point with increased winds).

Table 5-1. Boundary condition sources and timing for Tabbs Bay and Morgan's Point (near upper Galveston boundary of EFDC-SS model)

Model Time Period	Boundary Condition Source
09/01/2008 – 09/11/2008	NOAA Tidal Stage
09/11/2008 – 09/15/2008	SWAN+ADCIRC
09/15/2008 – 01/01/2010	NOAA Tidal Stage

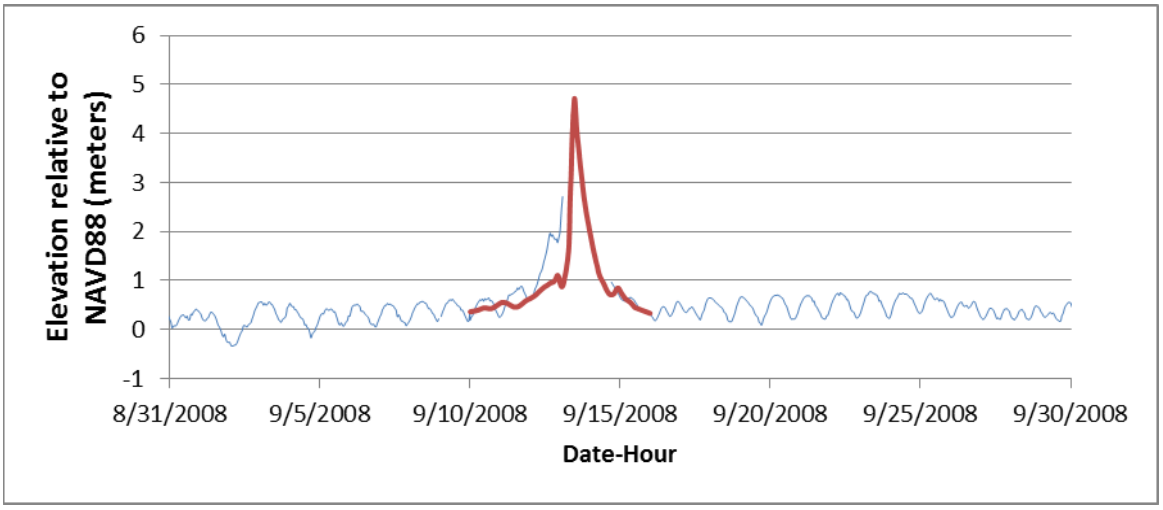

Figure 5-4. NOAA tidal stage at Morgan's Point open boundary for September 2008 (blue line) compared to SWAN+ADCIRC modeled Hurricane Ike (red line).

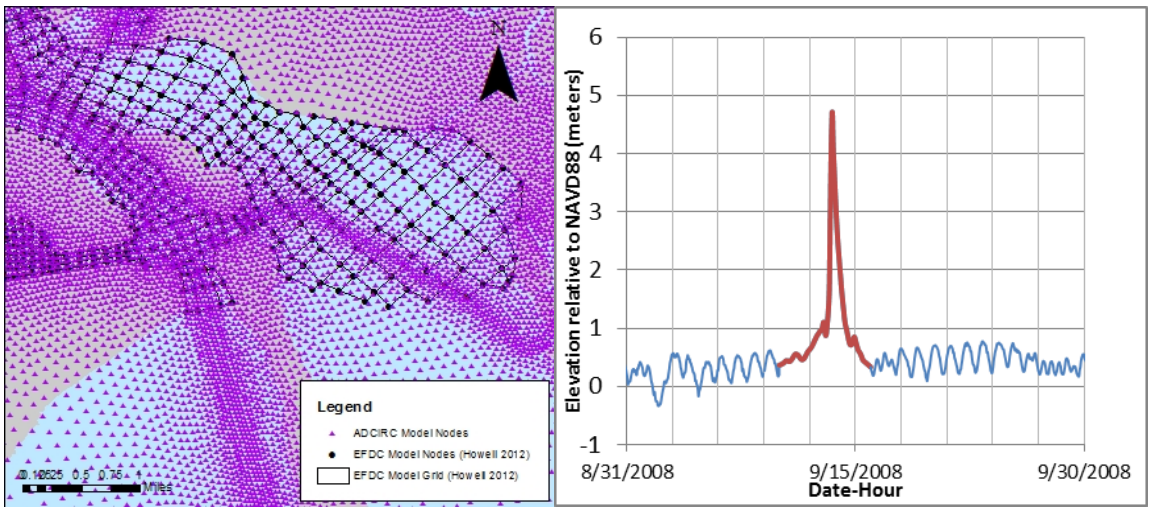

Figure 5-5. The surge boundary condition locations from Morgan's point through Tabbs Bay with the combined head boundary using NOAA tidal stage (blue line) and SWAN+ADCIRC storm surge water elevations (red line).

5.3.2 MODEL TIMING

A majority of the USGS flow gages shown in Figure 5-2 have hydrographs with a duration of approximately seven days with most falling in a 9 day window from September 11 to September 20 of 2008 (see Figure 5-6 and a detailed summary in Table 5-2). Based on these data and the duration of the runs from the SWAN+ADCIRC model, two temporal horizons will be used for the EFDC-SS model in this research. For short-term analysis (storm response), a duration of 13 days will be used with a time step of 0.5 seconds. A small time step was used to account for stability issues with the modeled caused by significant changes in water levels at the open boundary from storm surge. The total duration of the model represents the dates from September 10 (one day before response is seen in hydrographs) to September 23 (3 days after hydrographs for the flow boundaries return to normal levels). The model was started on September 1, 2008 and hot started from the EFDC model used in Howell (2012); a hot start refers to the use of initial conditions on September 1, 2008 from the existing results file of Howell (2012). The period between September 1, 2008 and September 10, 2008 represents a spin-up time for the model to equilibrate prior to the landfall of Hurricane Ike (numerical models such as EFDC require a spin-up period of time to allow stabilization of predicted water levels; model results from the spin-up period are typically discounted from the analysis).

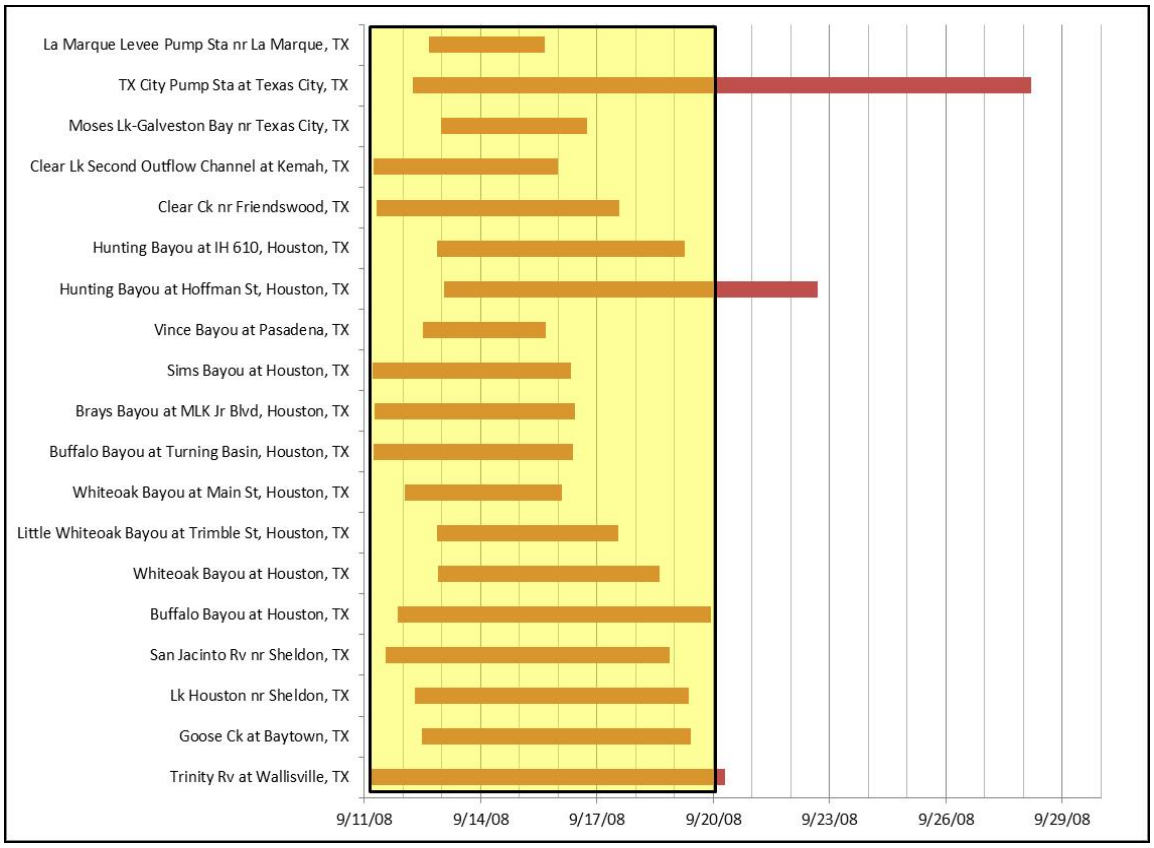

Figure 5-6. Storm duration for USGS gages in the Houston-Galveston Region

Table 5-2. Timing of hydrograph for USGS flow gages in the Houston-Galveston Region for Hurricane Ike

Site Number	Station Name	Latitude	Longitude	Gage Height (ft)	Start Time	Duration (days)	End Time	Peak 1	Peak 2	Peak 3	Peak 4
8067252	Trinity River at Wallisville, TX	29.812443	-94.731308	No	9/11/2008 4:30	9.10	9/20/2008 7:00	9/12/2008 16:00	9/13/2008 7:15		
8067525	Goose Ck at Baytown, TX	29.770781	-94.99965	Yes	9/12/2008 11:45	6.93	9/19/2008 10:00	9/13/2008 9:45	9/14/2008 11:00		
8072000	Lk Houston nr Sheldon, TX	29.916333	-95.141319	Yes	9/12/2008 7:00	7.06	9/19/2008 8:30	9/13/2008 4:00	9/14/2008 23:30		
8072050	San Jacinto Rv nr Sheldon, TX	29.876334	-95.093818	Yes	9/11/2008 13:00	7.33	9/18/2008 21:00	9/13/2008 9:45	9/15/2008 11:30		
8074000	Buffalo Bayou at Houston, TX	29.760228	-95.40855	Yes	9/11/2008 20:30	8.08	9/19/2008 22:30	9/13/2008 13:00	9/14/2008 13:15	9/17/2008 3:00	
8074500	Whiteoak Bayou at Houston, TX	29.775227	-95.397161	Yes	9/12/2008 21:15	5.72	9/18/2008 14:30	9/13/2008 10:15	9/14/2008 9:30		
8074540	Little Whiteoak Bayou at Trimble St, Houston, TX	29.792777	-95.368055	Yes	9/12/2008 21:00	4.68	9/17/2008 13:15	9/13/2008 9:00	9/14/2008 11:15		
8074598	Whiteoak Bayou at Main St, Houston, TX	29.766616	-95.358548	Yes	9/12/2008 1:15	4.03	9/16/2008 2:00	9/13/2008 11:00	9/14/2008 11:45		
8074710	Buffalo Bayou at Turning Basin, Houston, TX	29.749394	-95.291047	No	9/11/2008 5:45	5.13	9/16/2008 8:45	9/13/2008 9:30			
8075110	Brays Bayou at MLK Jr Blvd, Houston, TX	29.714166	-95.338888	Yes	9/11/2008 6:15	5.17	9/16/2008 10:15	9/13/2008 9:45	9/14/2008 10:15		
8075500	Sims Bayou at Houston, TX	29.674396	-95.28938	Yes	9/11/2008 4:45	5.14	9/16/2008 8:00	9/13/2008 10:00			
8075730	Vince Bayou at Pasadena, TX	29.694673	-95.216323	Yes	9/12/2008 12:00	3.19	9/15/2008 16:30	9/13/2008 9:00			
8075763	Hunting Bayou at Hoffman St, Houston, TX	29.808837	-95.313269	Yes	9/13/2008 1:00	9.65	9/22/2008 16:30	9/13/2008 12:45	9/14/2008 9:00		

Site Number	Station Name	Latitude	Longitude	Gage Height (ft)	State Time	Duration	End Time	Peak 1	Peak 2	Peak 3	Peak 4
8075770	Hunting Bayou at IH 610, Houston, TX	29.793282	-95.26799	Yes	9/12/2008 20:45	6.41	9/19/2008 6:30	9/13/2008 13:45	9/14/2008 10:30		
8077600	Clear Ck nr Friendswood, TX	29.517455	-95.178544	Yes	9/11/2008 7:30	6.26	9/17/2008 13:45	9/13/2008 15:45			
8077637	Clear Lk Second Outflow Channel at Kemah, TX	29.554396	-95.025761	No	9/11/2008 5:30	4.77	9/16/2008 0:00	9/13/2008 2:30			
8077650	Moses Lk-Galveston Bay nr Texas City, TX	29.447454	-94.920201	No	9/12/2008 23:30	3.76	9/16/2008 17:45	9/14/2008 15:15			
8077658	TX City Pump Sta at Texas City, TX	29.357456	-94.924922	No	9/12/2008 5:45	15.95	9/28/2008 4:30	9/13/2008 4:30	9/14/2008 19:00	9/16/2008 7:45	9/18/2008 8:15
8077740	La Marque Levee Pump Sta nr La Marque, TX	29.34579	-94.963257	No	9/12/2008 15:45	3.00	9/15/2008 15:45	9/13/2008 5:45			

5.3.3 CONSERVATIVE DYE TRACER SETUP FOR POLLUTANT RELEASE

A conservative dye tracer is simulated to represent a spill at one of the facilities in the HSC-IC. A 12-hour spill is assumed; the concentration of the spilled material is assumed to be 1,000 mg/L and is applied constantly over the time period at the surface (top) water layer. A 12-hour length for the spill is based on a reasonable time for facility to contain the spill or for the tank to no longer be inundated. Model sensitivity to the spill length is examined further in Section 5.5.3. The location of the spill is varied as will be seen in subsequent sections to determine the vulnerability of the HSC-IC to the spill location. The concentration of the spilled material is applied to the cell nearest the facility of interest. The timing of the spill relative to the hurricane event is also investigated. The duration and quantity of the spill is studied via sensitivity analysis but is not varied during the analysis of vulnerability.

The same three hurricane scenarios described earlier (Ike, Ike at Point 7, and Ike at Point 7 with increased wind speed) are simulated in this section. The WSE at the open boundaries of Tabbs Bay and Morgan's Point for the additional hurricane storms surge scenarios are shown in Figure 5-7 and Table 5-3; the maximum observed storm surge is shown for each case. The timing of the peak storm surge level is the same for both scenarios but the model maximum WSE increase to 5.8 and 7.4 m for Hurricane Ike at Point 7 and Hurricane at Point 7 with increased winds, respectively. Details of the model hurricane scenario were previously discussed in Chapter 3.

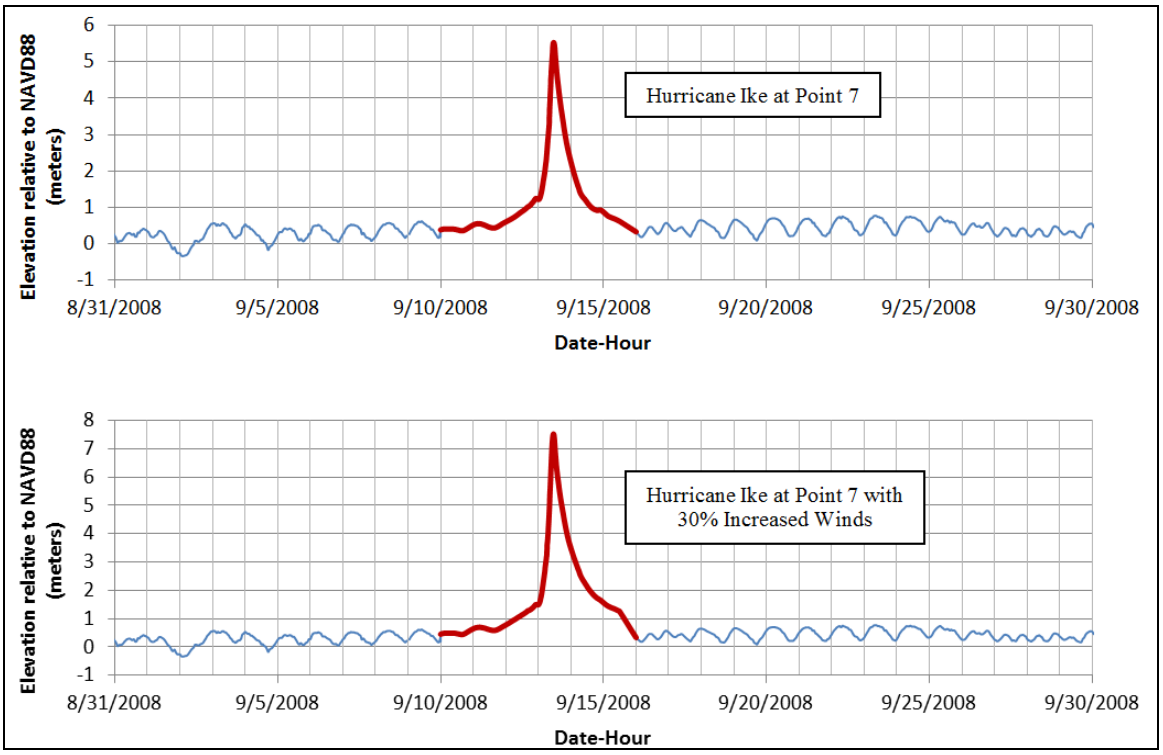

Figure 5-7. Combined open boundary at Morgan's Point applied in the EFDC-SS model for the Hurricane Ike at Point 7 (Top) and Hurricane Ike at Point 7 with 30% Increased Winds (bottom)

Table 5-3. EFDC Model Runs for Water Elevation

Run	Maximum WSE at the surge boundary (meters)
1) SWAN+ADCIRC Ike surge boundary condition	4.3
2) SWAN+ADCIRC Ike at Point 7 surge boundary condition	5.8
3) SWAN+ADCIRC Ike at Point 7 with 30% increase in winds surge boundary condition	7.4

Figure 5-8 shows the three locations (facilities 1, 5, and 9) that were modeled in an effort to provide a comparative analysis relative to findings from the vulnerability and FEDERAP components of the research. Facilities were selected to provide spill locations extending across the model domain. The three facilities represent potential spill scenarios to the far west (Facility 1), in the middle (Facility 5), and near the mouth (Facility 9) of

the HSC-IC. In addition, these facilities in particular were chosen because of the large potential losses modeled through FEDERAP in Chapter 4.

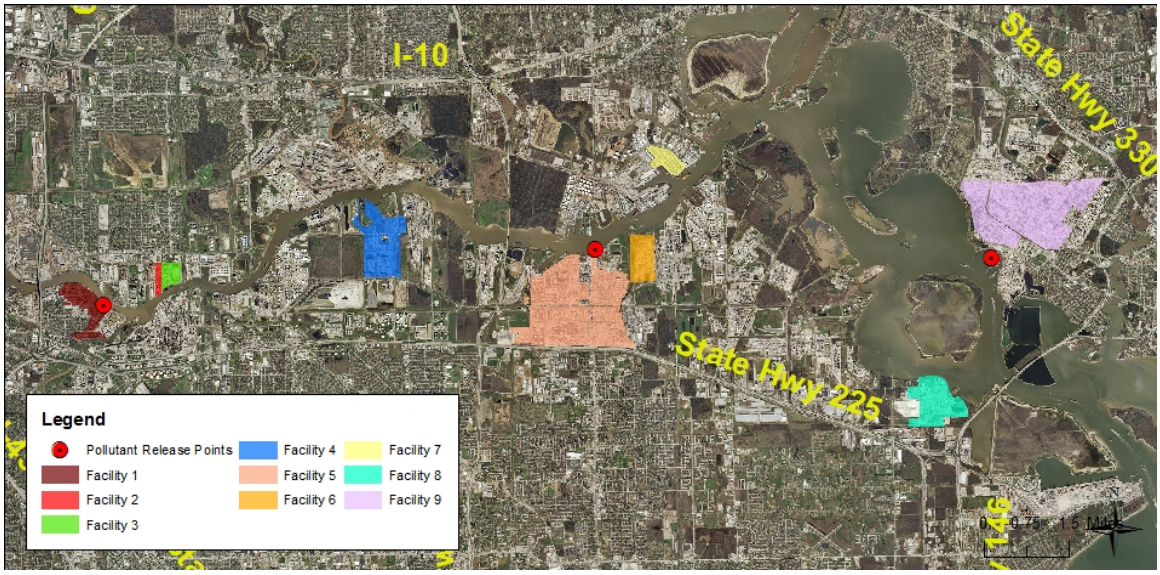

Figure 5-8. Conservative tracer release locations along the HSC associated with facilities 1, 5 and 9

Three different timings of pollutant release throughout the surge hydrograph were modeled: (a) prior to the peak, (b) at the peak, and (c) following the peak. Figure 5-9 shows the starting time of release on the hydrograph at the open boundary of EFDC-SS for Hurricane Ike. The same timing is used for the Hurricane Ike at Point 7 and Hurricane Ike at Point 7 with 30% increase in wind.

A set of model runs shown in

Table 5-4 were undertaken to simulate separately: location of spill, timing of spill, and the specific hurricane scenario that is being modeled. A combination of all of these variables results in a total of 27 model runs.

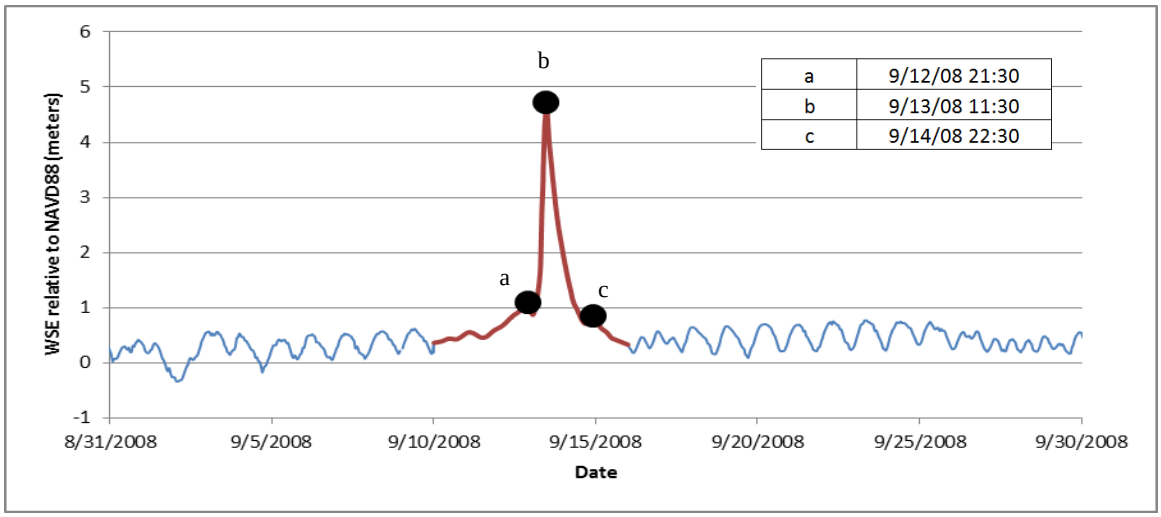

Figure 5-9. Pollutant release points (black dots) shown on the Morgan's Point open boundary condition for Hurricane Ike. The same timing is used for all three hurricane scenarios modeled.

5.3.4 CHANGES IN WATER AND SEDIMENT QUALITY DURING A HURRICANE IN THE HSC-IC

In addition to the potential for active contamination during a hurricane, the re-suspension of pollutant from bottom sediment as well as the potential mobilization of sediment would further pollute the waterway, even in the absence of other spills. Hence, to model the potential change in water and sediment quality, total suspended sediment (TSS), salinity, and bed shear stress were modeled using the three hurricane scenarios described previously (Ike, Ike at point 7, and Ike at point 7 with 30% increased winds, see Table 5-5). The purpose was to determine the potential effects on the spatial distribution and concentration of existing pollutant concentrations in the waterway.

Table 5-4. EFDC Modeled Spill Scenarios

Run	Maximum Water Elevation at the surge boundary (meters)	Location (Facility)	Timing
1.1a	4.0 (Ike Run)	1	a
1.1b	4.0 (Ike Run)	1	b
1.1c	4.0 (Ike Run)	1	c
1.5a	4.0 (Ike Run)	5	a
1.5b	4.0 (Ike Run)	5	b
1.5c	4.0 (Ike Run)	5	c
1.9a	4.0 (Ike Run)	9	a
1.9b	4.0 (Ike Run)	9	b
1.9c	4.0 (Ike Run)	9	c
2.1a	6.1 (Ike at Point 7)	1	a
2.1b	6.1 (Ike at Point 7)	1	b
2.1c	6.1 (Ike at Point 7)	1	c
2.5a	6.1 (Ike at Point 7)	5	a
2.5b	6.1 (Ike at Point 7)	5	b
2.5c	6.1 (Ike at Point 7)	5	c
2.9a	6.1 (Ike at Point 7)	9	a
2.9b	6.1 (Ike at Point 7)	9	b
2.9c	6.1 (Ike at Point 7)	9	c
3.1a	7.3 (Ike at Point 7 with 30% increase in winds)	1	a
3.1b	7.3 (Ike at Point 7 with 30% increase in winds)	1	b
3.1c	7.3 (Ike at Point 7 with 30% increase in winds)	1	c
3.5a	7.3 (Ike at Point 7 with 30% increase in winds)	5	a
3.5b	7.3 (Ike at Point 7 with 30% increase in winds)	5	b
3.5c	7.3 (Ike at Point 7 with 30% increase in winds)	5	c
3.9a	7.3 (Ike at Point 7 with 30% increase in winds)	9	a
3.9b	7.3 (Ike at Point 7 with 30% increase in winds)	9	b
3.9c	7.3 (Ike at Point 7 with 30% increase in winds)	9	c

Table 5-5. EFDC-SS model scenarios for simulating long-term sediment and water quality of the HSC-IC system after a severe storm surge event.

Run	Maximum Water Elevation at the surge boundary (meters)	Sediment Module	Water Quality Module
1.WQ	4.0 (Ike Run)	Yes	Yes
2.WQ	6.1 (Ike at Point 7)	Yes	Yes
3.WQ	7.3 (Ike at Point 7 with 30% increase in winds)	Yes	Yes

5.4 VALIDATION OF EFDC-SS TO SWAN+ADCIRC WATER SURFACE ELEVATIONS AND VELOCITIES

Water surface elevations at points within the study area were compared to water surface elevations computed in SWAN+ADCIRC for the three hurricane scenarios. Figure 5-10 shows the comparison at one of these points located near Facility 5. For Hurricane Ike, the water surface elevations for the ascent and decent parts of the hydrograph match well with computed water surface elevations from SWAN+ADCIRC. For model velocities, the velocity in the x-direction (east and west), y –direction (north and south), and the magnitude of the velocities for Hurricane Ike at a point located near Facility 5 is shown in Figure 5-11. In the x-direction, the models match in high and low velocities as well timing. However, the shift from velocities west to east occurs faster in the SWAN+ADCIRC and high velocities are sustained past the peak velocity. Since there are higher modeled velocities in EFDC-SS in the y-direction, the flow direction is northwest or southeast where as SWAN+ADCIRC is dominated to the west or east. The higher velocities modeled after the storm event in SWAN+ADCIRC may be due to water coming into the waterway from the inundated regions that is not captured in EFDC-SS without the inclusion of wetting and drying.

The peak storm surge modeled in EFDC-SS is higher than SWAN+ADCIRC by 0.9 m. For Hurricane Ike at Point 7, the EFDC-SS results compare well for the highest modeled WSEs but underestimate the water levels by 0.2 m for the days following the storm surge event. The validation of Hurricane Ike at Point 7 with increased winds shows that the EFDC model consistently underestimated the water surface elevations by 0.5 to 1.0 m. This could be a result of EFDC-SS inability to propagate higher storm surge levels

through the entire model due to the narrow grid and inflows from the San Jacinto River from the northern portion of the model grid working against the storm surge boundary condition. Even though water levels within the HSC-IC did not match with SWAN+ADCIRC for the scenario and given that the general shape of the WSE was matched well, the model was used for the remaining pollutant transport simulations.

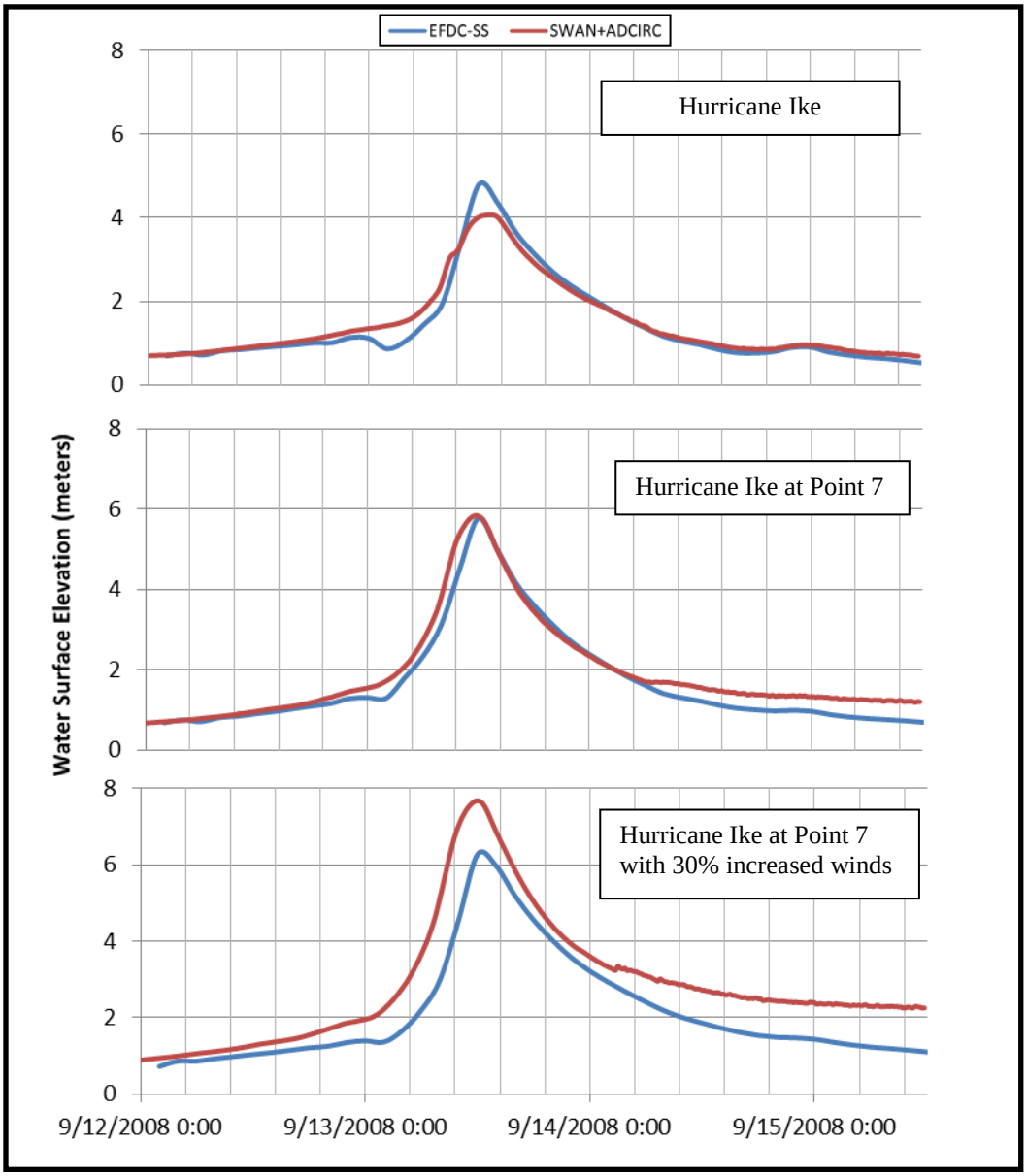

Figure 5-10. Comparison of WSE from EFDC-SS to modeled WSE from SWAN+ADCIRC at location in model domain near Facility 5.

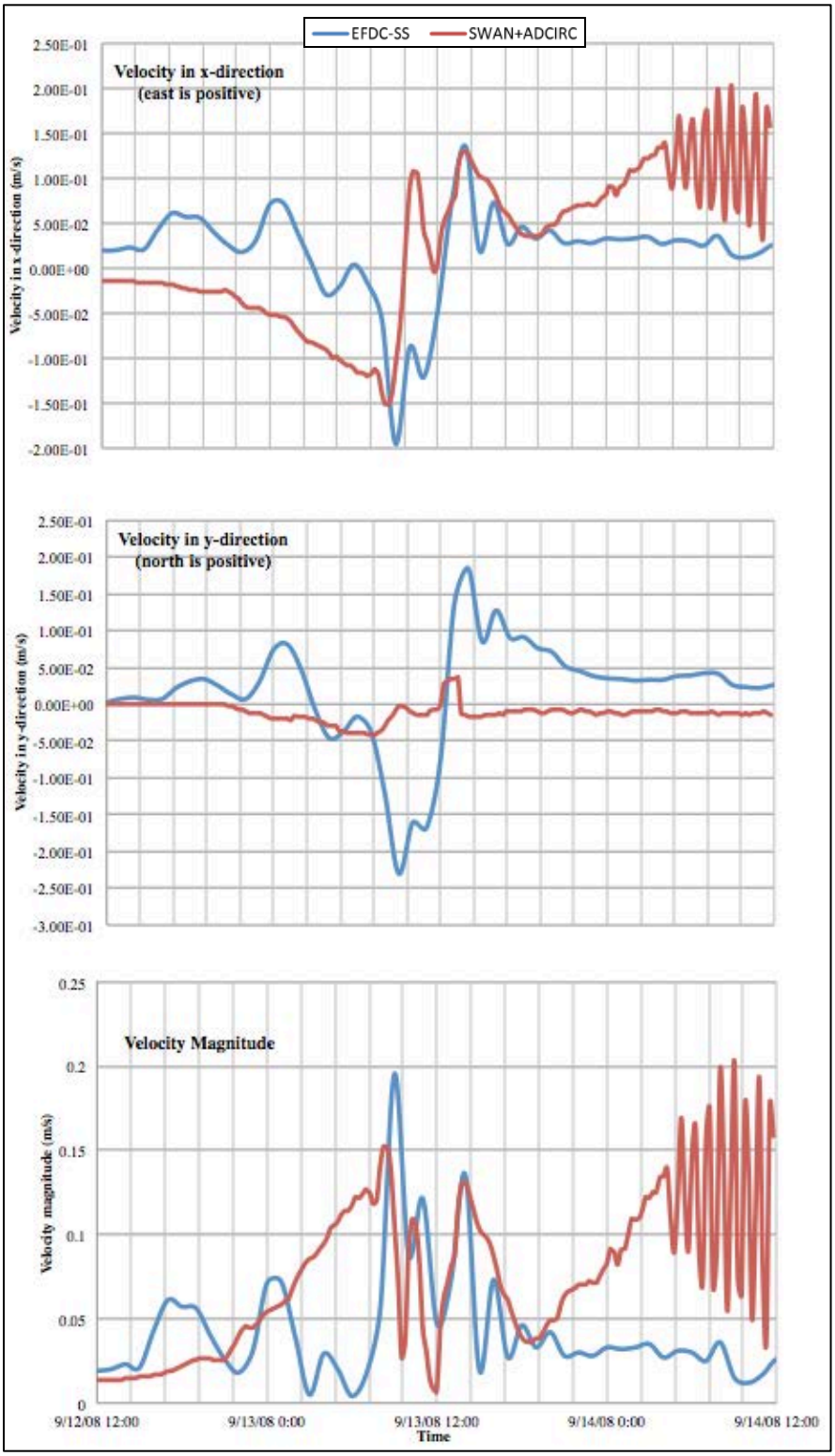

Figure 5-11. Comparison of modeled velocities from EFDC-SS to modeled velocities from SWAN+ADCIRC at location in model domain near Facility 5

5.5 POLLUTANT RELEASE RESULTS AND DISCUSSION

For the purpose of initially analyzing the impact of timing of the dye release, Hurricane Ike with a release at Facility 1 prior to peak storm surge is used as the "Base model" run (1.1a). The depth-averaged dye concentration at various times in the model run following the release is shown in Figure 5-12. Recall from Figure 5-8 that Facility 1 is located towards the far west of the HSC-IC and for this scenario the release occurs on 09/12/2008 at 9:30PM. By 09/15/2008 at 12:00AM, the conservative tracer has a spatial spread from the far west boundary of the HSC-IC to the southern boundary near Morgan's point. For the next 8 days, the dye concentration increases moving east with a high concentration developing west of Alexander Island in the Upper San Jacinto Bay (Figure 5-1). While depth-averaged dye concentration is used to assess the transport of the tracer for the different scenarios, there is observed differences in dye concentration within the water column. Figure 5-13 shows the concentration of dye in each of the five layers for various times in the model run. The high concentrations are observed lower in the water column over time due to mixing caused by advection caused by high water levels and inflows and diffusion at the point of the spill due to the high concentration at the top layer. In general, there is equal mixing in the system though as the dye moves away for the spill location, the high concentration of dye is modeled in the top three layers (upper 80% of the water column). A lower density non-conservative tracer would significantly change the distribution of dye concentrations in the water column; hence, the result focuses on depth-averaged dye concentrations throughout the system.

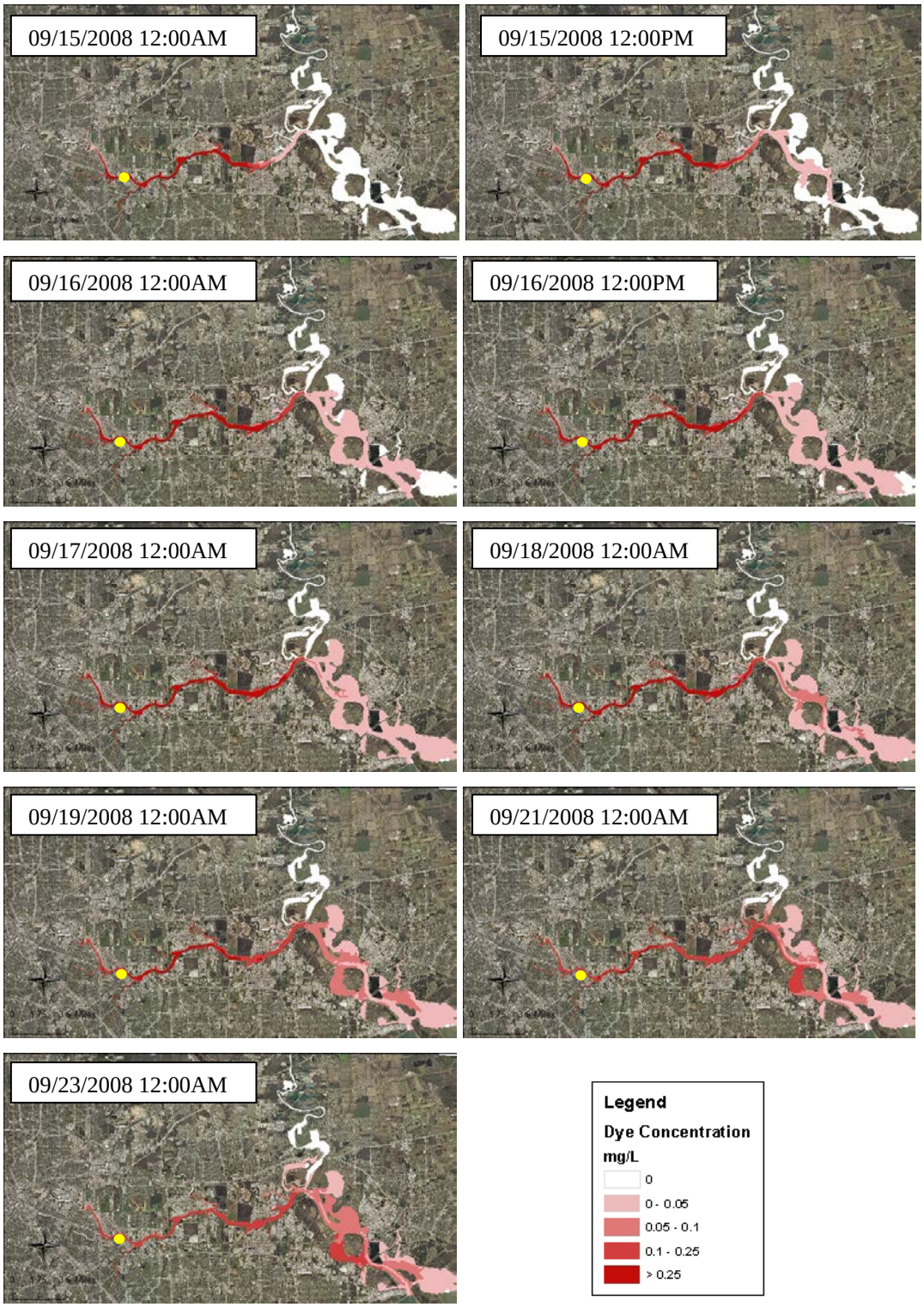

Figure 5-12. Dye concentration for model run 1.1a (Hurricane Ike with release at Facility 1 indicated by the yellow dot prior to peak storm surge) at various times during and following the storm surge event.

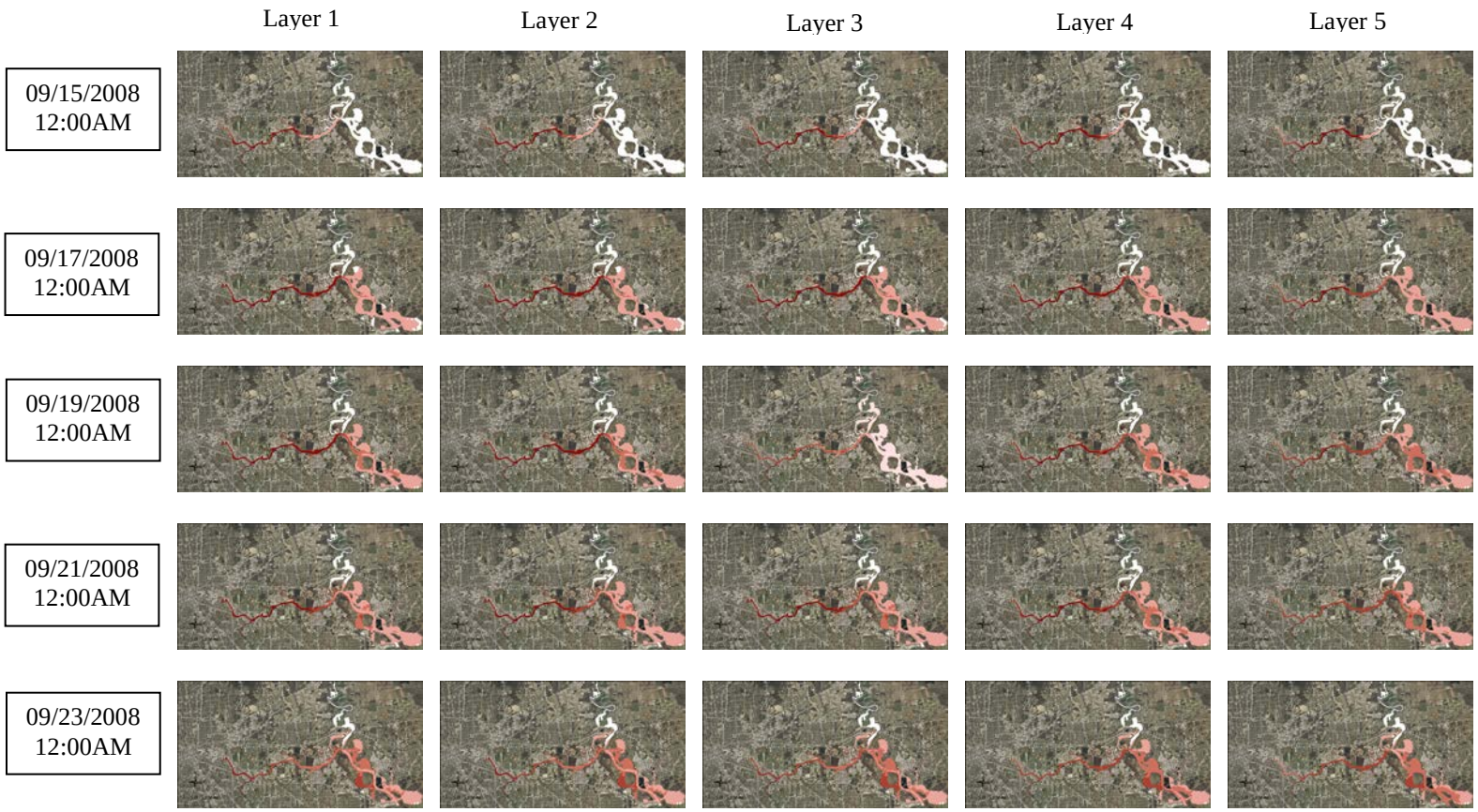

Figure 5-13. Dye concentration in each water layer (Layer 1 is the top layer) for model run 1.1a (Hurricane Ike with release at Facility 1) at various times during and following the storm surge event.

5.5.1 SPATIAL VARIABILITY OF POLLUTANT RELEASE IN HSC-IC

Figure 5-14 and Figure 5-15 present the depth-averaged dye concentration at various times in the model for Hurricane Ike with a release location at Facility 1 at the peak storm surge (1.1b) and following the peak storm surge (1.1c), respectively. For run 1.1b, the concentration of dye reaches the open boundary at Morgan's point at the same time as run 1.1a despite the release occurring almost 12 hours later indicating that a release that co-occurs with the peak storm surge or prior would result in similar spatial timing and spread. This is likely caused by the increase in velocities downstream as the water levels recede. In contrast, when the dye is released after the peak storm surge, the velocities are significantly lower resulting in the dye not reaching the open boundary until after 09/19/2008, over 4 days after the water levels have returned to typical elevations (between 0 and 1 m – NAVD88).

In general, for the three different release-timing scenarios, the highest concentrations of dye at 9/23/2008, ten days following Hurricane Ike, are located in Upper San Jacinto Bay and west of the battleship. Difference plots were developed from the three model runs. In Figure 5-16, the largest decrease of dye concentration at 9/23/2008 is observed to the west due to the force of the storm surge subsiding as the water level decreased from peak storm surge. For run 1.1b, release during peak surge, the northern shores and side bays are more vulnerable where the opposite is true when the release occurs after the storm surge has passed (run 1.1c). Therefore the timing of the release is a significant indicator of which parts of the system are polluted in the aftermath of a storm surge event.

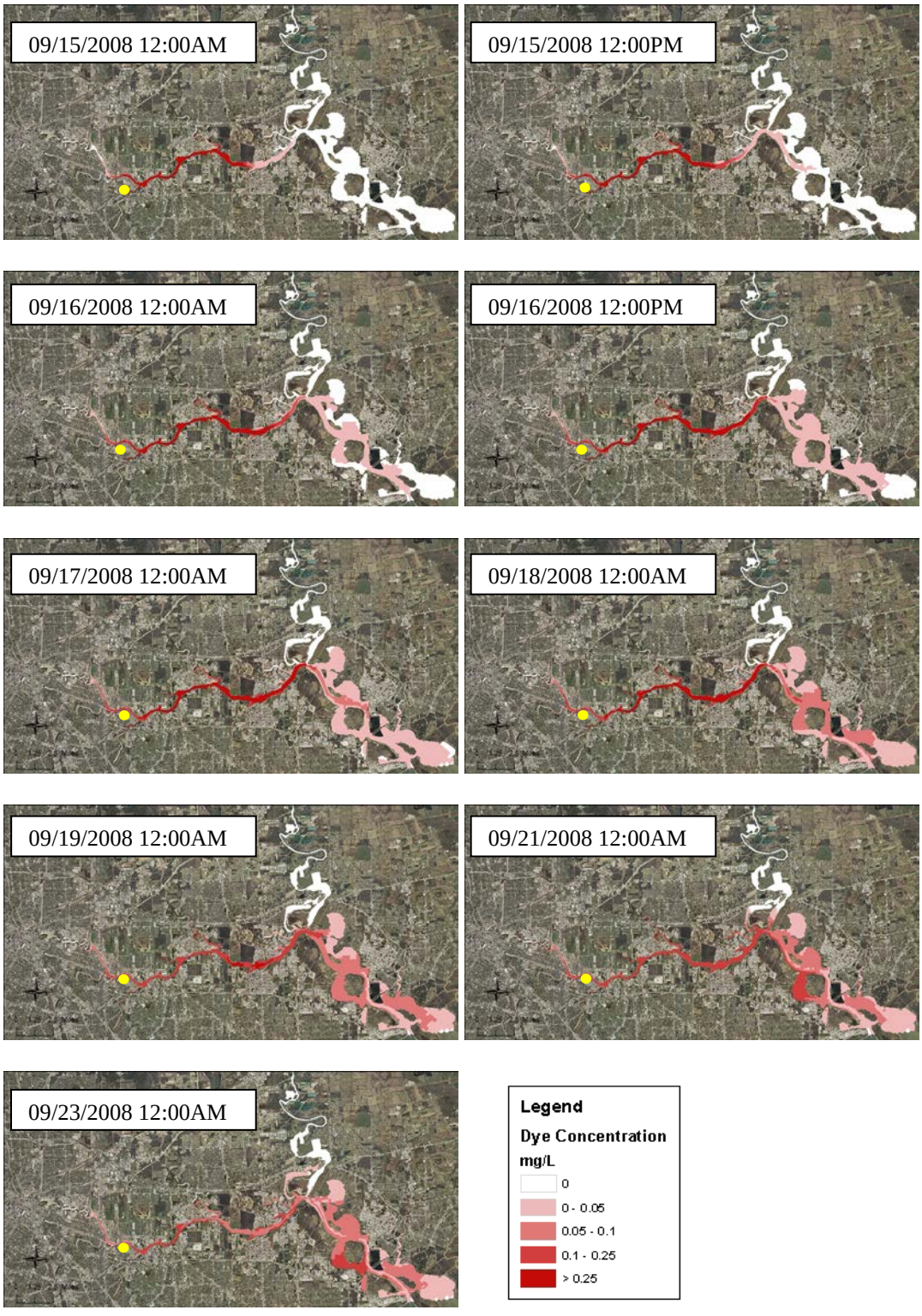

Figure 5-14. Dye concentration for model run 1.1b (Hurricane Ike with release at Facility 1 indicated by the yellow dot at peak storm surge) at various times during and following the storm surge event.

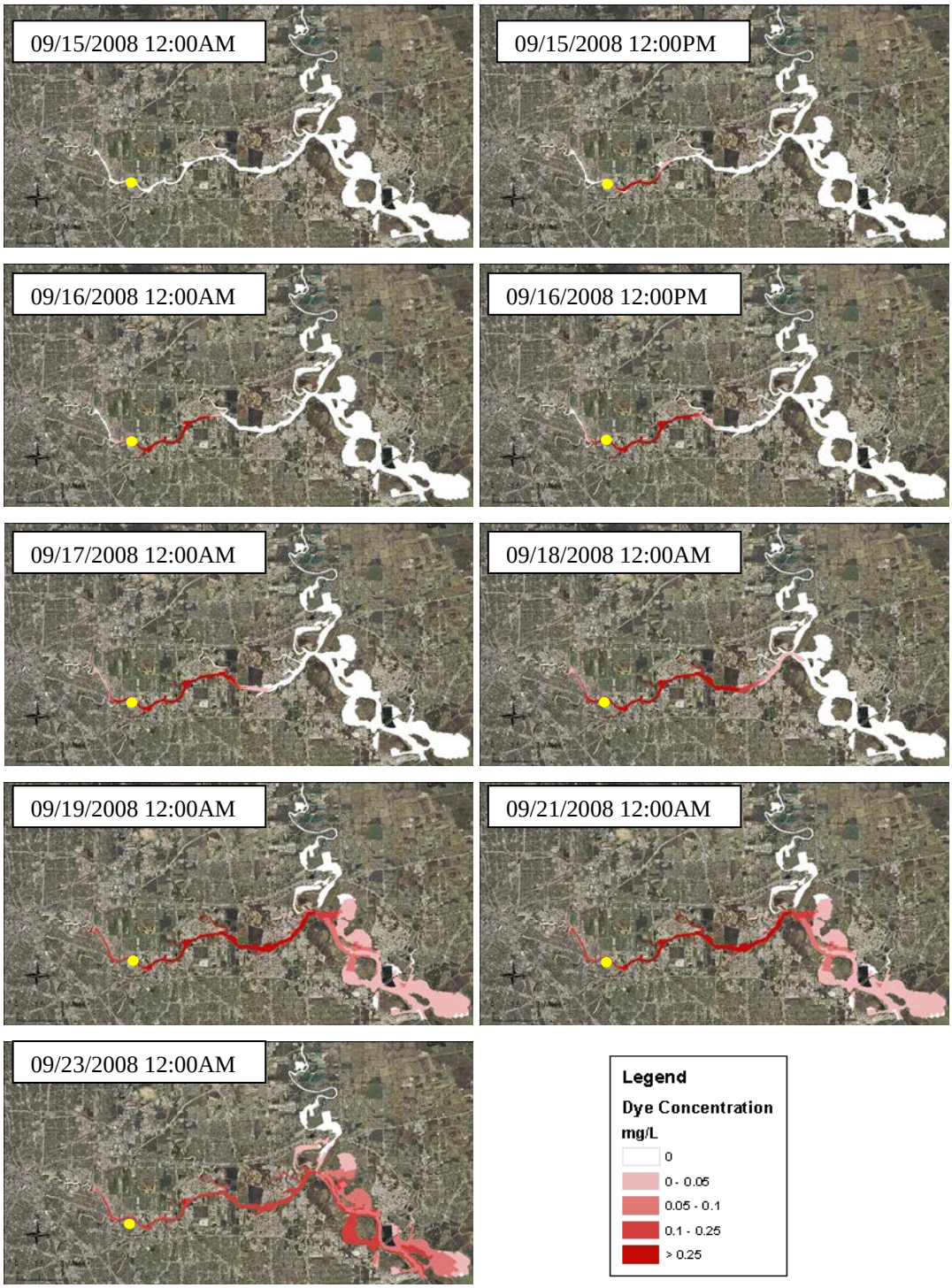

Figure 5-15. Dye concentration for model run 1.1c (Hurricane Ike with release at Facility 1 indicated by the yellow dot after peak storm surge) at various times during and following the storm surge event.

Figure 5-17 and Figure 5-18 show the depth-averaged dye concentration for a spill at the peak storm surge level for Hurricane Ike at Facility 5 and Facility 9, respectively. Since the model was designed to release at a certain concentration for the model cell closest to the facility of interest, the total amount of dye release varies due to the difference in model cell size for the three release locations and the water levels modeled during the time of release. In addition, a significantly larger portion of the dye at Facility 9 leaves through the open boundary resulting in very low concentrations compared to the other two locations. Hence, a different scale for visualization of the results is used for each. For a release at Facility 5 (run 1.5b), dye concentrations are observed at the open boundary significantly sooner than run 1.1b. Possibly due to the impact of the tributary inflows to the west of Facility 5, the dye does not reach past Green's Bayou. Green's Bayou has significant flows for this event and may be acting as a barrier to prevent a potential spill from moving west; in which case, it could be aiding in the movement east towards Galveston Bay. For a release at Facility 9 (run 1.9b), the dye concentration stays contained within the eastern portion of the Upper San Jacinto Bay with the highest residual dye concentrations by 09/23/2008 observed in and around Goose Creek. A spill near Facility 9 at peak storm surge shows minimal spatial movement within the model domain though this may be due to significant loss of dye through the open boundary (i.e., into Galveston Bay).

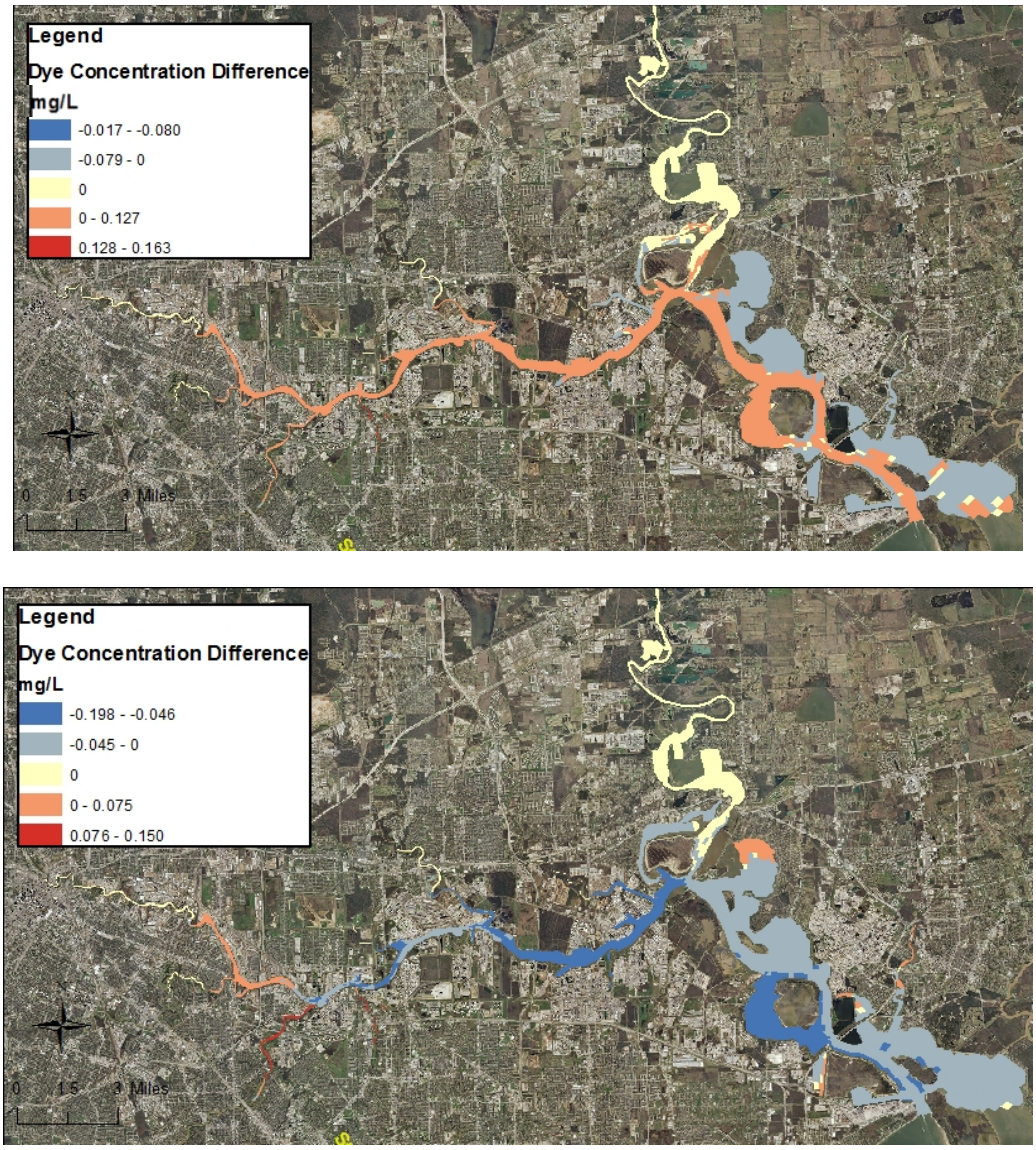

Figure 5-16. Difference in dye concentration at 09/23/2008 12:00AM compared to the base model run shown in Figure 5-9 based on the timing of dye release. (top) Comparison of 1.1a and 1.1b (bottom) Comparison of 1.1a and 1.1c

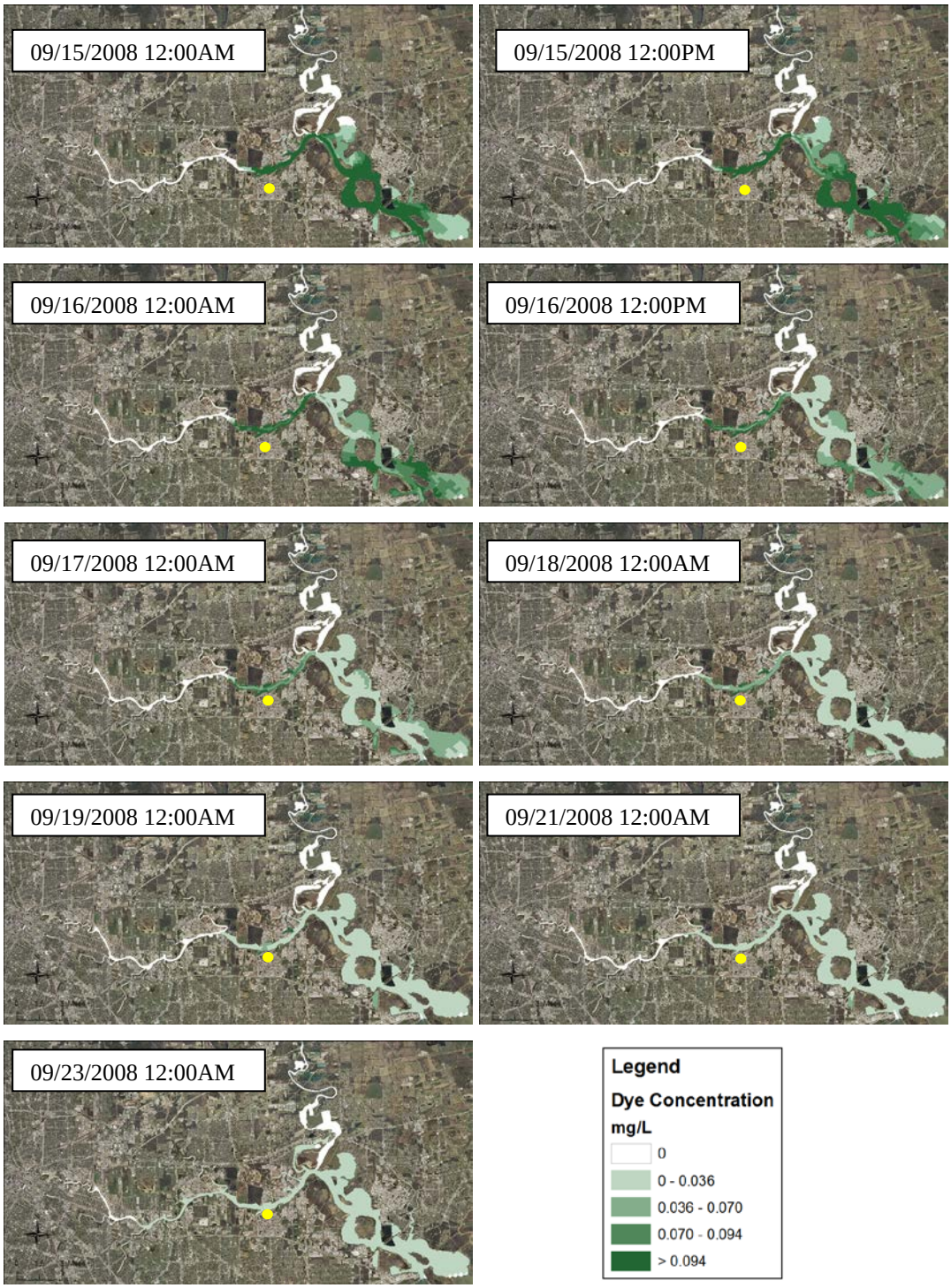

Figure 5-17. Dye concentration for model run 1.5b (Hurricane Ike at with release at Facility 5 indicated by the yellow dot at peak storm surge) at various times during and following the storm surge event.

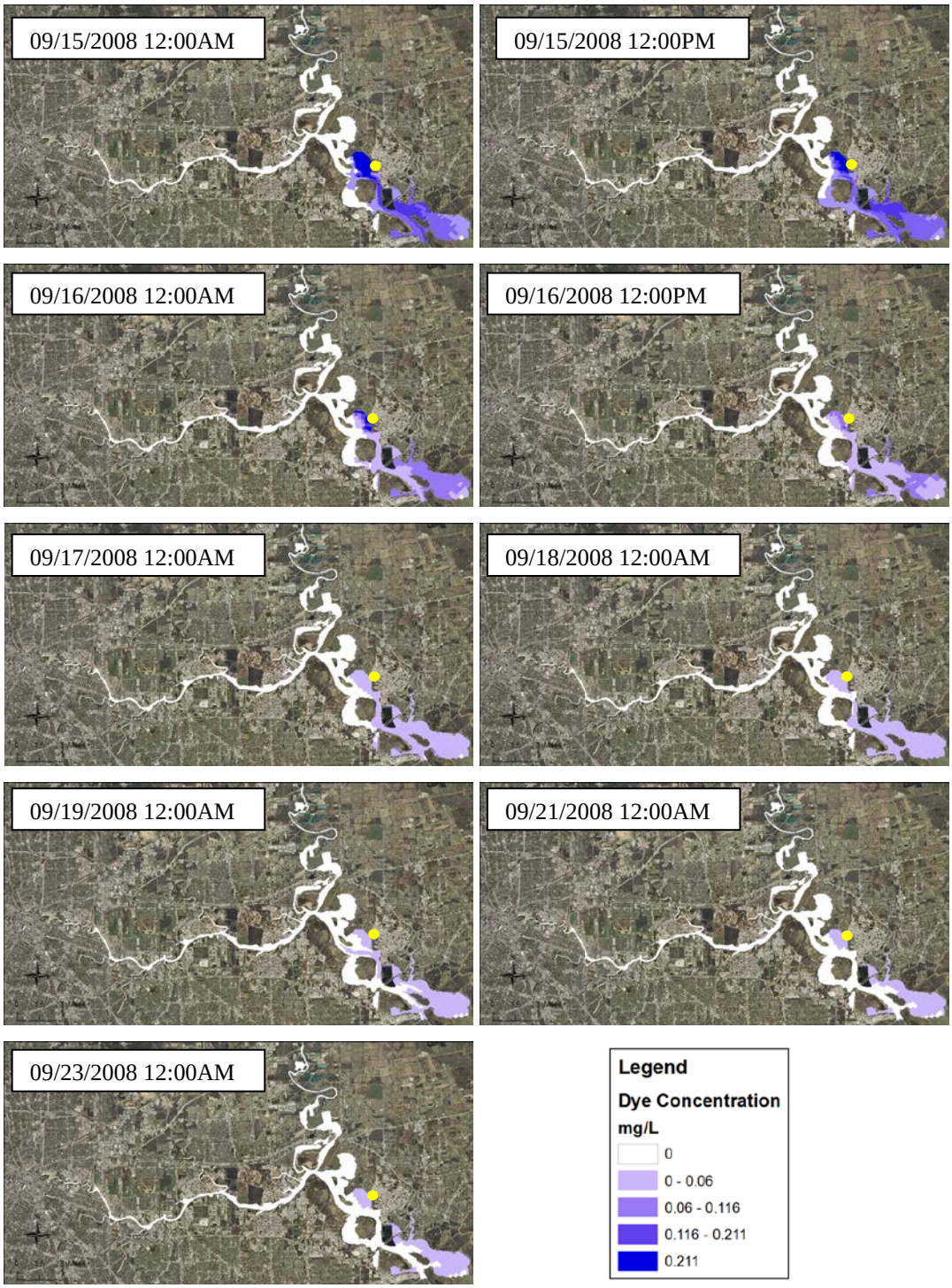

Figure 5-18. Dye concentration for model run 1.9b (Hurricane Ike at with release at Facility 9 indicated by the yellow dot at peak storm surge) at various times during and following the storm surge event.

Figure 5-19 and Figure 5-20 present the dye concentration at various times in the model for releases at Facility 1 at the peak of the storm surge for Hurricane Ike at Point 7 (2.1b) and Hurricane Ike at Point 7 with 30% increased winds (3.1b), respectively. Since, in general the timing of a release at the peak of the storm surge (scenario b) led to an increase in pollution across the HSC-IC, this timing was used in the comparative analysis for the different hurricane scenarios. For model run 2.1b, the higher concentrations of dye are observed to the west and the dye does not reach the open boundary toward Galveston Bay until 09/15/2008 at 12:00PM. Figure 5-21 shows the change in dye concentration at various time steps between Hurricane Ike (run 1.1b) and Hurricane Ike at Point 7 (run 2.1b). Within 24 hours after the storm surge event, higher concentrations are modeled in the eastern portion of the model domain. However, by 09/16/2008 at 12:00AM, the change in concentrations of dye begins to shift and higher concentrations are observed east of the Battleship. It is important to note that these differences are very small (near zero), which explains the sudden change observed on 09/21/2008 to 09/23/2008. For a storm surge event with large WSE levels (3.1b), similar results are observed with dye concentration pushing west in the HSC-IC into downtown Houston. With the increase in storm surge, the dye reaches the open boundary almost 12 hours earlier though lower concentrations are modeled east of the Battleship most likely due to the increased forcing to the north and east from high WSE modeled for Hurricane Ike at Point 7 with increased winds. Unlike run 2.1b, with a higher storm surge event, higher concentrations of dye become present east of the Battleship and near the open boundary significantly sooner (12 to 24 hours before this shift is observed when analyzing the difference between 1.1b and 2.1b). This result may indicate that a high storm surge event disperses higher

concentrations of a pollutant to the west and east of the HSC-IC when the spill co-occurs with the peak of the storm surge within the near-town part of the HSC.

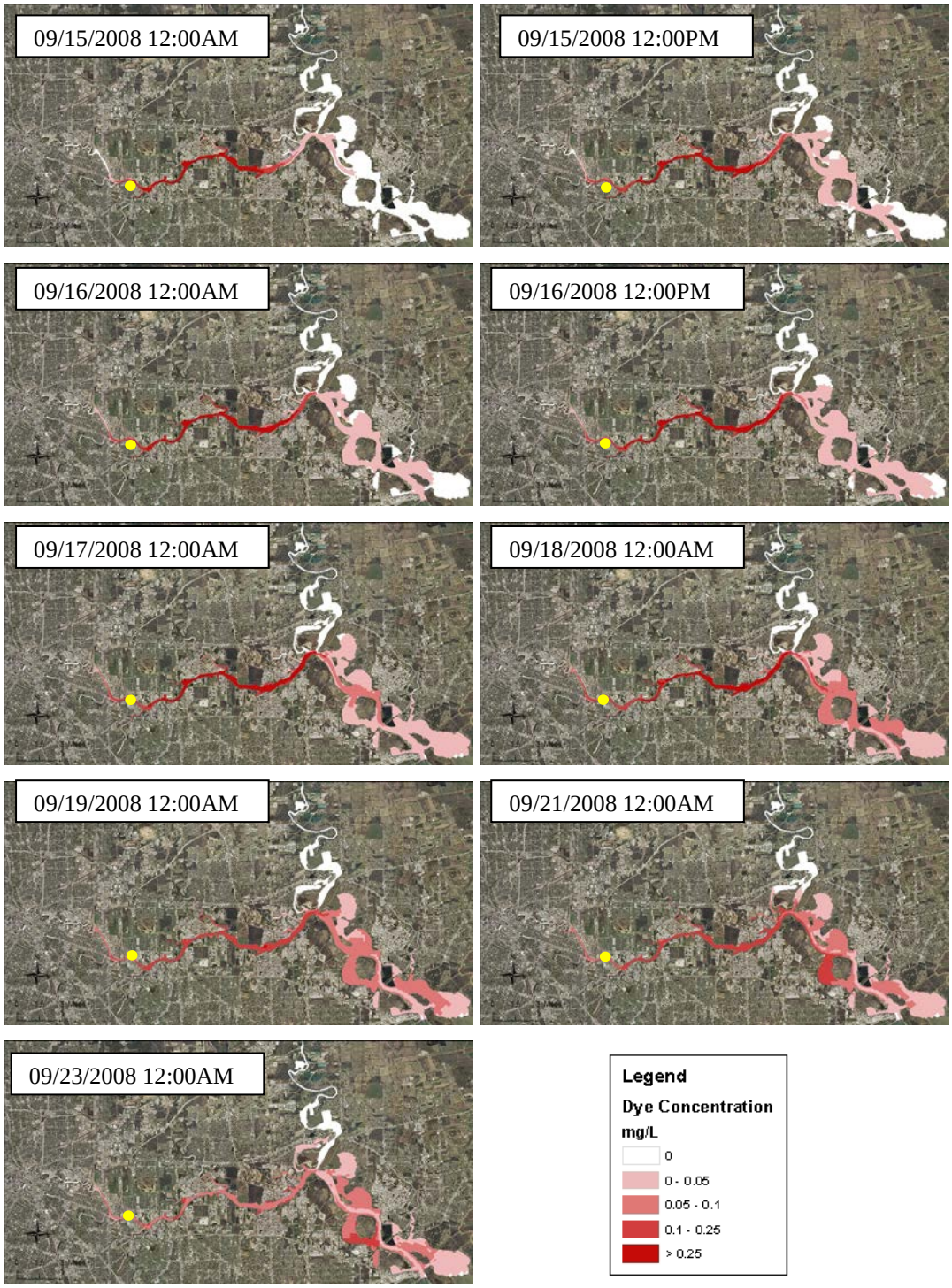

Figure 5-19. Dye concentration for model run 2.1b (Hurricane Ike at Point 7 with release at Facility 1 indicated by the yellow dot at peak storm surge) at various times during and following the storm surge event.

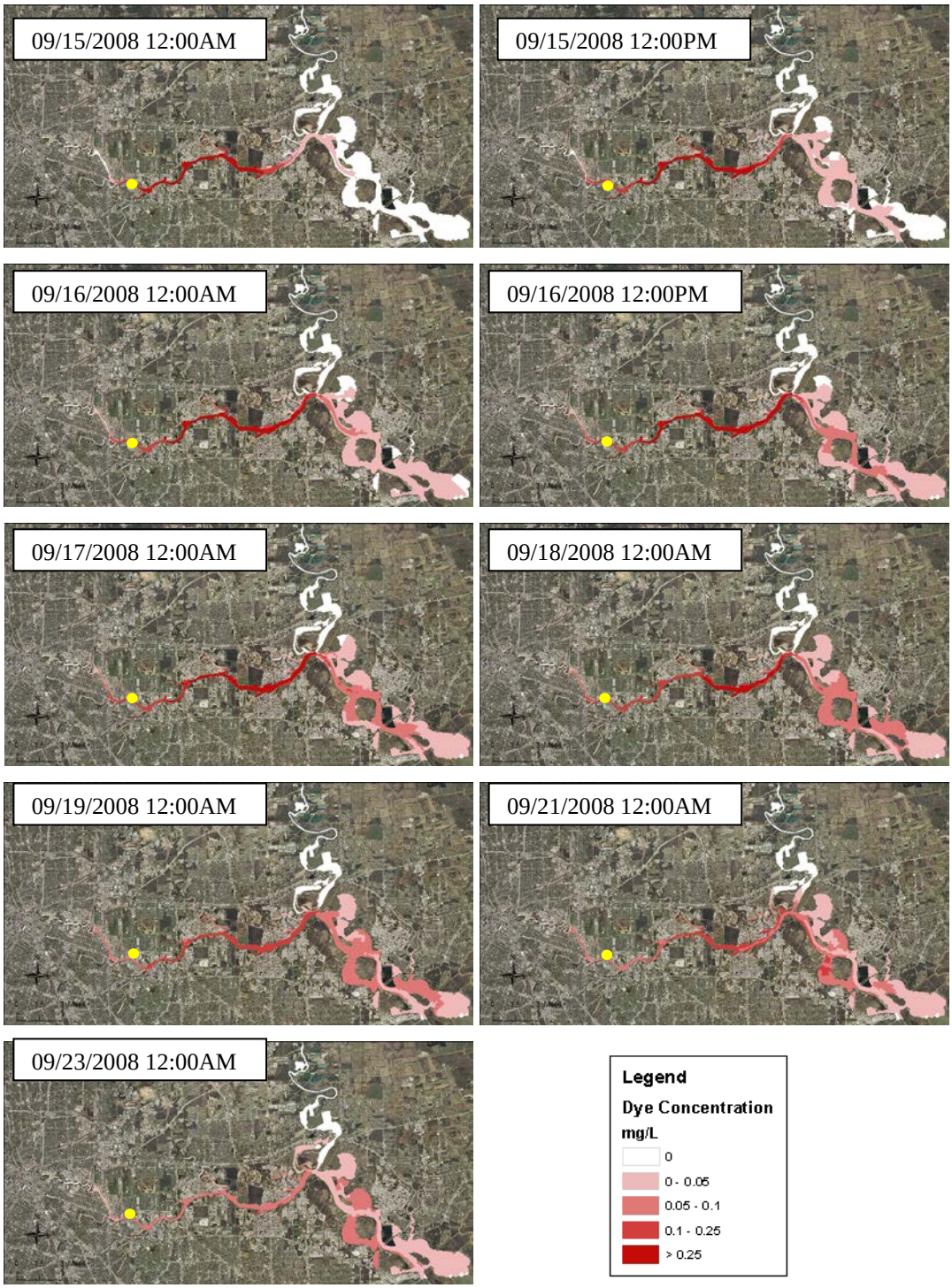

Figure 5-20. Dye concentration for model run 3.1b (Hurricane Ike at Point 7 with 30% increase in wind speed with release at Facility 1 indicated by the yellow dot prior to peak storm surge) at various times during and following the storm surge event.

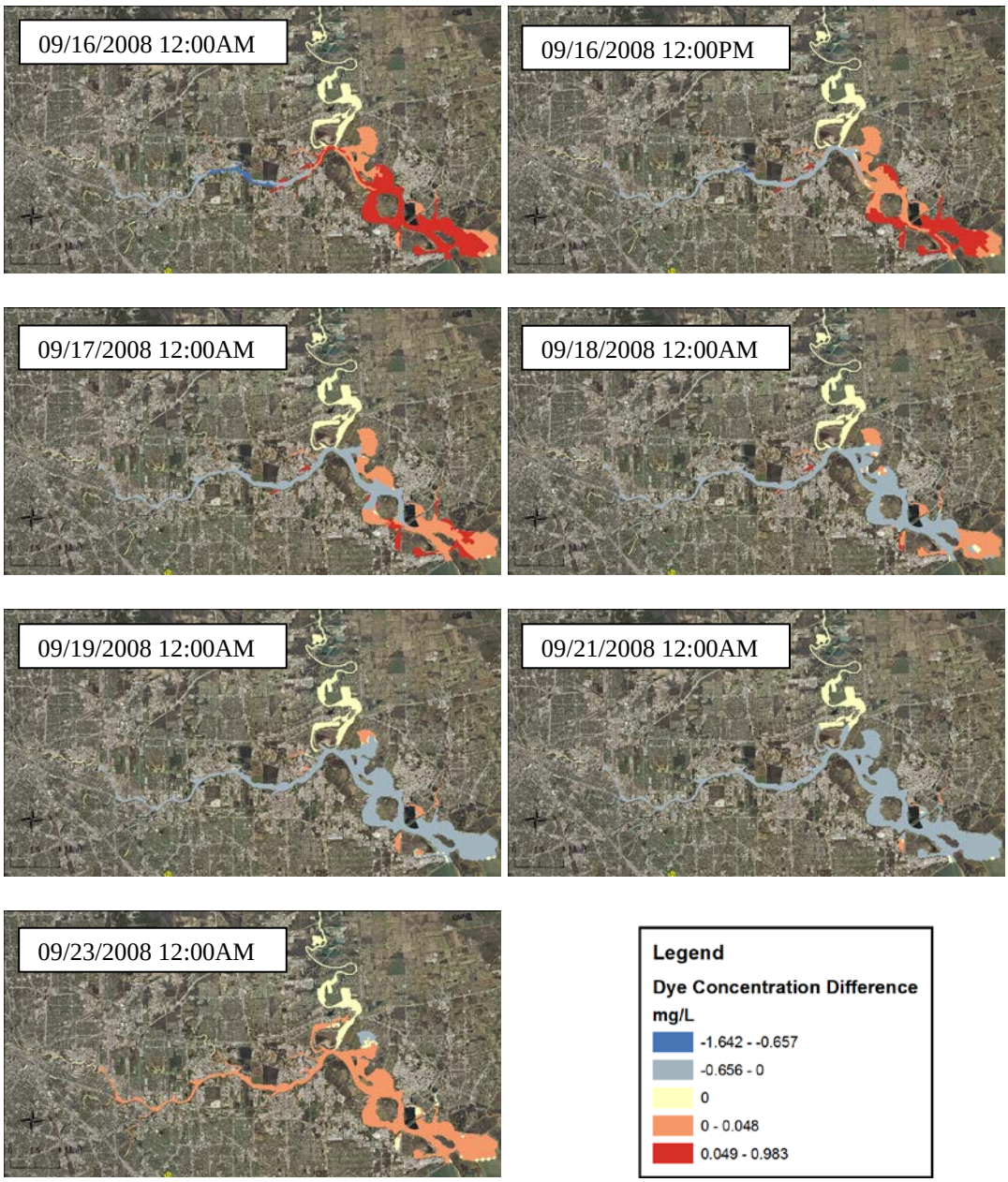

Figure 5-21. The change in dye concentration at various time steps from model run 1.1b (Hurricane Ike with release at Facility 1 at peak storm surge) when Hurricane Ike is shifted to Point 7 (2.1b).

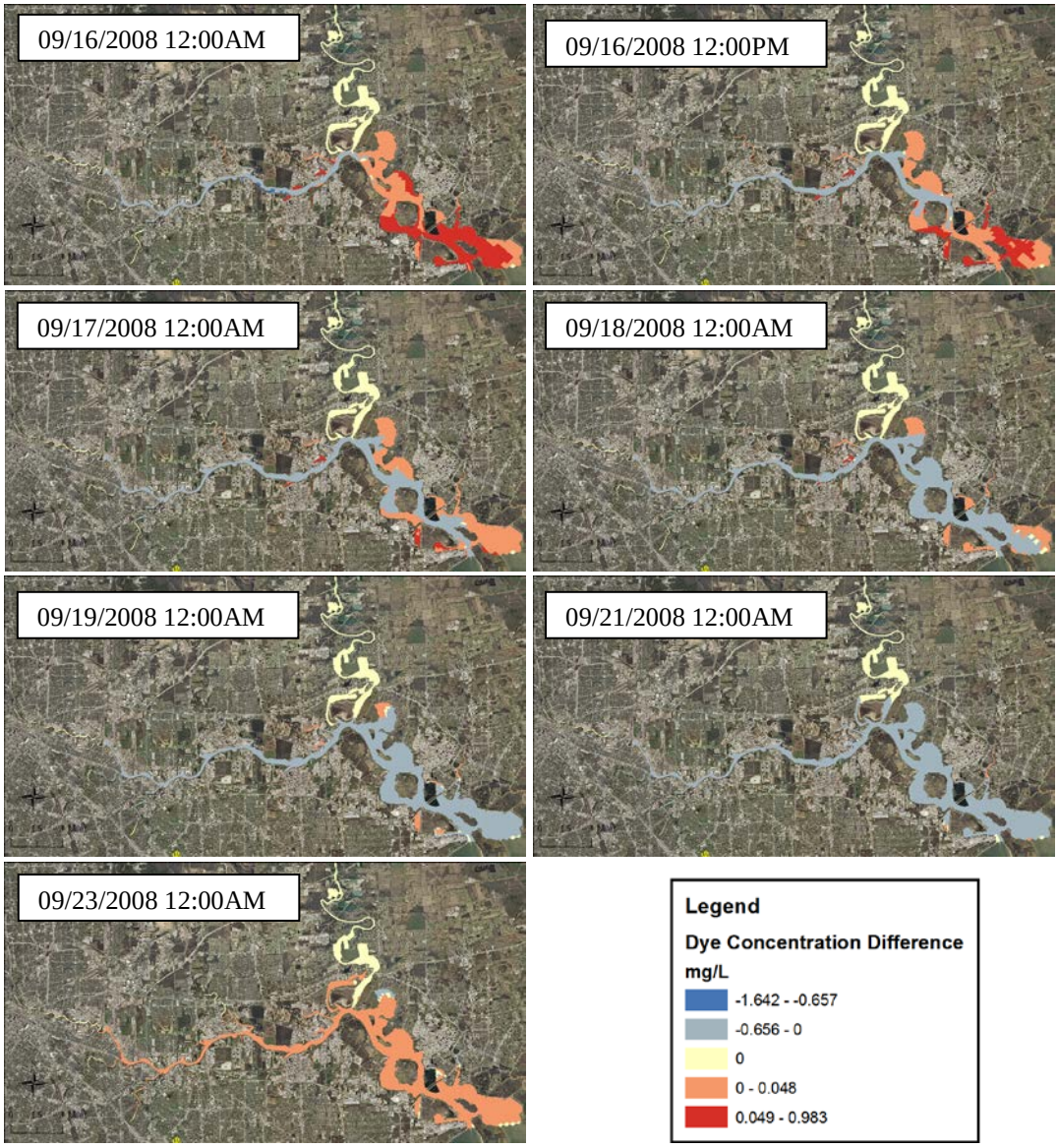

Figure 5-22. The change in dye concentration at various time steps from model run 1.1b (Hurricane Ike with release at Facility 1 at peak storm surge) when Hurricane Ike is shifted to point 7 with winds increased by 30% (3.1b).

5.5.2 MASS BALANCE OF CONSERVATIVE DYE IN HSC-IC

Table 5-6 presents the dye mass (metric tons or MT) that is spilled for each scenario based on a constant spill concentration of 1000 mg/L over a 12-hour time period in the model grid closest to the facility of interest. The dye lost through the open boundary at Tabbs Bay and Morgan's Point provides a quantitative method for determining the potential contamination that would enter Galveston Bay. Note, for the base model run (Facility 1 for Hurricane Ike prior to peak), 0.135 MT of the 42.6 MT dye released was unaccounted for in the system (0.3%). Therefore, EFDC-SS conserves dye mass.

For a spill scenario at Facility 1, the worst-case scenario is a spill occurring at the peak of storm surge. In addition, as storm surge increases, a higher percentage of the dye leaves through the open boundary (49% for Hurricane Ike and 59% for Hurricane Ike at Point 7 with increased winds). In the case of a release at Facility 5, a release prior to the peak storm surge was the worst-case timing for Galveston Bay as over 90% of the dye release leaves the boundary for all three-hurricane scenarios. At this location, an increase in hurricane strength does not have a significant impact on the amount of dye lost through the open boundary. Similarly, at Facility 9, a release prior to peak storm surge results in near all of the dye mass being pushed into Galveston Bay. Facility 9 is the closest spill location to the open boundary; results from spill simulations at this facility indicated that any spill east of the Battleship entrance to the HSC would lose at least 80% of its mass into Galveston Bay, approximately nine days after the storm surge event.

Table 5-6. Mass of dye leaving the model domain through the open boundary at Tabbs Bay and Morgan's Point for each of the model scenarios through 09/23/2008 at 12:00AM.

	Dye Spilled (MT)	Dye lost through Open Boundary (MT) Absolute	Dye lost through Open Boundary (MT) Normalized to Base run	Percent in Bay (%)
Base Run (1.1a)	42.6	20.8	-	49%
1.1b	49.7	24.3	20.9	49%
1.1c	46.5	11.8	10.8	25%
1.5a	42.4	38.9	39.1	92%
1.5b	49.7	39.9	34.2	80%
1.5c	49.5	29.8	25.7	60%
1.9a	42.7	42.7	42.7	100%
1.9b	49.7	42.9	36.8	86%
1.9c	49.4	40.7	35.1	82%
2.1a	42.6	21.9	21.9	51%
2.1b	49.6	26.1	22.4	53%
2.1c	46.5	12.3	11.2	26%
2.5a	46.0	26.2	24.3	57%
2.5b	49.5	30.2	26.0	61%
2.5c	46.2	40.5	37.4	88%
2.9a	42.7	43.3	43.2	100%
2.9b	49.8	43.6	37.4	88%
2.9c	45.8	41.3	38.4	90%
3.1a	42.6	23.3	23.3	55%
3.1b	49.6	29.2	25.1	59%
3.1c	46.3	14.5	13.3	31%
3.5a	42.6	39.2	39.2	92%
3.5b	49.9	40.9	34.9	82%
3.5c	46.4	14.6	13.4	31%
3.9a	42.7	42.7	42.7	100%
3.9b	49.8	43.9	37.6	88%
3.9c	49.2	44.2	38.3	90%

5.5.3 SENSITIVITY ANALYSIS OF EDFC-SS

A sensitivity analysis was undertaken to evaluate the effect of model variables that were not varied in the simulations discussed above. The length of time of the release and total dye amount were varied using model run 1.1a as the base run. Table 5-7 presents the results of the sensitivity analysis on these variables.

For length of time of spill, the concentration was varied so that the same quantity of dye was released into the system but over a 24-hour and a 6-hour period of time. For loss through the open boundary, doubling the time of release increased the amount of dye into Galveston Bay by less than 10%. For a shortened release period of 6 hours, the amount of dye entering Galveston Bay decreased by less than 5%. The results indicated that for the same quantity of spill, the vulnerability of Galveston Bay to contamination is relatively unchanged if the contaminant is released rapidly or more slowly. In addition, for this variable, the spatial sensitivity within the modeled system is shown in Figure 5-23 and Figure 5-24 for various times in the model. For a shorter release time, higher concentrations of dye are observed east of the release point and lower concentrations are noted near and to the west of Facility 1. The spatial spread of dye concentration matches coverage of the base run and once the releases cease, the magnitudes of these concentrations are relatively small indicating minimal sensitivity to the length of time of release for the HSC-IC.

Table 5-7. Sensitivity results for length of time for spill release, model time step, and dye concentration.

	Dye Spilled (MT)	Dye out through Open Boundary (MT)	Percent in Bay (%)
Base Run (1.1a)	42.6	20.8	48.8
Length of time for spill release (Base = 12 hours)			
24 hour	42.6	22.5	52.8
6 hour	42.6	19.2	45.1
Total Dye Spilled (42.6 metric ton)			
50% spill reduction	21.3	10.1	47.4
25% spill reduction	32.0	15.1	47.2
25% spill increase	53.3	25.2	47.3
50% spill increase	64.0	30.2	47.4

The results for sensitivity to dye spill amount had no impact on the spatial changes of the movement of the dye within the HSC-IC system and therefore are not presented. In Table 5-7, the total mass flux of dye into and out of the system for these changes in concentration are shown to have little change in the total percent of dye lost through the open boundary, between 45% and 50% for all of the sensitivity runs related to quantity of release. The total mass reaching Galveston Bay, however, is significantly higher as more dye was spilled indicating an increased vulnerability to the size of the spill.

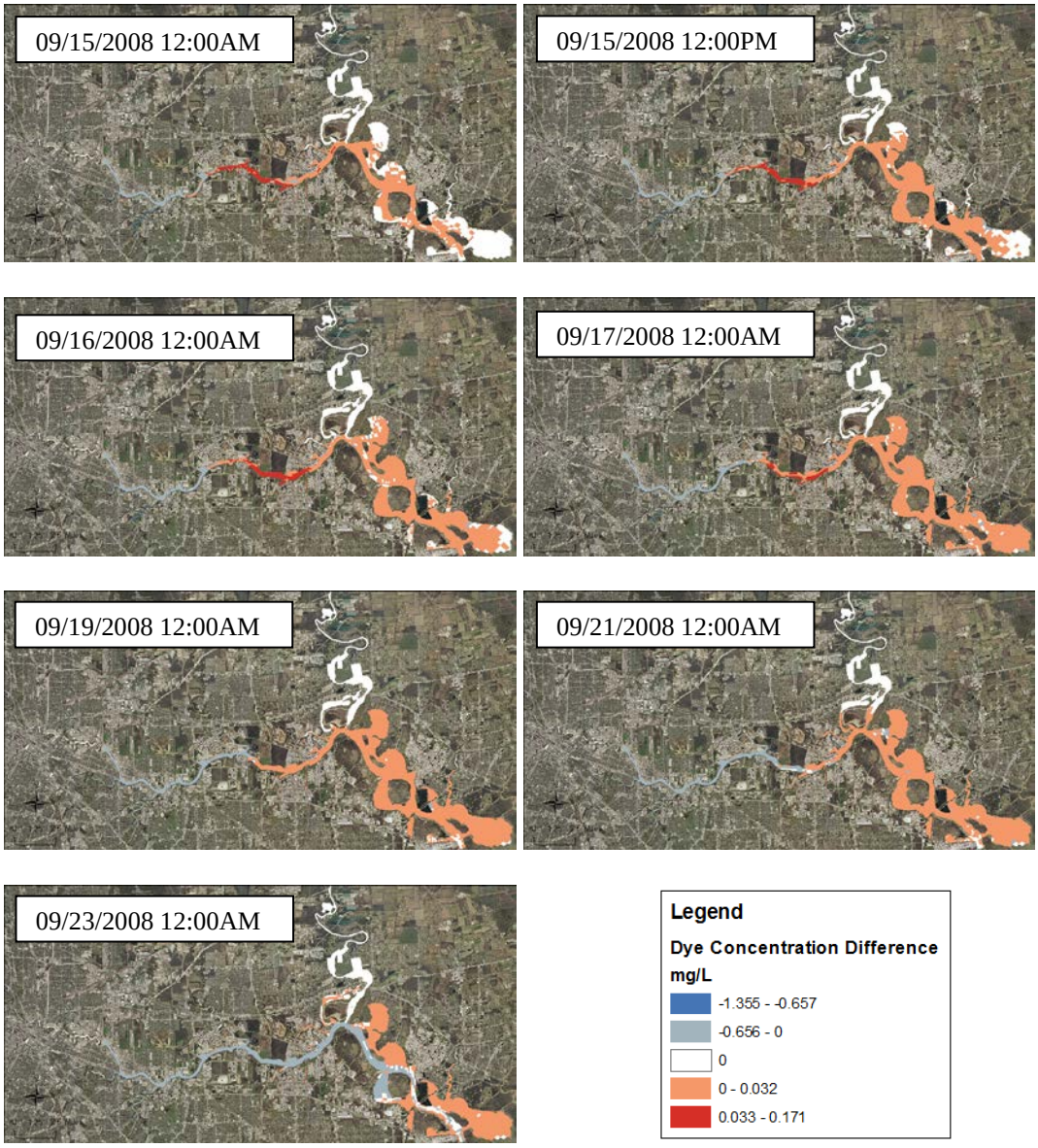

Figure 5-23. Change in dye concentration for dye release in half the time (6 hours) of the base model run.

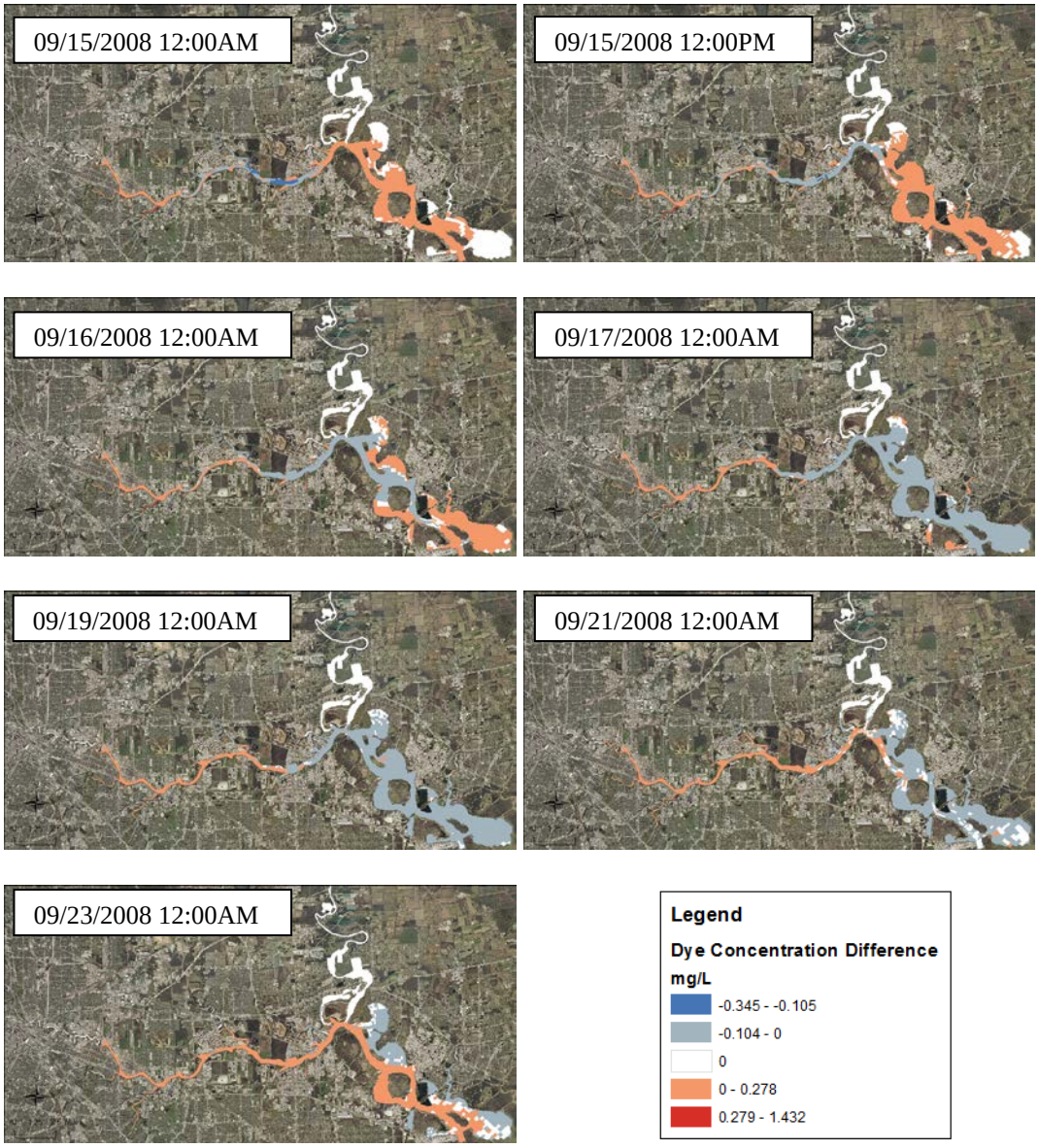

Figure 5-24. Change in dye concentration for dye release over a 24-hour period versus the base model run dye release of 12 hours.

5.5.4 ADAPTION TO ON ENVIRONMENTAL LOSS MODULE FOR FEDERAP MODEL

The FEDERAP model, presented in Chapter 4 of this thesis, applies a cleanup cost of $30.61 per liter spilled from a facility tank (Etkin, 2000), based on estimates for in-port spills. However, modeled spill scenarios from EFDC-SS showed significant loss of spill out of the port region and into Galveston Bay. Etkin (2000) does not have specific estimates for the change in cost in a bay system. However, the EPA Basic Oil Spill Cost Estimation Model (BOSCEM) developed by Etkin (2004) provides a model where in-port and bay spill costs can be differentiate through input criteria for the spill cost model are shown in Table 5-8. The input criteria and are applied to cost for response cost,

$$response\ cost\ (per gallon)\ X\ medium\ modifier\ X\ spill\ amount = total\ response\ cost, \quad (4)$$

socioeconomic cost,

$$socioeconomic\ cost(per gallon)\ X\ socioeconomic\ cost\ modifier\ X\ spill\ amount = total\ socioeconomic\ cost, \quad (5)$$

and environmental cost,

$$environmental\ cost\ (per gallon)\ X\ 0.5(freshwater\ modifier + wildlife\ modifier)\ X\ spill\ amount = total\ environmental\ damage\ cost. \quad (6)$$

The total spill cost is the sum of Equations 4 thru 6. The key inputs that differentiate spill costs for the channel and the bay are freshwater vulnerability category and habitat, socioeconomic and cultural value and wildlife sensitivity (Table 5-8). A description is included in the table for each factor chosen.

Table 5-8. EPA BOSCEM input criteria (Etkin, 2004) for the HSC-IC and Galveston Bay

Input Criteria	**HSC-IC Input Criteria**	**Galveston Bay Input Criteria**
Per-Gallon Oil Response Cost	$82 (Crude)	$82 (Crude)
Socioeconomic Base Per-Gallon Cost	$60 (Crude)	$60 (Crude)
Environmental Base Per- Gallon Cost	$30 (Crude)	$30 (Crude)
Response Cost Modifier for Location Medium Type	1 (Open Water/Shore)	1 (Open Water/Shore)
Socioeconomic and Cultural Value Ranking	0.1 (Heavy Industrial areas)	1 (Recreational areas)
Response Method Factor	1	1
Freshwater Vulnerability Category	0.4 (Industrial)	1 (Recreation)
Habitat and Wildlife Sensitivity	0.4 (Urban/Industrial)	1.2 (Estuary)

Table 5-9 presents the original environmental loss estimates from FEDERAP for facility 1, 5, and 9. Since the timing of the spill impacts the percent of pollutant released into Galveston Bay, estimates using the Etkin (2004) model were determined for spills prior to peak, at peak, and after peak storm surge. The percent of spill released to Galveston Bay was applied to the total spill amount for the corresponding storm surge level. Storm surge levels of 15, 18 and 22 ft were chosen to match with the modeled Ike, Ike at point 7, and Ike at point 7 with increased wind, respectively. The Galveston Bay input criteria (Table 5-8) were applied to spill quantities leaving the HSC-IC. The cost of the remaining spill quantity is determined using the HSC-IC input criteria (Table 5-8). In general, using the refined spill loss model produces same order of magnitude cost estimates as using FEDERAP. The costs of BOSCEM are higher for spills at Facility 1 at all storm surge levels but generally very similar or a little lower than FEDERAP for spills at Facility 5 or Facility 9. It is noted that while the spill costs are similar for FEDERAP

and the EFDC-SS, the modeling provides an in-depth understanding of the specific consequences from spills along different parts of the HSC-IC. Facilities farther west in the HSC-IC have a potential for inland pollution in addition to the spilled material reaching Galveston Bay. In contrast, spills near to the mouth of the HSC-IC get flushed out to Galveston Bay fairly rapidly with at least 80% of the spilled material being discharged to the Bay.

Table 5-9. Environmental losses from FEDERAP and EPA BOSCEM using spill results from EFDC-SS

	Storm Surge Level (ft)	FEDERAP Predicted Environmental Losses (million)	EPA BOSCEM Losses (million)		
			Before peak	At peak	After peak
Facility 1	15	$336	$505	$505	$471
	18	$796	$1103	$1106	$1067
	22	$1112	$1519	$1525	$1485
Facility 5	15	$691	$776	$752	$713
	18	$917	$902	$910	$963
	22	$2815	$2606	$2586	$2486
Facility 9	15	$296	$339	$327	$324
	18	$557	$564	$554	$556
	22	$2534	$2269	$2259	$2261

As can be seen from Table 5-9, by accounting for the timing of the spill, cleanup costs change by $30 to $120 million for the various scenarios shown in the Table. On average, there is 0.3 to 6% variability between the lowest and highest estimates when comparing spills that occur before, at, and after the peak storm surge.

5.6 SEDIMENT AND WATER QUALITY RESULTS

Figure 5-25 shows the salinity concentrations (mg/L) in the HSC-IC study area during the modeled Hurricane Ike event. As expected, salinity concentrations increase

north as the storm surge rises yield high concentrations for as high as the HSC Battleship (see Figure 5-1 for reference) for 8 hours. By 09/14/2008 at 12:00AM, high salinity concentrations begin to recede back towards the bay and by the end of the model run (09/23/2008 at 12:00AM), the spatial distribution and concentration levels are similar to those observed before the hurricane event.

Figure 5-26 and Figure 5-27 present the modeled salinity concentrations (mg/L) for Hurricane Ike at Point 7 and Hurricane Ike at Point 7 with 30% increased winds, respectively. Around 09/13/2008 at 12:00PM, high concentrations of salinity are modeled west past the HSC Battleship; however the retention time for the higher observed concentrations is similar to Hurricane Ike and by 09/23/2008 at 12:00AM, salinity concentration have normalized back to pre-storm concentrations.

Figure 5-25 shows the depth-averaged TSS concentrations (mg/L) in the HSC-IC study area during the modeled Hurricane Ike event. High TSS concentrations are observed in the deepest portion of the HSC-IC (navigable portion) starting at 09/13/2008 at 08:00AM north of Morgan's Point. While experiencing high storm surge elevations, the high TSS concentrations are forced north near the HSC Battleship and south towards the outlet of Cedar Bayou, north of Tabbs Bay. Between 09/14/2008 12:00AM and 09/15/2008 12:00AM, higher TSS concentrations are observed from the Upper San Jacinto Bay to Morgan's Point. This is a result of lower WSE and not suspended sediment being added to the system. The total mass of TSS that has been forced in from Galveston Bay through the storm surge event remains constant but depth-averaged concentrations increase since there is less water diluting the concentration. As the storm surge scenario increases in intensity, the TSS on 09/14/2008 at 12:000AM and

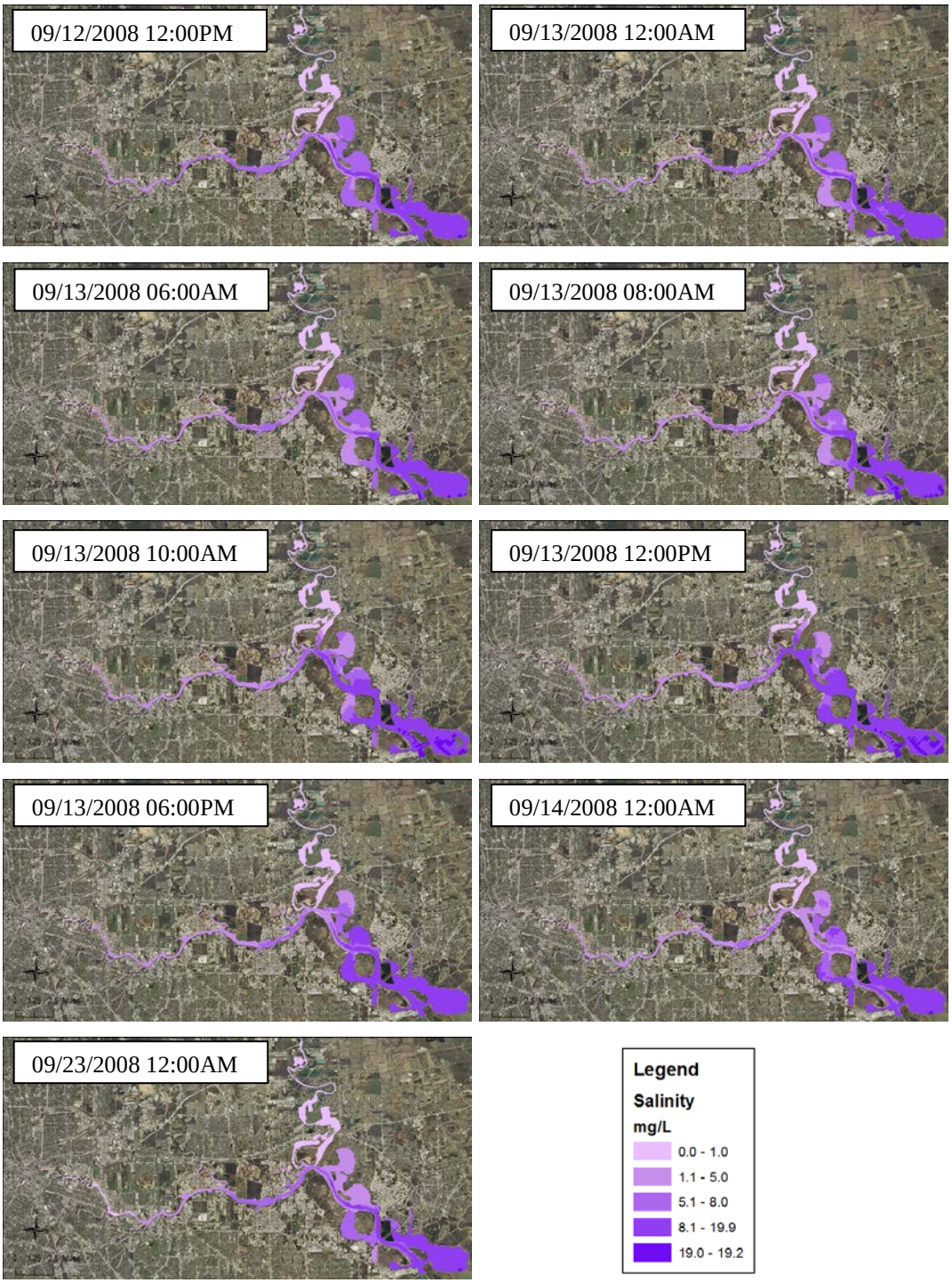

Figure 5-25. Modeled salinity changes during Hurricane Ike for the HSC-IC

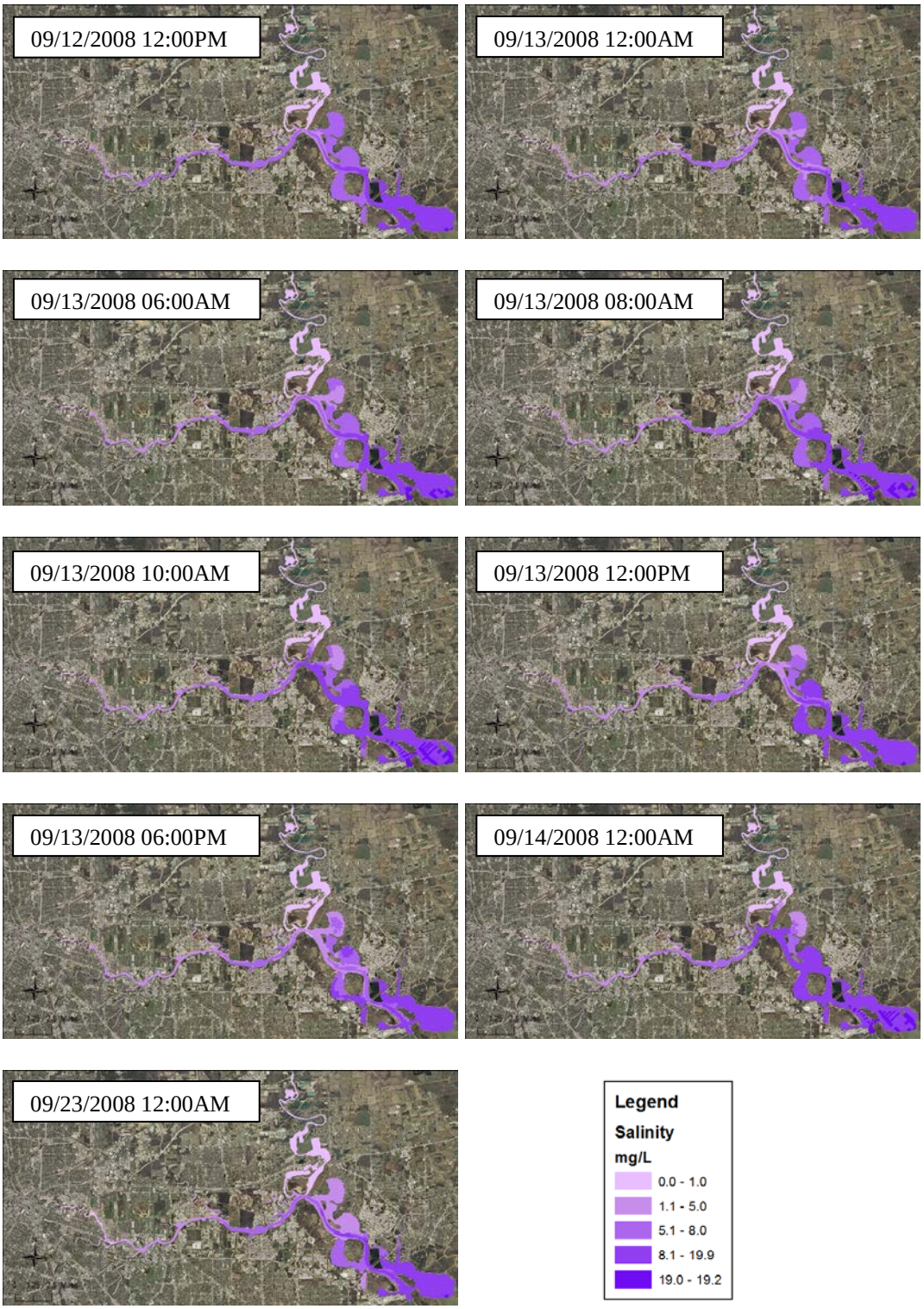

Figure 5-26. Modeled salinity changes during Hurricane Ike at Point 7 for the HSC-IC

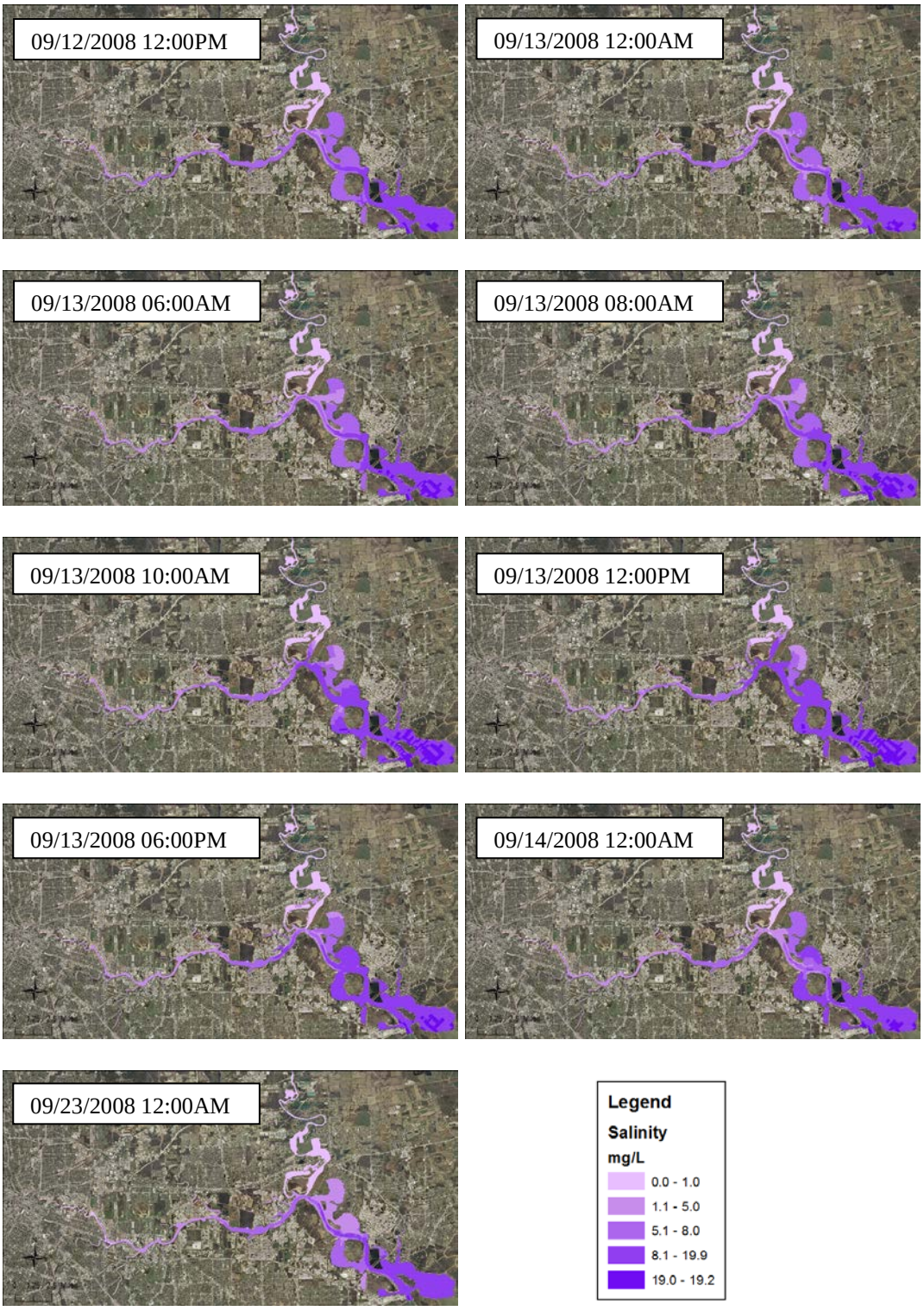

Figure 5-27. Modeled salinity changes during Hurricane Ike at Point 7 with increased winds for the HSC-IC

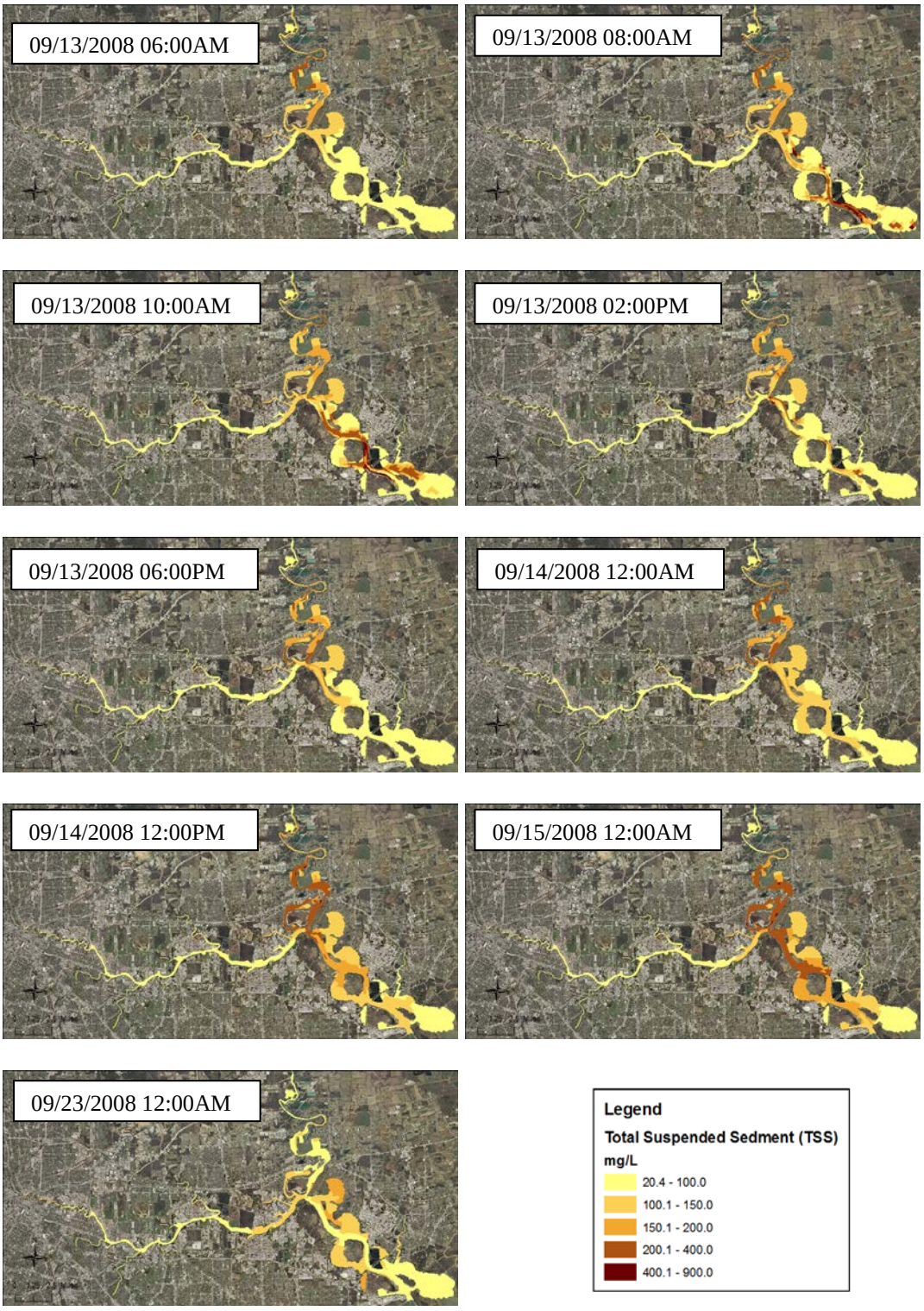

Figure 5-28. Modeled TSS changes during Hurricane Ike for the HSC-IC

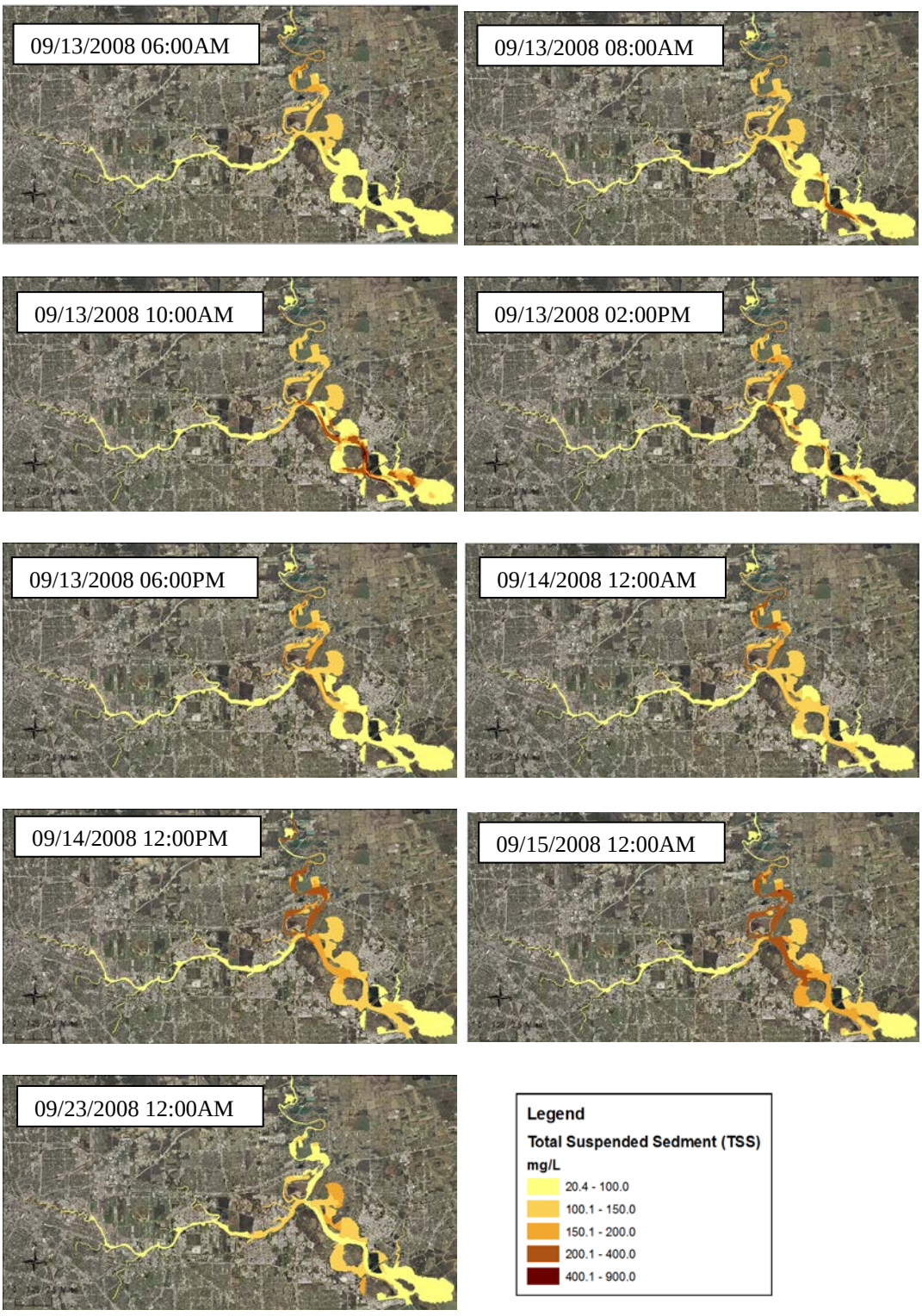

Figure 5-29. Modeled TSS changes during Hurricane Ike at Point 7 for the HSC-IC

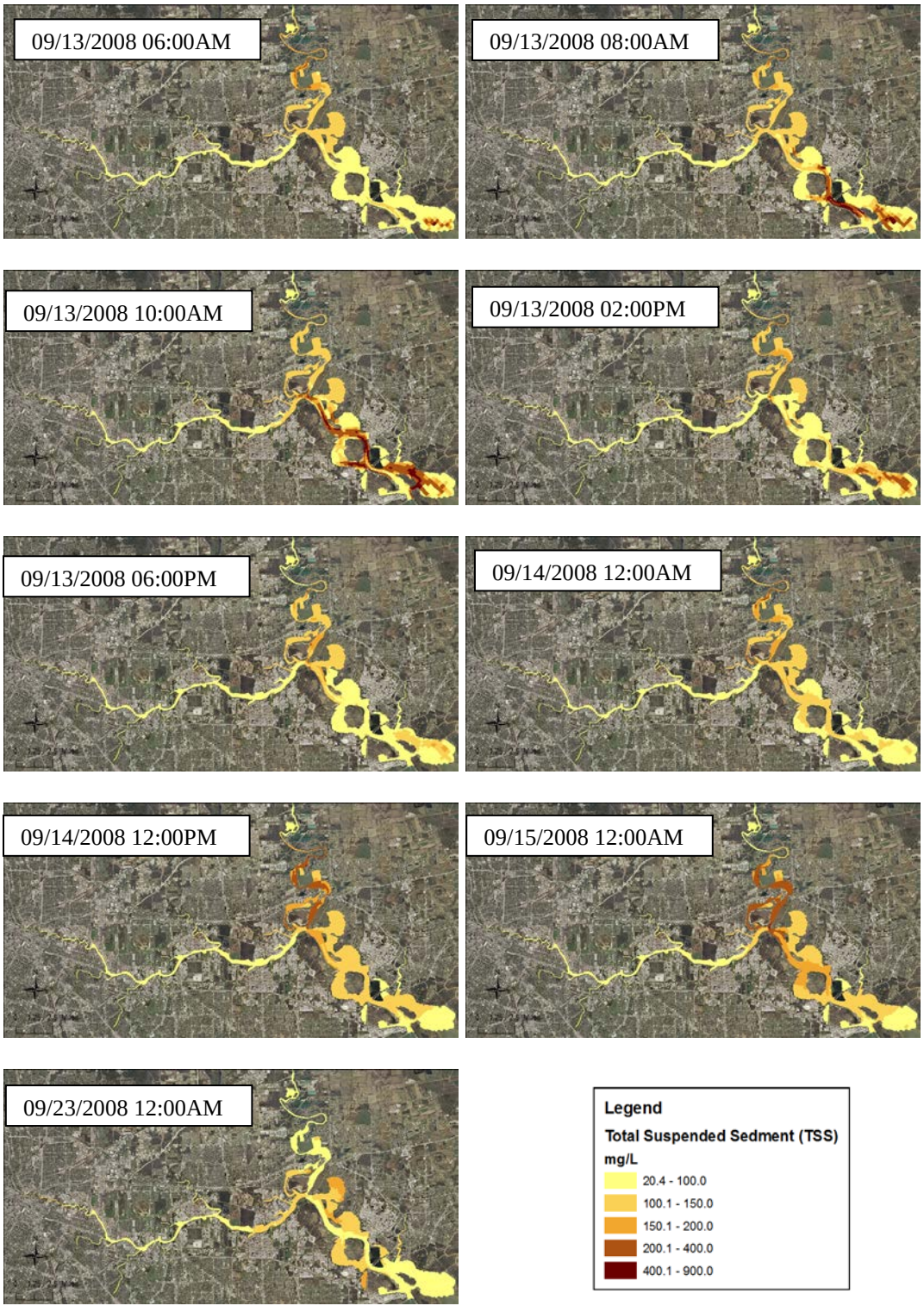

Figure 5-30. Modeled TSS changes during Hurricane Ike at Point 7 with increased winds for the HSC-IC

09/15/2008 concentrations decrease in this region between Upper San Jacinto Bay and Morgan's Point due to increased TSS leaving the system through the open boundary to Galveston Bay. This indicates that suspended sediment remaining in the modeled system is dependent on the storm surge level observed. At higher storm surge levels, more sediment leaves the system potentially explaining higher PCB concentrations observed at locations in Galveston bay in water and sediment following Hurricane Ike (Howell, 2012).

High bed shear stress causes significant resuspension of sediment and will certainly change the dynamics in the existing pollutant distribution with the estuary. Under hurricane forces, it is expected that shear stress would increase. From an ecological and environmental perspective, it is important to understand this phenomenon. Hence, for Hurricane Ike, bed shear stresses were modeled using EFDC-SS. The results are shown in Figure 5-29. The highest bed shear stresses are observed in the navigable portion of the channel and in the area north of Tabbs Bay near the outlet of Cedar Bayou (corresponding to high modeled TSS). Howell and Rifai (2015) observed changes in the diffusive flux (PCB-Σ65) to the sediment bed in this area pre-Hurricane Ike and a year later. The change was towards net sediment-to-water diffusive fluxes potentially explained by the modeled bed shear stress results from EFDC-SS. In addition, based on visual inspection of changes in PCB concentrations from 2008 (pre-Ike) to 2009 (post-Ike) presented in Rifai (2009) there was an increase in PCB concentrations for water and sediment in regions of high bed shear stress though, in general, concentrations increased for locations across the model domain. The areas of highest modeled bed shear stress do not indicate areas of greatest change in PCB concentrations. While the results of the

water quality modeling during hurricane storm surge further support the theory that Hurricane Ike significantly changed the spatial contaminant distribution in the HSC-IC, the results also emphasize the need for further sampling following future storm surge events in order to understand the full impact of a hurricane on the ecosystems involved.

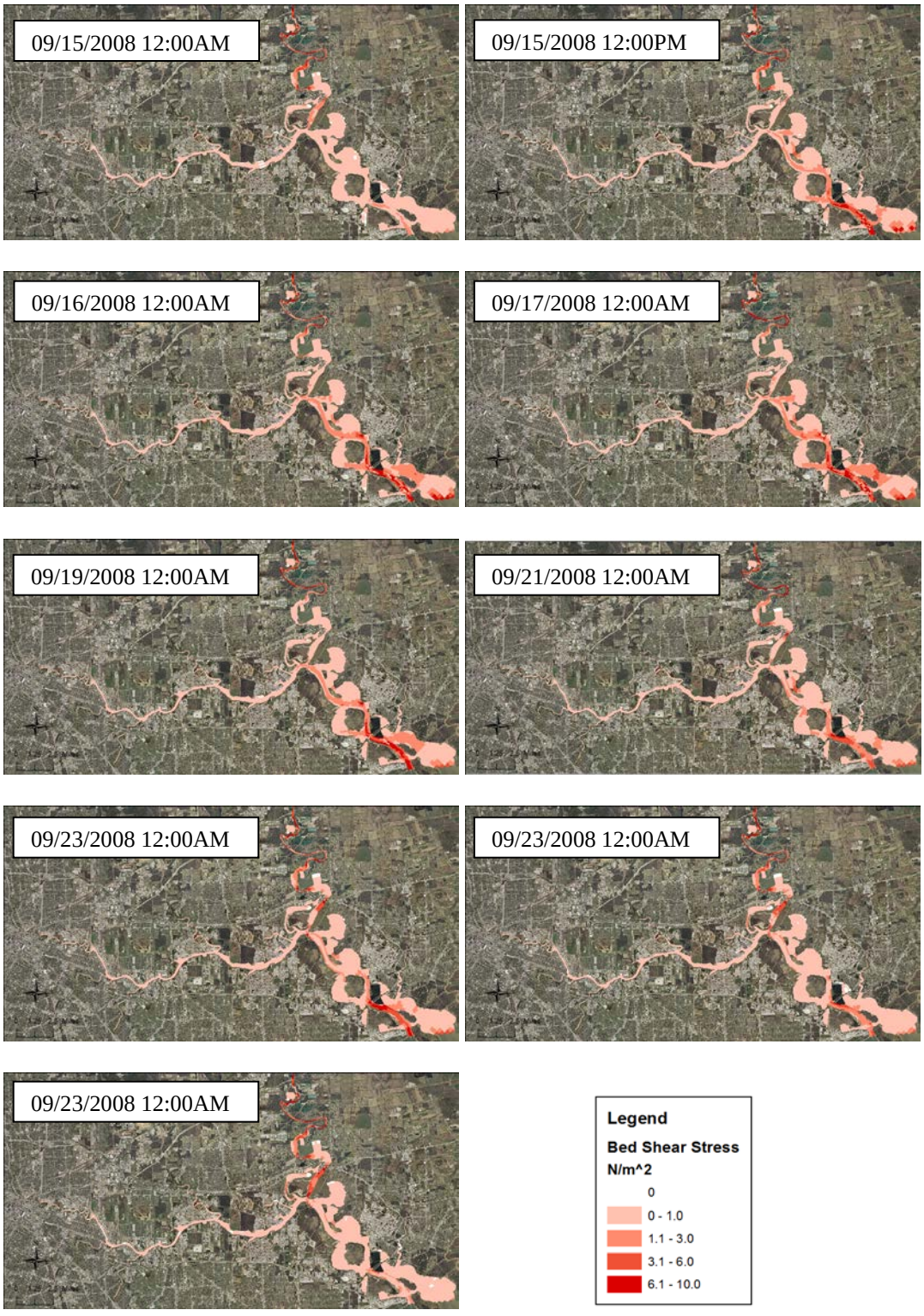

Figure 5-31. Bed shear stress during Hurricane Ike for the HSC-IC

CHAPTER 6. SUMMARY AND CONCLUSIONS

Preparing and mitigating the risk from storm surge for a hurricane event requires an understanding of vulnerability of coastal regions. However, current approaches to vulnerability assessments do not account for the complexities related to industrial and environmental losses. This dissertation introduces vulnerability frameworks, tools, and models at the regional and facility level that address this gap and demonstrates the developed tools and models using the Houston Ship Channel Industrial Complex as a case study. The research addresses the limitations of the current one-size-fits-all vulnerability approaches and brings to light the importance of taking into account the unique and important aspects of a coastal region. Because coastal communities are diverse along the Gulf Coast, the appropriate understanding of the potential impact from severe storm surge events should include the infrastructure that would be most affected as that has a significant impact on the regional economy. In addition, the HSC-IC is not a system of isolated facilities and vulnerabilities, but is interconnected and dynamic, thereby causing the impact on one facility to have larger impacts on the entire region. There is no standard model for understanding facility vulnerability from an economic and environmental perspective and the modeling of the impact on water quality in its estuary is limited at best. This last issue was a key driver in the development of the EFDC-SS model because it is vital to have an understanding of how the system reacts to spills under different hurricane storm surge scenarios.

The conceptual model for evaluating the vulnerability of industrialized coastal regions to storm surge identifies key variables for the study region. The framework integrated hurricane scenarios modeled from SWAN+ADCIRC and cross-linked the

results with geospatial information for facilities within the industrial region to identify geospatial and environmental vulnerabilities to storm surge. The implementation of the framework within the HSC-IC found a relationship between storm surge and the total area inundated at a given storm surge level. Additionally, the research establishes a relationship between storm surge level and the total number of storage tanks affected. With other storm surge events, the relationship can predict the total area inundated in the region. As part of a potential economic analysis, a cost per inundated acre can be applied to predict or assess the total damage from inundation due to storm surge in the HSC-IC region. In addition, this relationship is consistent with previous work and shows that the 100-yr FEMA floodplain in its current form may not be sufficient for considering significant storm surge impacts. Consideration should be given to incorporating the vulnerability of areas that will experience economic and/or environmental losses at the storm surge level.

In addition, the regional vulnerability framework demonstrated a methodology for evaluating environmental vulnerabilities for an industrial region and for specific facilities in the region by using releases from storage tanks, records of past historical releases, and Risk Management Planning. By combining the geospatial vulnerability results and the vulnerabilities based on a comprehensive environmental release dataset, it is possible to categorize the facilities in the HSC-IC and rank them from most vulnerable to least vulnerable based on both storm surge and environmental releases. Although there is variation in facility vulnerability between storm surge levels of approximately 4 m and 7.7 m, this variation is almost non-existent when storm surge exceeds 7 m. At storm surge levels of 7 m and higher, almost every facility in the HSC-IC will experience

significant economic and/or environmental losses. Hence, plans for mitigation and protection whether at the individual facility level or regionally via berms and/or surge gates need to consider this information in the decision-making.

The Facility Economic Damage and Environmental Release Planning (FEDERAP) provided a modeling framework that allows for investigating the complex relationship between storm surge level and the specific losses that would be experienced by a specific facility or an entire industrial region. The model demonstrates that industrial regions should be evaluated using tools that consider their unique characteristics. In addition, the FEDERAP model demonstrates that property loss is a relatively small component when compared to other losses that could be incurred due to storage tank damage or damage to process units. This research also demonstrates that storm surge levels are directly related to incurred damages and losses at industrial facilities and that storm surge above a facility's specific threshold value would increase losses at a steeper slope due to environmental pollution and loss of productivity.

In an attempt to strengthen the regional understanding of facility loss in the HSC-IC, the development and validation of a detailed regression model was performed and applied, though the resulting regional losses did not increase with increasing surge level for all studied levels as was the case with the 12 facilities that were analyzed with FEDERAP. The regression approach will require further refinement before it can be used for region-wide analysis; however, the regression can be applied with accuracy for chemical and refining facilities where the match to FEDERAP data was very good.

Alternate approaches for regional loss estimates were developed using relationships derived from the facilities modeled in FEDERAP based on total area and

inundated area of the studied facilities for each storm surge level. In addition, the FEDERAP model results were refined using detailed tank spill probabilities obtained from structural fragility analyses completed by others. The results show the rigor of the FEDERAP framework in that it can be modified to incorporate more data and approaches as they become available. Like other damage models (HAZUS), localized data provide a greater understanding of loss for a particular study area. As illustrated in Chapters 4 and 5, FEDERAP is a framework that can be continually updated and improved as more knowledge is acquired from both a hurricane standpoint and industrial infrastructure.

EFDC-SS (the coupled EFDC and SWAN+ADCIRC model) represents a more rigorous approach for modeling environmental impact by simulating potential spill scenarios and water quality changes during a hurricane event. The model was instrumental in understanding potential spill movement and settling locations in the HSC-IC during a hurricane for various spill scenarios; however, the model was not used in evaluating long-term impacts of hurricane events. Results demonstrated that the timing of the release was a key factor in predicting the location of high dye concentrations. A mass flux analysis at the open boundary showed the location of the release was a major factor in determining the percent of the spill released into the Galveston Bay system. For all of the model runs, at least 45% of the spill quantity would be released into the Galveston Bay system indicating a need for expanding the modeling efforts beyond the current HSC-IC study area. Mitigation strategies such as gates or levee systems have been discussed extensively for these types of estuary systems and would significantly change the results of this thesis. In the event that a gate is implemented, EFDC-SS could be used to model changes in spill transport and cleanup costs for various strategies.

In addition, key areas of resuspension of sediment were identified from the modeled TSS and bed shear stress. Using areas of highly contaminated sediments (such as with PCBs) from previous studies in the HSC-IC, certain areas were identified as high risk to movement of existing contaminants. This information could be used to aid decision makers in prioritizing areas of remediation, especially in regions like the HSC-IC with a history of extreme events and persistent contamination in the water and sediment.

EFDC-SS was also used to improve cleanup estimates in FEDERAP by accounting for percent of pollutant mass lost into Galveston Bay since cleanup cost within an industrial corridor and a bay differ. The updated losses accounted for this complexity by connected two separately developed models. To date, vulnerability and pollutant transport studies for hurricanes have not been used in collaboration. This dissertation developed and applied a framework that joins two typically separate areas of study in disaster research resulting in a more refined understanding of environmental and economic vulnerability in a region like the HSC-IC.

Lastly, it is important to note the research presented in this dissertation is not probabilistic in nature and does not include the risk of incurring a specific storm surge level. However, the model can be readily adapted to incorporate risk and probability when data on hurricane risks are available. It would be possible to associate the modeled storm surge levels from the various hurricane scenarios with an “event risk” value, representing a probability of occurrence as determined by on-going FEMA work. The risk for facilities may then be estimated based on their geospatial, environmental, economic vulnerability, and the event risk for each storm surge level.

Future work should incorporate wetting and drying in the EFDC-SS model in order to account for complexities related to inundation. Using the developed models and frameworks, non-conservative tracers would promote understanding regarding how a contaminant may react with the natural system including long-term impacts beyond the 23 days modeled in this work.

The insights derived from the results presented in this research can be used to inform stakeholders about the potential impact of storm surge events on the HSC-IC and can be used to communicate to the need for mitigation strategies to protect this vital resource in the Houston-Galveston region. Given real-time surge level inputs, the developed models can be used to identify regions of high environmental vulnerability thereby informing emergency coordinators of regions that should be evacuated and that may require cleanup due to an environmental disaster.

Ultimately, a better understanding of the vulnerabilities and economic impact on a surrounding region can support public policy related to promoting resilience in coastal communities, and informing emergency managers. By identifying the facilities with the greatest vulnerability and impact on the surrounding region, evacuation and mitigation plans specific to a given scenario can be executed that otherwise would be unknown.

REFERENCES

Adams, C., E. C. Witt, J. Wang, D. K. Shaver, D. Summers, Y. Filali-Meknassi, H. Shi, R. Luna and N. Anderson (2007). "Chemical Quality of Depositional Sediments and Associated Soils in New Orleans and the Louisiana Peninsula Following Hurricane Katrina." Environmental Science & Technology 41(10): 3437-3443.

Adger, W. N., T. P. Hughes, C. Folke, S. R. Carpenter and J. Rockstrom (2005). "Social-ecological resilience to coastal disasters." Science 309(5737): 1036-1039.

Alarcon, V. J., D. Johnson, W. H. McAnally, J. van der Zwaag, D. Irby and J. Cartwright (2014). "Nested Hydrodynamic Modeling of a Coastal River Applying Dynamic-Coupling." Water Resources Management 28(10): 3227-3240.

Anderson, M. A. (2010). "Influence of pumped-storage hydroelectric plant operation on a shallow polymictic lake: Predictions from 3-D hydrodynamic modeling." Lake and Reservoir Management 26(1): 1-13.

Ashley, N. A., K. T. Valsaraj and L. J. Thibodeaux (2008). "Elevated in-home sediment contaminant concentrations – The consequence of a particle settling–winnowing process from Hurricane Katrina floodwaters." Chemosphere 70(5): 833-840.

Birkmann, J. (2006). Measuring Vulnerability to Natural Hazards: Towards Disaster Resilient Societies. Tokyo, United Nations University Press.

Blake, E. S. and E. J. Gibney (2011). “The deadliest, costliest, and most intense United States Tropical Cyclones from 1851 to 2010 (and other frequently requested hurricane facts).” Miami, Fl, NOAA - National Hurricane Center.

Bonvicini, S., G. Antonioni, P. Morra and V. Cozzani (2014). "Quantitative assessment of environmental risk due to accidental spills from onshore pipelines." Process Safety and Environmental Protection(0).

Booij, N., R. C. Ris and L. H. Holthuijsen (1999). "A third-generation wave model for coastal regions 1. Model description and validation." Journal of Geophysical Research 104(C4): 7649-7666.

Brody, S., R. Blessing, A. Sebastian and P. Bedient (2012). "Delineating the Reality of Flood Risk and Loss in Southeast, Texas." Natural Hazards Review.

Bunya, S., J. C. Dietrich, J. J. Westerink, B. A. Ebersole, J. M. Smith, J. H. Atkinson, R. Jensen, D. T. Resio, R. A. Luettich, C. Dawson, V. J. Cardone, A. T. Cox, M. D. Powell, H. J. Westerink and H. J. Roberts (2010). "A High-Resolution Coupled Riverine Flow, Tide, Wind, Wind Wave, and Storm Surge Model for Southern Louisiana and Mississippi. Part I: Model Development and Validation." Monthly Weather Review 138(2): 345-377.

Burleson, D. W., H. S. Rifai, J. K. Proft, C. N. Dawson and P. B. Bedient (2015a). "Vulnerability of an industrial corridor in Texas to storm surge." Natural Hazards: 1-21.

Burleson, D. W., H. S. Rifai and P. B. Bedient (2015b). "A GIS Framework and Toolbox for Modeling Industrial Facility Damage and Economic Losses due to Storm Surge." Journal of Environmental Informatics: (accepted awaiting publication).

Carpenter, S., B. Walker, J. M. Anderies and N. Abel (2001). "From metaphor to measurement: Resilience of what to what?" Ecosystems 4(8): 765-781.

Cauffman, S. A., L. T. Phan, F. Sadek, W. P. Fritz, D. Duthinh and W. J. Rossiter (2006). "Performance of Physical Structures in Hurricane Katrina and Hurricane Rita: A Reconnaissance Report (NIST TN 1476)." National Institute of Standards and Technology 222.

Chakraborty, J., G. Tobin and B. Montz (2005). "Population Evacuation: Assessing Spatial Variability in Geophysical Risk and Social Vulnerability to Natural Hazards." Natural Hazards Review 6(1): 23-33.

Chen, Q. (2005). "Prediction of Wind Waves in a Shallow Estuary." J. Waterway, Port, Coastal, Ocean Eng. 131(4): 137.

Christopher, V. M., M. G. Allen, E. T. David and P. B. Ellen (2012). "Coastal Hazard Vulnerability Assessment of Sensitive Historical Sites on Rainsford Island, Boston Harbor, Massachusetts." Journal of Coastal Research 28(1A): 20.

Cigler, B. (2009). "Post-Katrina Hazard Mitigation on the Gulf Coast." Public Organization Review 9(4): 325-341.

Craig, P. M. (2012). User's Manual for EFDC_Explorer7: A Pre/Post Processor for the Environmental Fluid Dynamics Code (Rev 00). L. Dynamic Solutions Intl. Knoxville, TN.

Cruz, A., L. Steinberg and R. Luna (2001). "Identifying Hurricane-Induced Hazardous Material Release Scenarios in a Petroleum Refinery." Natural Hazards Review 2(4): 203-210.

Cutter, S. L., L. Barnes, M. Berry, C. Burton, E. Evans, E. Tate and J. Webb (2008). "A place-based model for understanding community resilience to natural disasters." Global Environmental Change 18(4): 598-606.

Cutter, S. L., B. J. Boruff and W. L. Shirley (2003). "Social vulnerability to environmental hazards." Social Science Quarterly 84(2): 242-261.

Cutter, S. L., R. L. Schumann and C. T. Emrich (2014). "Exposure, Social Vulnerability and Recovery Disparities in New Jersey after Hurricane Sandy." Journal of Extreme Events 01(01): 1450002.

Dietrich, J. C., S. Tanaka, J. J. Westerink, C. N. Dawson, R. A. Luettich, Jr., M. Zijlema, L. H. Holthuijsen, J. M. Smith, L. G. Westerink and H. J. Westerink (2012). "Performance of the Unstructured-Mesh, SWAN+ADCIRC Model in Computing Hurricane Waves and Surge." Journal of Scientific Computing 52(2): 468-497.

Dietrich, J. C., M. Zijlema, J. J. Westerink, L. H. Holthuijsen, C. Dawson, R. A. Luettich, R. E. Jensen, J. M. Smith, G. S. Stelling and G. W. Stone (2011). "Modeling hurricane waves and storm surge using integrally-coupled, scalable computations." Coastal Engineering 58(1): 45-65.

Ding, A., J. White, P. Ullman and A. Fashokun (2008). "Evaluation of HAZUS-MH Flood Model with Local Data and Other Program." Natural Hazards Review 9(1): 20-28.

Eggleston, K. (2014). "Valero Refinery Expansions Pushed Forward by Eagle Ford Production Growth – $730 Million." Eagle Ford Shale Retrieved 02/16/15, 2015, from http://eaglefordshale.com/pipeline-midstream-news/valero-refinery-expansions-pushed-forward-by-eagle-ford-production-growth/.

Etkin, D. S. (2000). “Worldwide analysis of oil spill cleanup cost factors”. 23rd Arctic & Marine Oilspill Program Tech. Sem.

Etkin, D.S., (2004). “Modeling oil spill response and damage costs”. In: Proceedings of 5th Biennial Freshwater Spills Symposium, 6–8 April.

Fahey, J. (2012) "Hurricane Isaac: Gas Prices Spike Across The Country." Huffington Post

Folke, C. (2006). "Resilience: The emergence of a perspective for social-ecological systems analyses." Global Environmental Change-Human and Policy Dimensions 16(3): 253-267.

Folke, C., S. Carpenter, T. Elmqvist, L. Gunderson, C. S. Holling and B. Walker (2002). "Resilience and sustainable development: Building adaptive capacity in a world of transformations." Ambio 31(5): 437-440.

Folke, C., S. R. Carpenter, B. Walker, M. Scheffer, T. Chapin and J. Rockstrom (2010). "Resilience Thinking: Integrating Resilience, Adaptability and Transformability." Ecology and Society 15(4).

Francis, R. and B. Bekera (2013). "A metric and frameworks for resilience analysis of engineered and infrastructure systems." Reliability Engineering & System Safety(0).

Frazier, T. G., N. Wood, B. Yarnal and D. H. Bauer (2010). "Influence of potential sea level rise on societal vulnerability to hurricane storm-surge hazards, Sarasota County, Florida." Applied Geography 30(4): 490-505.

Fries, J. S., R. T. Noble, G. M. Kelly and J. L. Hsieh (2007). "Storm impacts on potential pathogens in estuaries." Eos, Transactions American Geophysical Union 88(8): 93-95.

Funakoshi, Y. (2008). "Coupling of Hydrodynamic and Wave Models: Case Study for Hurricane Floyd (1999) Hindcast." J. Waterway, Port, Coastal, Ocean Eng. 134(6): 321.

Godoy, L. A. (2007). "Performance of Storage Tanks in Oil Facilities Damaged by Hurricanes Katrina and Rita." Journal of Performance of Constructed Facilities 21(6): 441-449.

Godoy, L. A. (2009). Hurricane failures of tanks for the oil industry. International Association for Shell and Spatial Structures (IASS) Symposium, Valencia, Spain.

Guo, W. J. and Y. X. Wang (2009). "A numerical oil spill model based on a hybrid method." Marine Pollution Bulletin 58(5): 726-734.

Hagy, J., J. Lehrter and M. Murrell (2006). "Effects of Hurricane Ivan on water quality in Pensacola Bay, Florida." Estuaries and Coasts 29(6): 919-925.

Hallegatte, S., N. Ranger, O. Mestre, P. Dumas, J. Corfee-Morlot, C. Herweijer and R. Wood (2011). "Assessing climate change impacts, sea level rise and storm surge risk in port cities: a case study on Copenhagen." Climatic Change 104(1): 113-137.

Hamrick, J. M. (1992). A three-dimensional environmental fluid dynamics computer code: Theoretical and computational aspects.

Hamrick, J. M. (1996). Users manual for the environmental fluid dynamic computer code, The College of William and Mary, Virginia Institute of Marine Science. Special Report 328**:** 224.

Harris, S. P. and D. O. Wilson (2008). "Mitigating Hurricane storm surge perils at the DeLisle Plant." Process Safety Progress 27(3): 177-184.

Holling, C. S. (1973). "Resilience and Stability of Ecological Systems." Annual Review of Ecology and Systematics 4(1): 1-23.

Hope, M. E., J. J. Westerink, A. B. Kennedy, P. C. Kerr, J. C. Dietrich, C. Dawson, C. J. Bender, J. M. Smith, R. E. Jensen, M. Zijlema, L. H. Holthuijsen, R. A. Luettich, M. D. Powell, V. J. Cardone, A. T. Cox, H. Pourtaheri, H. J. Roberts, J. H. Atkinson, S. Tanaka, H. J. Westerink and L. G. Westerink (2013). "Hindcast and validation of Hurricane Ike (2008) waves, forerunner, and storm surge." Journal of Geophysical Research: Oceans 118(9): 4424-4460.

Howell, N. L. (2012). Bed and suspended sediment as source and transport mechanisms for polychlorinated biphenyls in the Houston Ship Channel Estuary System. PhD, University of Houston.

Howell, N. L. and H. S. Rifai. (2015). “Longitudinal estimates of sediment-water diffusive flux of PCB congeners in the Houston Ship Channel.” Estuarine, Coastal and Shelf Science Volume 164: 19-27.

Huang, W.-P., C.-A. Hsu, C.-S. Kung and J. Z. Yim (2007). "Numerical studies on typhoon surges in the Northern Taiwan." Coastal Engineering 54(12): 883-894.

Hufschmidt, G. (2011). "A comparative analysis of several vulnerability concepts." Natural Hazards 58(2): 621-643.

Irish, J. L., D. T. Resio and J. J. Ratcliff (2008). "The Influence of Storm Size on Hurricane Surge." Journal of Physical Oceanography 38(9): 2003-2013.

Jelesnianski, C. P., J. Chen and W. A. Shaffer (1992). SLOSH: Sea, lake, and overland surges from hurricanes. NOAA Techical Report NWS 48, National Oceanic and Atmospherica Administration.

Jelesnianski, C. P., J. Chen and W. A. Shaffer (1992). SLOSH: Sea, Lake, and Overland Surges from Hurricanes. Technical Report of National Weather Service. Silver Springs, MD. 48:71.

Ji, Z. G., M. R. Morton and J. M. Hamrick (2001). "Wetting and Drying Simulation of Estuarine Processes." Estuarine, Coastal and Shelf Science 53(5): 683-700.

Kameshwar, S., Padgett, J.E. (2015). “Fragility Assessment of Above Ground Petroleum Storage Tanks under Storm Surge.” 12th International Conference on Applications of Statistics and Probability in Civil Engineering, Vancouver, Canada, July 12-15, 2015.

Kameshwar, S. (2015). Personal Communication on 07-08-20015, preliminary results from tank fragility analysis.

Kerr, P. C., A. S. Donahue, J. J. Westerink, R. A. Luettich, L. Y. Zheng, R. H. Weisberg, Y. Huang, H. V. Wang, Y. Teng, D. R. Forrest, A. Roland, A. T. Haase, A. W. Kramer, A. A. Taylor, J. R. Rhome, J. C. Feyen, R. P. Signell, J. L. Hanson, M. E. Hope, R. M. Estes, R. A. Dominguez, R. P. Dunbar, L. N. Semeraro, H. J. Westerink, A. B. Kennedy, J. M. Smith, M. D. Powell, V. J. Cardone and A. T. Cox (2013). "U.S. IOOS coastal and ocean modeling testbed: Inter-model evaluation of tides, waves, and hurricane surge in the Gulf of Mexico." Journal of Geophysical Research: Oceans 118(10): 5129-5172.

Kim, M., E. Miller-Hooks and R. Nair (2011). "A Geographic Information System-Based Real-Time Decision Support Framework for Routing Vehicles Carrying Hazardous Materials." Jounral of Intelligent Transportation Sytems. 15(1): 28-41.

Kleinosky, L., B. Yarnal and A. Fisher (2007). "Vulnerability of Hampton Roads, Virginia to Storm-Surge Flooding and Sea-Level Rise." Natural Hazards 40(1): 43-70.

Lei, Y., J. a. Wang, Y. Yue, H. Zhou and W. Yin (2014). "Rethinking the relationships of vulnerability, resilience, and adaptation from a disaster risk perspective." Natural Hazards 70(1): 609-627.

Lin, N., K. A. Emanuel, J. A. Smith and E. Vanmarcke (2010). "Risk assessment of hurricane storm surge for New York City." Journal of Geophysical Research 115(D18121).

Link, L. E. (2010). "The anatomy of a disaster, an overview of Hurricane Katrina and New Orleans." Ocean Engineering 37(1): 4-12.

Liu, Y., R. H. Weisberg, C. Hu and L. Zheng (2011). "Tracking the Deepwater Horizon Oil Spill: A Modeling Perspective." Eos, Transactions American Geophysical Union 92(6): 45-46.

Lopez Marrero, T. (2008). Adaptive capacity and resilience to floods in the Caribbean: A case study of two flood-prone communities in Puerto Rico Ph.D., The Pennsylvania State University.

Marc, L. and H. Carol (2005). Development of Vulnerability Functions for Industrial/ Petrochemical Facilities due to Extreme Winds and Hurricanes. Solutions to Coastal Disasters 2005, American Society of Civil Engineers**:** 494-503.

Mattocks, C. and C. Forbes (2008). "A real-time, event-triggered storm surge forecasting system for the state of North Carolina." Ocean Modelling 25(3-4): 95-119.

Mercado, A. (1994). "On the use of NOAA's storm surge model, SLOSH, in managing coastal hazards — the experience in Puerto Rico." Natural Hazards 10(3): 235-246.

Naito, C., D. Cox, Q. Yu and H. Brooker (2012). "Fuel Storage Container Performance during the 2011 Tohoku, Japan, Tsunami." Journal of Performance of Constructed Facilities 27(4): 373-380.

NOAA. (2012). "Hurricanes in History." Retrieved July 22, 2014, 2014.

Pandoe, W. W. and B. L. Edge (2008). "Case Study for a Cohesive Sediment Transport Model for Matagorda Bay, Texas, with Coupled ADCIRC 2D-Transport and SWAN Wave Models." Journal of Hydraulic Engineering 134(3): 303-314.

Pardue, J. H., W. M. Moe, D. McInnis, L. J. Thibodeaux, K. T. Valsaraj, E. Maciasz, I. van Heerden, N. Korevec and Q. Z. Yuan (2005). "Chemical and Microbiological Parameters in New Orleans Floodwater Following Hurricane Katrina." Environmental Science & Technology 39(22): 8591-8599.

Petrova, E. (2006). "Vulnerability of Russian regions to natural risk: experience of quantitative assessment." Nat. Hazards Earth Syst. Sci. 6(1): 49-54.

Pine, J. (2006). "Hurricane Katrina and oil spills: Impacts on coastal and ocean environment." Oceanography 19(2): 37-39.

Qi, H. and M. S. Altinakar (2011). "A GIS-based decision support system for integrated flood management under uncertainty with two dimensional numerical simulations." Environmental Modelling and Software 26(6): 817-821.

Rao, A., P. Chittibabu, T. Murty, S. Dube and U. Mohanty (2007). "Vulnerability from storm surges and cyclone wind fields on the coast of Andhra Pradesh, India." Natural Hazards 41(3): 515-529.

Reible, D., C. Haas, J. Pardue and W. Walsh (2006). "Toxic and Contaminant Concerns Generated by Hurricane Katrina." Journal of Environmental Engineering 132(6): 565-566.

Rifai, H.S. (2010). “Dioxin and PCB Contamination in HSC and Galveston Bay: Past, Present, and Future [Powerpoint Slides].” Retrieved from http://www .taep.org/assets/docs/rifai_taep_nov18_2010.pdf. Acceess date: 07/17/2015.

Robertson, I., H. Riggs, S. Yim and Y. Young (2007). "Lessons from Hurricane Katrina Storm Surge on Bridges and Buildings." Journal of Waterway, Port, Coastal, and Ocean Engineering 133(6): 463-483.

Santella, N., L. J. Steinberg and H. Sengul (2010). "Petroleum and Hazardous Material Releases from Industrial Facilities Associated with Hurricane Katrina." Risk Analysis 30(4): 635-649.

Sebastian, A., J. Proft, J. C. Dietrich, W. Du, P. B. Bedient and C. N. Dawson (2014). "Characterizing hurricane storm surge behavior in Galveston Bay using the SWAN + ADCIRC model." Coastal Engineering 88(0): 171-181.

Sengul, H., N. Santella, L. J. Steinberg and A. M. Cruz (2012). "Analysis of hazardous material releases due to natural hazards in the United States." Disasters 36(4): 723-743.

Sharma, U. and A. Patwardhan (2008). "Methodology for identifying vulnerability hotspots to tropical cyclone hazard in India." Mitigation and Adaptation Strategies for Global Change 13(7): 703-717.

Sheng, Y. P. (1990). Evolution of a three-dimensional curvilinear-grid hydrodynamic model for estuaries, lakes and coastal waters: CH3D. Estuarine and Coastal Modeling (1989), ASCE.

Sheng, Y. P., Y. Zhang and V. A. Paramygin (2010). "Simulation of storm surge, wave, and coastal inundation in the Northeastern Gulf of Mexico region during Hurricane Ivan in 2004." Ocean Modelling 35(4): 314-331.

Smith, J. M., M. A. Cialone, T. V. Wamsley and T. O. McAlpin (2010). "Potential impact of sea level rise on coastal surges in southeast Louisiana." Ocean Engineering 37(1): 37-47.

Smith, J. M., A. R. Sherlock and D. T. Resio (2001). STWAVE: Steady-state spectral wave model user's manual for STWAVE, Version 3.0, DTIC Document.

Srinivas, H. and Y. Nakagawa (2008). "Environmental implications for disaster preparedness: Lessons Learnt from the Indian Ocean Tsunami." Journal of Environmental Management 89(1): 4-13.

Stearns, M. and J. Padgett (2011). "Impact of 2008 Hurricane Ike on Bridge Infrastructure in the Houston/Galveston Region." Journal of Performance of Constructed Facilities 26(4): 441-452.

Stewart, M. G. (2003). "Cyclone damage and temporal changes to building vulnerability and economic risks for residential construction." Journal of Wind Engineering and Industrial Aerodynamics 91(5): 671-691.

The Wamdi Group (1988). "The WAM Model—A Third Generation Ocean Wave Prediction Model." Journal of Physical Oceanography 18(12): 1775-1810.

Topuz, E., I. Talinli and E. Aydin (2011). "Integration of environmental and human health risk assessment for industries using hazardous materials: A quantitative multi criteria approach for environmental decision makers." Environment International 37(2): 393-403.

Unanwa, C. O., J. R. McDonald, K. C. Mehta and D. A. Smith (2000). "The development of wind damage bands for buildings." Journal of Wind Engineering and Industrial Aerodynamics 84(1): 119-149.

Verter, V. and B. Y. Kara (2001). "A GIS-Based Framework for Hazardous Materials Transport Risk Assessment." Risk Analysis: An International Journal 21(6): 1109-1120.

Vickery, P. J., J. Lin, P. F. Skerlj, J. L. A. Twisdale and K. Huang (2006). "HAZUS-MH Hurricane Model Methodology. I: Hurricane Hazard, Terrain, and Wind Load Modeling." Natural Hazards Review 7(2): 82-93.

Vickery, P. J., P. F. Skerlj, J. Lin, J. L. A. Twisdale, M. A. Young and F. M. Lavelle (2006). "HAZUS-MH Hurricane Model Methodology. II: Damage and Loss Estimation." Natural Hazards Review 7(2): 94-103.

Walker, B., C. S. Hollin, S. R. Carpenter and A. Kinzig (2004). "Resilience, adaptability and transformability in social-ecological systems." Ecology and Society 9(2).

Walton, T. L., Jr. and R. G. Dean (2009). "Influence of florida bathymetry on wind stress components of storm surge." Coastal Engineering Journal 51(4): 297-308.

Wamsley, T. V., M. A. Cialone, J. M. Smith, B. A. Ebersole and A. S. Grzegorzewski (2009). "Influence of landscape restoration and degradation on storm surge and waves in southern Louisiana." Natural Hazards 51(1): 207-224.

Wang, C. and B. Yarnal (2012). "The vulnerability of the elderly to hurricane hazards in Sarasota, Florida." Natural Hazards 63(2): 349-373.

Wang, J. and Y. Shen (2010). "Modeling oil spills transportation in seas based on unstructured grid, finite-volume, wave-ocean model." Ocean Modelling 35(4): 332-344.

Weather Research Center (2015). “What is the size of a hurricane?”. Retrieved from http://www.wxresearch.org/family/pg5.html . Access date 07/17/15.

Weaver, R. J. and D. N. Slinn (2010). "Influence of bathymetric fluctuations on coastal storm surge." Coastal Engineering 57(1): 62-70.

Weisberg, R. and L. Zheng (2006). "Hurricane storm surge simulations for Tampa Bay." Estuaries and Coasts 29(6): 899-913.

Westerink, J. J., R. A. Luettich, J. C. Feyen, J. H. Atkinson, C. Dawson, H. J. Roberts, M. D. Powell, J. P. Dunion, E. J. Kubatko and H. Pourtaheri (2008). "A basin- to channel-scale unstructured grid hurricane storm surge model applied to southern Louisiana." Monthly Weather Review 136(3): 833-864.

Wilson, R. P. (2014). "Hurricane Sandy: Environmental Impact and Agency Efforts." Environmental Claims Journal 26(2): 126-156.

Wu, S.-Y., B. Yarnal and A. Fisher (2002). "Vulnerability of coastal communities to sea-level rise: a case study of Cape May County, New Jersey, USA." Climate Research 22(3): 255-270.

Yang, Z., M. K. Lindell and C. S. Prater (2009). "Vulnerability of community businesses to environmental disasters." Disasters 33(1): 38-57.

Zhang, K. Q., C. Y. Xiao and J. She (2008). "Comparison of the CEST and SLOSH models for storm surge flooding." Journal of Coastal Research 24(2): 489-+.

Zhou, H., J. A. Wang, J. Wan and H. Jia (2010). "Resilience to natural hazards: a geographic perspective." Natural Hazards 53(1): 21-41.

Zimmerman, R. (2014). "Planning Restoration of Vital Infrastructure Services Following Hurricane Sandy: Lessons Learned for Energy and Transportation." Journal of Extreme Events 01(01): 1450004.

Zografos, K. G., G. M. Vasilakis and I. M. Giannouli (2000). "Methodological framework for developing decision support systems (DSS) for hazardous materials emergency response operations." Journal of Hazardous Materials 71(1): 503-521.